



COVARIANCE ANALYSIS OF VISION AIDED NAVIGATION BY  
BOOTSTRAPPING

THESIS

Andrew L. Relyea, Captain, USAF

AFIT/GE/ENG/12-36

DEPARTMENT OF THE AIR FORCE  
AIR UNIVERSITY

**AIR FORCE INSTITUTE OF TECHNOLOGY**

Wright-Patterson Air Force Base, Ohio

APPROVED FOR PUBLIC RELEASE; DISTRIBUTION UNLIMITED

The views expressed in this thesis are those of the author and do not reflect the official policy or position of the United States Air Force, the Department of Defense, or the United States Government.

This material is declared a work of the U.S. Government and is not subject to copyright protection in the United States

COVARIANCE ANALYSIS OF VISION AIDED NAVIGATION BY  
BOOTSTRAPPING

THESIS

Presented to the Faculty  
Department of Electrical and Computer Engineering  
Graduate School of Engineering and Management  
Air Force Institute of Technology  
Air University  
Air Education and Training Command  
in Partial Fulfillment of the Requirements for the  
Degree of Master of Science in Electrical Engineering

Andrew L. Relyea, B.S.E.E.

Captain, USAF

March 2012

APPROVED FOR PUBLIC RELEASE; DISTRIBUTION UNLIMITED

COVARIANCE ANALYSIS OF VISION AIDED NAVIGATION BY  
BOOTSTRAPPING

Andrew L. Relyea, B.S.E.E.  
Captain, USAF

Approved:

M. Pachter  
Meir Pachter, PhD (Chairman)

Feb. 17, 2012  
Date

Michael Stepaniak  
Lt Col Michael Stepaniak, PhD (Committee Member)

17 Feb 2012  
Date

Kenneth A. Fisher  
Maj Kenneth Fisher, PhD (Committee Member)

17 Feb 2012  
Date

## Abstract

Inertial Navigation System (INS) aiding using bearing measurements taken over time of stationary ground features is investigated. A cross country flight, in two and three dimensional space, is considered, as well as a vertical drop in three dimensional space. The objective is to quantify the temporal development of the uncertainty in the navigation states of an aircraft INS which is aided by taking bearing measurements of ground objects which have been geolocated using ownship position. It is shown that during wings level flight at constant speed and a fixed altitude, an aircraft that tracks ground objects and over time sequentially transitions to tracking new ground objects which were geolocated by the aircraft as they came into view, will have the beneficial effect of considerably reducing the long term uncertainty in the INS-provided navigation state. It is also shown that a munition in “free fall” tracking previously geolocated ground features will also have the beneficial effect of reducing the uncertainty in the INS-provided navigation state.

*I would like to dedicate this paper to my wife and baby for your support and patience. I  
know you may never read this paper, but I wrote this paper for you.  
I LOVE YOU BOTH!*

## Table of Contents

	Page
Abstract . . . . .	iv
Dedication . . . . .	v
List of Figures . . . . .	viii
List of Tables . . . . .	x
List of Symbols . . . . .	xi
List of Abbreviations . . . . .	xiv
1 Introduction . . . . .	1
1.1 Background . . . . .	1
1.2 Motivation . . . . .	1
1.3 Scope . . . . .	2
1.4 Approach/Methodology . . . . .	3
2 Literature Review . . . . .	4
2.1 Overview . . . . .	4
2.2 Reference Frames . . . . .	4
2.2.1 Earth-fixed reference frame . . . . .	4
2.2.2 Navigation reference frame . . . . .	4
2.2.3 Body-fixed reference frame . . . . .	4
2.3 Inertial Navigation . . . . .	5
2.4 SLAM . . . . .	8
2.5 Recent Research . . . . .	9
3 Methodology . . . . .	12
3.1 Introduction . . . . .	12
3.2 Two-Dimensional Case . . . . .	12
3.2.1 Dynamics Error Model . . . . .	12
3.2.2 Modeling/Calibrating the Free INS . . . . .	18
3.2.3 Measurement Model . . . . .	19
3.2.4 Initialization . . . . .	23
3.2.5 Performance of Aided INS . . . . .	23
3.2.6 Transitioning Between Measurement Epochs . . . . .	24
3.3 Three-Dimensional Horizontal Case . . . . .	27

3.3.1	Dynamics . . . . .	27
3.3.2	Modeling/Calibrating the Free INS . . . . .	33
3.3.3	Measurement Equation . . . . .	34
3.3.4	Performance of Aided INS . . . . .	41
3.3.5	Initialization . . . . .	42
3.3.6	Transitioning Between Measurement Epochs . . . . .	42
3.4	Three Dimensional Vertical Case . . . . .	46
3.4.1	Dynamics . . . . .	46
3.4.2	Modeling/Calibrating the Free INS . . . . .	48
3.4.3	Measurement Model . . . . .	49
3.4.4	Performance of Aided INS . . . . .	51
3.4.5	Initialization . . . . .	53
3.4.6	Transitioning Between Measurement Epochs . . . . .	54
4	Covariance Analysis Results . . . . .	56
4.1	Introduction . . . . .	56
4.2	Two Dimensional Results . . . . .	56
4.3	Horizontal Three Dimensions . . . . .	58
4.4	Vertical Three Dimensions . . . . .	60
5	Conclusion . . . . .	66
5.1	Conclusions . . . . .	66
5.2	Follow-On Topics . . . . .	66
	Appendix A: 2-D Standard Deviation Plots . . . . .	68
	Appendix B: 3-D Horizontal Plots . . . . .	72
	Appendix C: 3-D Vertical Plots . . . . .	76
	Appendix D: General Form Dynamics . . . . .	82
	Appendix E: General Form Measurement Model . . . . .	85
	Bibliography . . . . .	99

## List of Figures

Figure	Page
2.1 Earth-Fixed Reference Frame. . . . .	5
2.2 Navigation Reference Frame. . . . .	6
2.3 Body-Fixed Reference Frame. . . . .	7
2.4 Basic SLAM problem. . . . .	9
3.1 Relationship between the body and inertial frame for the 2-D horizontal case. .	13
3.2 Showing the scenario set up. . . . .	24
3.3 Relationship between the body and inertial frame for the 3-D horizontal case. .	28
3.4 Relationship between the body and inertial frame for 3-D Vertical Case. . . .	47
3.5 Geometry 1 Ground Feature Locations. . . . .	52
3.6 Geometry 2 Ground Feature Locations. . . . .	53
4.1 2-D Unaided INS Position Standard Deviation. . . . .	58
4.2 2-D Aided INS Position Standard Deviation. . . . .	59
4.3 3-D Unaided INS Position Standard Deviation. . . . .	60
4.4 3-D Aided INS Position Standard Deviation. . . . .	61
4.5 Vertical Drop Unaided INS Position Standard Deviation. . . . .	62
4.6 Vertical Drop Aided INS Position Navigation State Standard Deviation for Geometry 1. . . . .	63
4.7 Vertical Drop Aided INS Position Navigation State Standard Deviation for Geometry 2. . . . .	63
A.1 2D Unaided INS Velocity Standard Deviations. . . . .	68
A.2 2D Unaided INS Velocity Standard Deviations. . . . .	69
A.3 2D Unaided INS Attitude Standard Deviation. . . . .	69
A.4 2D Unaided INS Attitude Standard Deviation. . . . .	70
A.5 2D Ground Object Position Uncertainty. . . . .	70

A.6	2D Ground Object Position Uncertainty. . . . .	71
B.1	3D Unaided INS Velocity Standard Deviations. . . . .	72
B.2	3D Unaided INS Velocity Standard Deviations. . . . .	73
B.3	3D Unaided INS Attitude Standard Deviation. . . . .	73
B.4	3D Unaided INS Attitude Standard Deviation. . . . .	74
B.5	3D Ground Object Position Uncertainty. . . . .	74
B.6	3D Ground Object Position Uncertainty. . . . .	75
C.1	Vertical Case Unaided INS Velocity Error Standard Deviation. . . . .	76
C.2	Vertical Case Unaided INS Angle Error Standard Deviation. . . . .	77
C.3	Vertical Case Aided INS Velocity Navigation State Standard Deviation For Geometry 1. . . . .	77
C.4	Vertical Case Aided INS Attitude Navigation State Standard Deviation For Geometry 1. . . . .	78
C.5	Vertical Case Ground Object 1 Position Standard Deviation For Geometry 1 . . .	78
C.6	Vertical Case Ground Object 2 Position Standard Deviation For Geometry 1 . . .	79
C.7	Vertical Case Aided INS Velocity Navigation State Standard Deviation For Geometry 2. . . . .	79
C.8	Vertical Case Aided INS Attitude Navigation State Standard Deviation For Geometry 2. . . . .	80
C.9	Vertical Case Ground Object 1 Position Standard Deviation For Geometry 2 . . .	80
C.10	Vertical Case Ground Object 2 Position Standard Deviation For Geometry 2 . . .	81

## List of Tables

Table	Page
4.1 Navigation States Standard Deviations for 2-D Case . . . . .	57
4.2 Navigation States Standard Deviations for 3-D Case . . . . .	62
4.3 Navigation States Standard Deviations for Geometry 1 of Vertical 3-D Case . .	64
4.4 Navigation States Standard Deviations for Geometry 2 of Vertical 3-D Case . .	65

## List of Symbols

Symbol	Page
$\mathbf{C}_b^n$ DCM from Body to Navigation Frame . . . . .	12
$\mathbf{f}$ Specific Force Measured by Accelerometer . . . . .	13
$\mathbf{a}$ Total A/C Acceleration . . . . .	13
$\mathbf{g}$ Specific Gravity Vector . . . . .	13
$(n)$ Indicates Navigation Frame . . . . .	13
$(b)$ Indicates Body Frame . . . . .	13
$f_x^{(b)}$ Specific Force Measured by Longitudinal Accelerometer . . . . .	13
$f_z^{(b)}$ Specific Force Measured by Vertical Accelerometer . . . . .	13
$\theta$ A/C Pitch Angle . . . . .	14
$\star$ Any Angle . . . . .	14
$\dot{\mathbf{V}}$ A/C Acceleration . . . . .	14
$_x$ $x$ Direction . . . . .	14
$_z$ $z$ Direction . . . . .	14
$\mathbf{V}$ A/C Velocity . . . . .	14
$_x$ $x$ Position . . . . .	14
$_z$ $z$ Position . . . . .	14
$\mathbf{A}$ Error State Dynamics Matrix . . . . .	15
$\delta \mathbf{x}$ Navigation Error State Vector . . . . .	15
$\delta \mathbf{u}$ Disturbance Vector . . . . .	15
$\mathbf{g}$ Constant Pull of Gravity . . . . .	15
$\mathbf{a}$ Longitudinal A/C Acceleration . . . . .	15
$t$ Current Time . . . . .	16
$T$ Duration of a Measurement Epoch . . . . .	16
$h$ Height Above Surface of the Earth . . . . .	16

$l$	Discrete Time Step Counter . . . . .	17
$\sigma_a$	Standard Deviation of the Uncertainty of the Accelerometer Bias . . . . .	18
$\sigma_g$	Standard Deviation of the Uncertainty of the Gyroscope Bias . . . . .	18
$\alpha$	Accelerometer Bias Constant . . . . .	19
$\beta$	Gyroscope Bias Constant . . . . .	19
$\xi$	Angle from Longitudinal Body Axis to LOS Vector . . . . .	19
$x_f$	$x$ Coordinate of Ground Feature on Camera Focal Plane . . . . .	19
$f$	Focal Length . . . . .	19
$x_p$	Inertial Frame $x$ Position of ground feature . . . . .	19
$z_p$	Inertial Frame $z$ Position of ground feature . . . . .	19
$\mathbf{C}_n^b$	DCM from Navigation to Body Frame . . . . .	20
$c$	Indicates Calculated Value from INS . . . . .	20
$m$	Indicates a Measured Value . . . . .	21
$\mathbf{H}(l)$	Time Dependent Measurement Matrix . . . . .	22
$u$	Indicates Ground Feature's Position is Unknown . . . . .	22
$k$	Indicates Ground Feature's Position is Known . . . . .	23
$\mathbf{R}$	Measurement Uncertainty . . . . .	25
$\psi$	A/C Yaw Angle . . . . .	27
$\phi$	A/C Roll Angle . . . . .	28
$\delta\Psi$	Angular Errors Vector . . . . .	28
$y_p$	Inertial Frame $y$ Position of Ground Feature . . . . .	34
$y_f$	$y$ Coordinate of Ground Feature on Camera Focal Plane . . . . .	34
$t_{term}$	Time Munition Reaches Terminal Velocity . . . . .	46
$h_{term}$	Munition Altitude When Munition Reaches Terminal Velocity . . . . .	48
$v_{term}$	Munition Terminal Velocity . . . . .	48
$h_{final}$	Altitude For Last Measurement Update . . . . .	55

$\mu$	Angle from Lateral Axis to Ground Feature . . . . .	85
$z_f$	$z^{(b)}$ Coordinate of Ground Feature on Camera Focal Plane for Vertical Case . .	95
$y_{xf}$	$y^{(b)}$ Coordinate of Ground Feature on Camera Focal Plane for Vertical Case . .	97

## List of Abbreviations

Abbreviation	Page
INS	Inertial Navigation Systems . . . . . 1
GPS	Global Positioning System . . . . . 1
SLAM	Simultaneous Localization and Mapping . . . . . 1
LO	Low Observable . . . . . 1
A/C	Aircraft . . . . . 1
HVT	High Value Target . . . . . 1
FOV	Field of View . . . . . 2
DCM	Direction Cosine Matrix . . . . . 12
$c\star$	$\cos \star$ . . . . . 14
$s\star$	$\sin \star$ . . . . . 14
LOS	Line of Sight . . . . . 19
LHS	Left Hand Side . . . . . 20
RHS	Right Hand Side . . . . . 22
FOTSE	First Order Taylor Series Expansion . . . . . 82

# Covariance Analysis of Vision Aided Navigation by Bootstrapping

## 1 Introduction

### 1.1 Background

There are many techniques to provide navigation information. They range from an individual standing on the ground holding a map and looking at his surroundings to modern military aircraft with high quality Inertial Navigation Systems (INS) with Global Positioning System (GPS) providing very precise position and velocity updates. The use of GPS is very prolific in military operations. However, General Schwartz, the Chief of Staff for the United States Air Force, is quoted as saying [4],

“Global positioning has transformed an entire universe of war-fighting capability. Our dependence on precision navigation in time will continue to grow, . . . It seemed critical to me that the joint force reduce its dependence on GPS aid, . . . Our operations cannot grind to a halt for a degraded or denied system, . . . We must . . . proceed to build more resilient systems. . . .”

This paper looks at using vision-aided navigation à la Simultaneous Localization and Mapping (SLAM) to provide a robust navigation solution in environments where GPS may be denied.

### 1.2 Motivation

Consider a Low Observable (LO) aircraft (A/C) carrying a LO munition on a mission into enemy territory to eliminate a relocatable High Value Target (HVT). During the mission briefing the location of the HVT was limited to a small area. The adversary

actively uses anti-GPS technologies, thus denying the precision and accuracy of GPS. The aircraft has a navigation quality INS, but the length of the flight is long enough that the errors produced by the INS are too large for a targeting solution. The pilot needs a better navigation solution, but does not want to inform the enemy of his aircraft's presence by using active navigation techniques, such as radar. The pilot needs a better navigation estimate than the INS alone can provide, but he also needs to maintain the autonomy provided by the INS.

Enter vision aided navigation. The aircraft uses its INS estimate to geolocate ground features, track those features to aid the INS, and using that aided estimate geolocate new features as the original features leave the camera Field of View (FOV). This aiding scheme constrains the error enough to obtain target solution. The munition, with its lower quality INS, uses a similar visual scheme. It looks within the area given during the mission briefing for the HVT. Once it geolocates the HVT, it also geolocates and tracks multiple ground features as it falls. The munition impacts the HVT and the aircraft begins the return trip home without emitting any signal giving away the its location.

### 1.3 Scope

There are several important aspects of visual navigation that will not be discussed in this paper. They include image processing, to include autonomous, without human assistance, feature detection and feature correspondence. It is assumed that autonomous feature detection and tracking are possible, such as by the SIFT image processing algorithm [5] or by the stochastic process set forth in [10].

This paper focuses exclusively on gauging the performance of an inertial navigation system aided by a vision based SLAM during

1. A horizontal flight in two dimensional space
2. A horizontal flight in three dimensional space

### 3. A vertical drop in three dimensional space

The measure of performance will be the uncertainty, or standard deviation, of the navigation states provided by the aided INS. These values will be compared to the uncertainty of the navigation states in the free INS.

#### **1.4 Approach/Methodology**

To document this research, each chapter will begin with a brief overview of the topics discussed in the chapter. Chapter 2 provides background information for the INS, the reference frames used when working with an INS, a brief discussion of SLAM and concludes with recent, relevant research. Chapter 3 shows the mathematical development of the 2-D case, including the dynamics and measurement model development, the state space representation and the use of the Kalman filter mechanization. This information was then extended to look at the 3-D case for both a horizontal flight and a vertical fall. Chapter 4 looks at the results of the covariance analysis. Finally, Chapter 5 summarizes the key points of the paper, focusing on the impact the INS aiding scheme provided. A list of potential follow-on research topics is also provided.

## 2 Literature Review

### 2.1 Overview

This chapter provides foundational information regarding the topics discussed in the following chapter. Section 2.2 discusses the different coordinate frames of reference used in this paper. Section 2.3 discusses the fundamentals of inertial navigation, including a brief discussion of the sensors used and how they work. Section 2.4 discusses SLAM. Finally, Section 2.5 reviews recent research that contributed to this paper.

### 2.2 Reference Frames

*2.2.1 Earth-fixed reference frame.* The Earth-fixed reference frame has its origin fixed to an arbitrary point on the surface of the Earth. The axis  $X_E$  points due North,  $Y_E$  points due east and  $Z_E$  points to the gravitational center of the Earth. This reference frame is shown in Figure 2.1.

*2.2.2 Navigation reference frame.* The navigation frame is a modified version of the Earth-fixed reference frame. The origin of this reference frame is also placed arbitrarily on the surface of the Earth, where  $z = 0$  at the surface of the earth. The only difference between the navigation frame and the Earth-fixed frame is that the axis are rotated 180° about the  $X$  axis. Therefore  $Y_n$  points due west and  $Z_n$  points exactly away from the center of the Earth. This reference frame is shown in Figure 2.2.

*2.2.3 Body-fixed reference frame.* This reference frame has its origin located somewhere on an A/C. Normally the origin is set at the A/C center of gravity to allow the use of the equations of motion. However, as fuel is used during flight, the center of gravity does not remain constant. Therefore in this research, the origin is set at the origin of the camera. The fact that it is “body-fixed” indicates that the axis do not change with respect

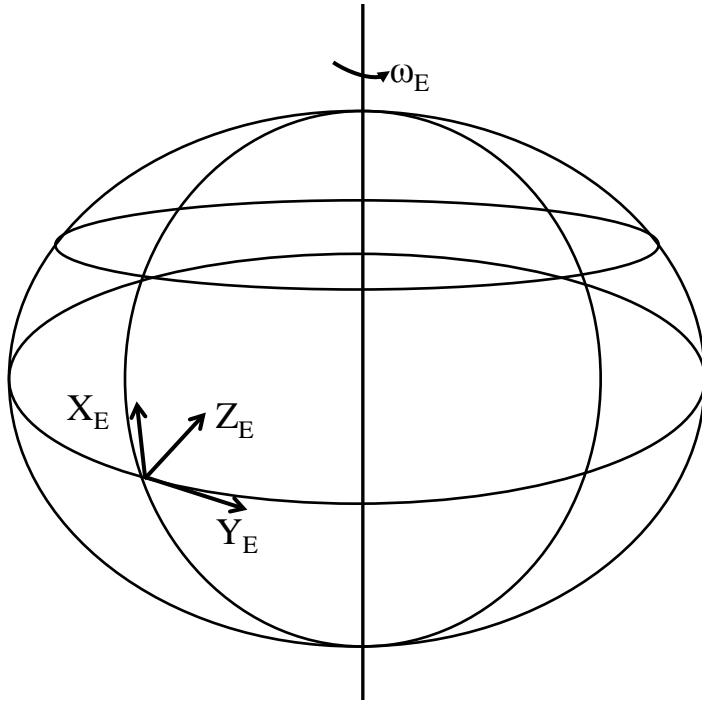


Figure 2.1: Earth-fixed reference frame

to the A/C body as A/C's trajectory changes. Rather, the  $X_b$  axis is the longitudinal axis and typically runs through the nose of the A/C, the  $Y_b$  axis is the lateral axis and runs parallel with the left wing, and the  $Z_b$  axis is the vertical axis and runs out the top of the A/C. This reference frame is shown on a F-35 Lightning II in Figure 2.3

### 2.3 Inertial Navigation

The INS provides the navigation state based on perceived changes in the inertia and moment of inertia of the sensors utilized. These changes are quantified based on Newton's mechanical laws. INSs are used in many vehicle types, including air, sea, ground and space, but the focus in this research will be on air based vehicles. An INS employs a suite of sensors, typically three accelerometers and three gyroscopes, one for each of the body axes, and an onboard computer to compile and integrate the information provided by the

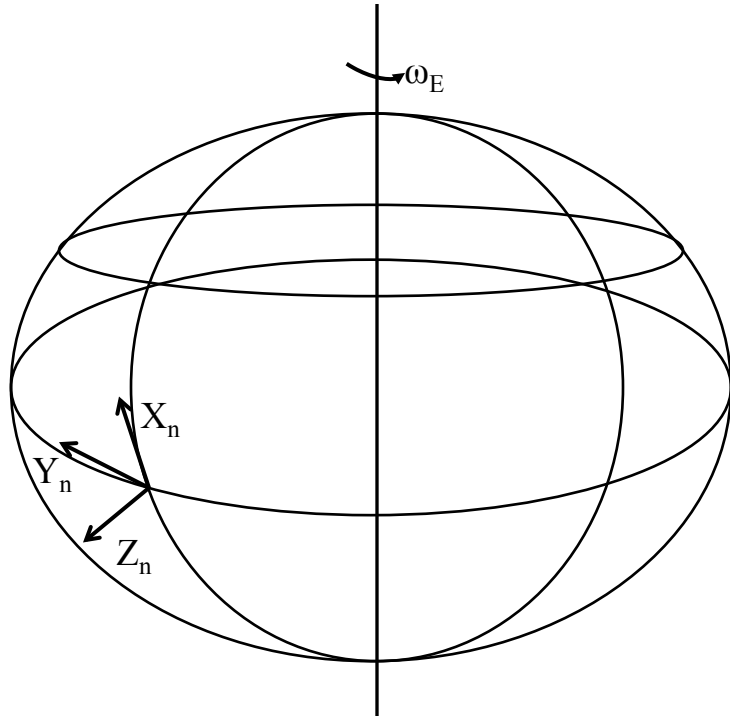


Figure 2.2: Navigation reference frame

sensors. This integrated data provides the operator of the A/C with an estimate of the current navigation state based on the initial navigation state.

An INS is initialized prior to take off using external sources, i.e., GPS for position, pilot setting velocity to zero, and runway markers and levels for the Euler angles. This initialization is critical because all later estimates build upon the initial values. If the starting point for the INS is incorrect, it will only get worse as time goes on. Once initialized, the INS can autonomously provide a navigation state estimate without any external assistance, thus it is unaffected by adversary jamming or atmospheric interference.

The onboard accelerometers indicate translational changes in an A/C's position. They sense acceleration along the A/C's axes. The detected acceleration is integrated to calculate the A/C's velocity, which in turn is integrated to provide position. However, there is no orientation data. As such, if there were no other sensors, the A/C would only

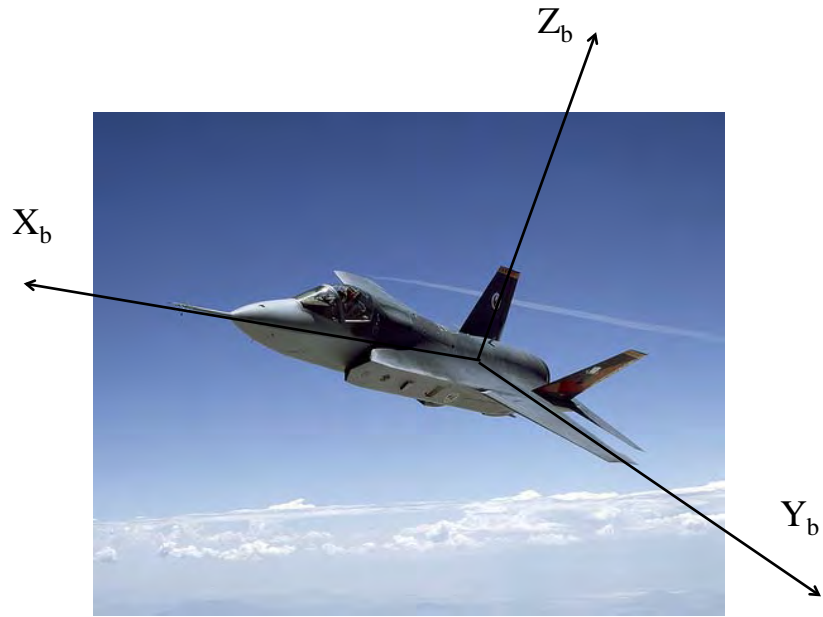


Figure 2.3: Body-fixed reference frame shown on F-35 Lightning II

know how much it moved left or right, forward or backward, and up or down relative to itself. It would be akin to being blindfolded, and placed in a car. One would feel acceleration forward or backward by being pressed into the seat or against the seatbelt, respectively.

Conversely, the gyroscopes indicate rotation rate. Then based on the initialized values, the rotation rate is integrated to determine the A/C's angles. This provides the orientation data that the accelerometers could not provide. However, the gyroscopes cannot detect the magnitude of the translation vector. This would be like being in a car blindfolded. One would feel the turns, and would know the direction of the turn but not how fast the car was traveling outside of the turn.

Both sensors, when operating independently, offer valuable, if incomplete information. It is when the information from both are brought together that a strong navigation state estimate is provided to the user. The translational information combined

with the orientation information takes the data from the body-fixed reference frame and makes it useful by putting it in the navigation, or inertial, reference frame. For example, the sensed movements left or right would translate to calculated movement North or South from the starting location, based on the orientation of the A/C.

The autonomy of the INS does have a major limitation: the sensors are prone to drift and noise. These sensor errors accumulate over time as the readings from the gyroscopes, to include the errors, are integrated into the angles. The accelerometers provide a double dose of the errors because they are integrated twice to calculate the position estimate. These errors cause the INS navigation state estimate to drift over time, with no upper limit to the estimate error. The only way to constrain the error is through an external measurement. Common examples of measurements used are barometric altimeters, GPS, doppler, and, more recently, visual bearings-only measurements.

## 2.4 SLAM

SLAM is a growing topic of interest in the robotics community. It is commonly believed that the ability for a robot to discern its environment and, at the same time, determine its position within the environment is a crucial step to true robotic autonomy [2]. The fundamental issue with SLAM is shown in Figure 2.4 [2].

The typical scenario is that a robot, with some sort of onboard sensor, i.e., laser range finder, camera, sonar etc., is placed in an environment with no a priori information regarding the environment. The robot then begins to probabilistically estimate its own position and that of the ground features around it, typically with some flavor of a Kalman filter. Because the features in the environment are being estimated, each feature adds some number of states to the state vector. The number depends on the type of information being used. For example, in a 2-d case, if the position of the ground feature is being estimated, and the feature is stationary, two states would have been to be concatenated on the end of

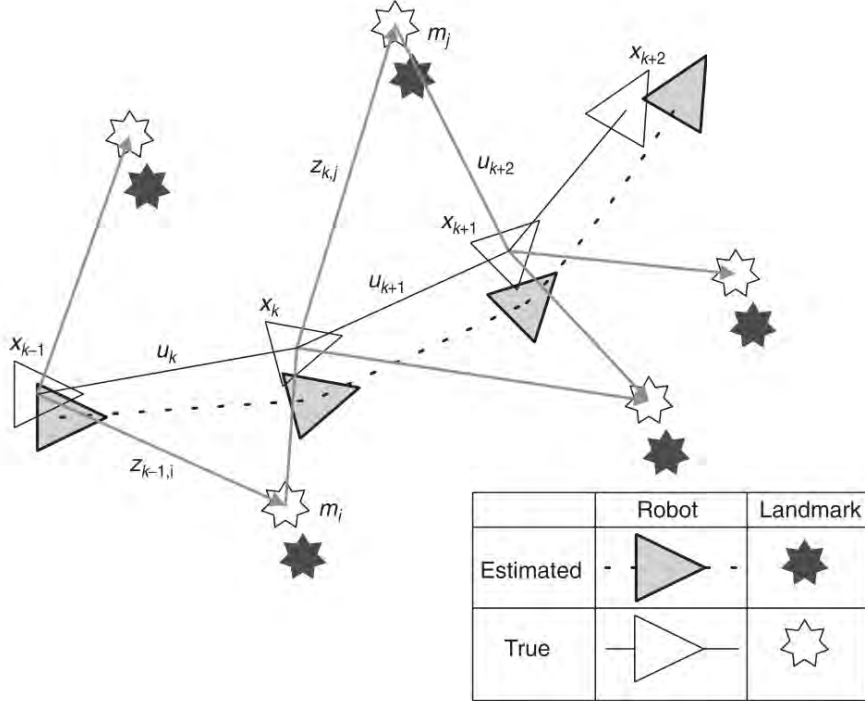


Figure 2.4: This shows fundamental problem of how the vehicle must estimate its own position at the same time that it is estimating the position of the features used for tracking. Neither position is ever truly known[2].

the state vector. In a 3-d case, for a moving feature, six states would have to be added to the state vector. This has potential to create a very large state vector quickly, which, depending on the filtering method used, can become computationally burdensome [2].

Feature recognition and tracking is crucial to SLAM. If the robot cannot track or correlate features from one update to the next, it will not be able to build a viable map. At best it would have a series of independent measurements with no way of connecting the dots to see the big picture. It is this aspect of the problem that has been the truly limiting factor for SLAM.

## 2.5 Recent Research

In [8], Pachter et. al explored the concept of using bearings-only visual measurements to aid an INS in three dimensions. It was theoretical work, meaning there

was no simulation or empirical data substantiate the theory. It did however develop the mathematics for observing the angle to a ground feature over time and using that information to update an INS, thus constraining the error.

In [3], Giebner used visual measurements to aid an A/C INS, via Kalman filter, while flying a circular orbit around a single ground feature, both in simulation and in an actual test environment. He found that using visual-measurements reduced the uncertainty of the position of the A/C, in three dimensions after 6 minutes of flight time, from 350 meters, in the unaided INS case, down to 50 meters when combined with barometric altimeter readings.

In [7] observability of a vision-aided INS was explored. The measurements were time dependent due to the fact that the position of the ground feature(s) being tracked, relative to the A/C, changed with time. Because the measurement matrix was time dependent, the observability Grammian was used. It was found that when the INS was only aided by bearings-only visual measurements of a single ground feature, the observability Grammian was rank deficient, thereby indicating incomplete INS aiding action. However, if a second ground feature was simultaneously tracked, the observability Grammian had full rank, thus there was complete INS aiding action; that is that all of the navigation states received some improvement from the measurement when compared to the unaided case.

In [2] a detailed history of SLAM was provided. It also provided fundamental information regarding implementing SLAM with various filter methods. It showed that the uncertainty of detected features, as well as the navigation estimate, will decrease as more measurements are taken. An example was provided where a robot was piloted remotely through an indoor environment. The pilot did not have visual access to the robot. Instead, the pilot navigated based on the map rendered by the robot. The robot then autonomously returned to the starting point. Other examples were provided as well.

In [1] an algorithm for single a camera to perform SLAM in real time, called MonoSLAM, was developed. The authors were concerned with mapping and localizing a small area. They found that even in a feature sparse environment they could build a map of points and eliminate drift once the robot began tracking a previously tracked feature. MonoSLAM was then used on a humanoid robot fitted with three cameras walking in a circle. They found, until the robot tracked a previously tracked feature, the feature uncertainty continued to grow. However, once features came back into view, the uncertainty stopped growing. They concluded that a robot would be able to repeat the task indefinitely without any drift in the localization accuracy.

### 3 Methodology

#### 3.1 Introduction

This chapter is broken up into three main sections. Section 3.2 discusses the two-dimensional case, including the error dynamics model development, calibrating the unaided INS, measurement model development and how the calculations were accomplished. Section 3.3 will cover the same topics as Section 3.2, but for the three-dimensional case where the A/C is flying wings level, constant altitude with its longitudinal axis aligned with the  $X_n$  axis and small angle assumptions are valid for the A/C's Euler angles. The Section 3.4 will expand on Section 3.3 for the vertical free fall case where all the body axes are still aligned with the navigation axes. Development of the general form, where small angle assumptions are not used on the A/C's Euler angles, of the dynamics model is shown in Appendix D, and the development of the general form of the measurement model is shown in Appendix E.

#### 3.2 Two-Dimensional Case

The two-dimensional case is the simpler of the two cases, and, as such, is the advantageous place to start. This research will start with the development of the dynamics model, which is the error state equations.

*3.2.1 Dynamics Error Model.* The navigation frame is the “inertial” ( $X_n, Z_n$ ) frame and the A/C body axes are ( $X_b, Z_b$ ). The A/C's position is ( $x, z$ ) and  $\theta$  is the pitch angle. A strapdown [9] INS arrangement is considered. When flying in the vertical plane of a non-rotating flat Earth as shown in Figure 3.1, the reference frames can be related by the Direction Cosine Matrix (DCM),  $\mathbf{C}_b^n$  [9]:

$$\mathbf{C}_b^n = \begin{bmatrix} \cos \theta & \sin \theta \\ -\sin \theta & \cos \theta \end{bmatrix} \quad (3.1)$$

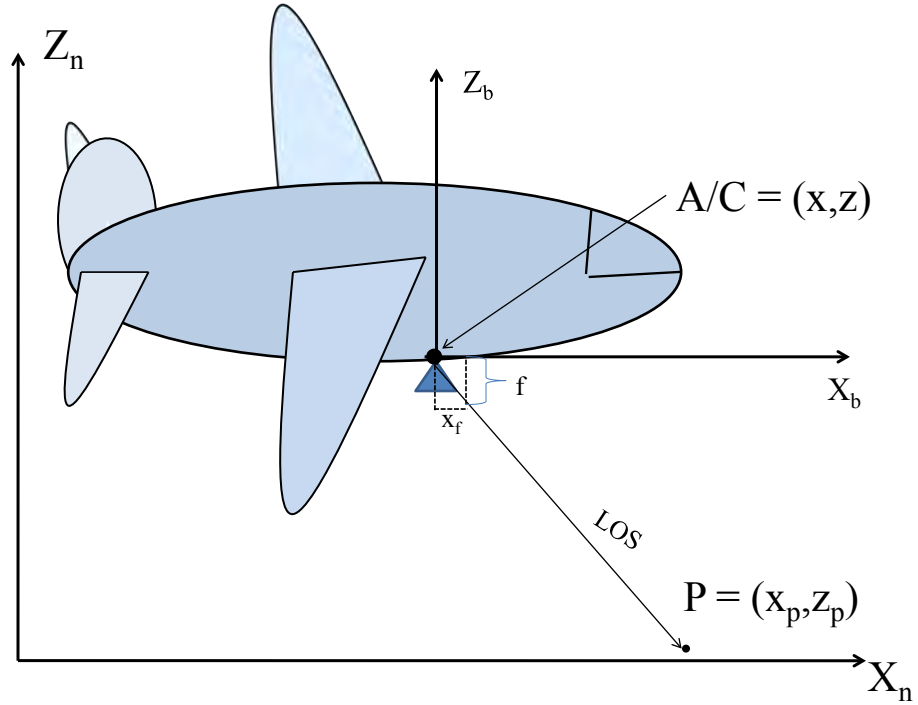


Figure 3.1: The A/C in the vertical plane. Notice that the origin of the body frame is at the camera.

The specific force,  $\mathbf{f}$  measured by an accelerometer is

$$\mathbf{f} = \mathbf{a} - \mathbf{g} \quad (3.2)$$

where  $\mathbf{a}$  is the A/Cs acceleration and  $\mathbf{g}$  is the Earth's gravitational force. The specific force resolved in the inertial frame is

$$\begin{bmatrix} f_x^{(n)} \\ f_z^{(n)} \end{bmatrix} = \mathbf{C}_b^n \begin{bmatrix} f_x^{(b)} \\ f_z^{(b)} \end{bmatrix}$$

$$f_x^{(n)} = f_x^{(b)} \cos\theta + f_z^{(b)} \sin\theta$$

$$f_z^{(n)} = -f_x^{(b)} \sin\theta + f_z^{(b)} \cos\theta$$

where the superscript indicates which frame of reference is being used, <sup>(n)</sup> for the inertial navigation frame frame and <sup>(b)</sup> for the body frame,  $f_x^{(b)}$  and  $f_z^{(b)}$  are the specific forces

measured by the longitudinal and vertical accelerometers, respectively, and  $\theta$  is the pitch angle. In an effort to conserve space, which is necessary in subsequent sections,  $\cos(\star)$  and  $\sin(\star)$  will be abbreviated with  $c\star$  and  $s\star$  respectively, where  $\star$  can be any angle.

The specific forces are fed into the states by

$$\begin{aligned}\dot{V}_x^{(n)} &= f_x^{(n)} + g_x^{(n)} \\ \dot{V}_z^{(n)} &= f_z^{(n)} + g_z^{(n)}\end{aligned}$$

and

$$V_x^{(n)} = \dot{x}^{(n)}$$

$$V_z^{(n)} = \dot{z}^{(n)}$$

$$\omega = \dot{\theta}$$

where  $\dot{V}$  is the acceleration of the A/C with the subscripts  $x$  and  $z$  indicating which direction. The A/C's acceleration is integrated to determine its  $x$  and  $z$  velocity,  $V$ , which produces the respective positions  $x$  and  $z$  by a second integration.

However, the sensors have uncertainty, so these equations must be perturbed using a first order Taylor series expansion. This produces

$$\begin{aligned}\delta f_x^{(n)} &= (-f_x^{(b)} \sin \theta + f_z^{(b)} \cos \theta) \delta \theta + \delta f_x^{(b)} \cos \theta + \delta f_z^{(b)} \sin \theta \\ &= f_z^{(n)} \delta \theta + \delta f_x^{(b)} \cos \theta + \delta f_z^{(b)} \sin \theta\end{aligned}\tag{3.3}$$

and

$$\begin{aligned}\delta f_z^{(n)} &= (-f_x^{(b)} \cos \theta - f_z^{(b)} \sin \theta) \delta \theta - \delta f_x^{(b)} \sin \theta + \delta f_z^{(b)} \cos \theta \\ &= -f_x^{(n)} \delta \theta - \delta f_x^{(b)} \sin \theta + \delta f_z^{(b)} \cos \theta\end{aligned}\tag{3.4}$$

where  $\delta f_x^{(b)}$  and  $\delta f_z^{(b)}$  are the errors of the accelerometers. Thus the error equations are formed

$$\delta \dot{x}^{(n)} = \delta V_x^{(n)} \quad (3.5)$$

$$\delta \dot{z}^{(n)} = \delta V_z^{(n)} \quad (3.6)$$

$$\delta \dot{V}_x^{(n)} = \delta f_x^{(n)} \quad (3.7)$$

$$\delta \dot{V}_z^{(n)} = \delta f_z^{(n)} \quad (3.8)$$

$$\delta \dot{\theta} = \delta \omega \quad (3.9)$$

and substituting Eqs. (3.3)-(3.4) into Eqs. (3.7)-(3.8) yields

$$\delta \dot{V}_x^{(n)} = f_z^{(n)} \delta \theta + \delta f_x^{(b)} \cos \theta + \delta f_z^{(b)} \sin \theta \quad (3.10)$$

$$\delta \dot{V}_z^{(n)} = -f_x^{(n)} \delta \theta - \delta f_x^{(b)} \sin \theta + \delta f_z^{(b)} \cos \theta \quad (3.11)$$

Eqs. (3.5), (3.6), (3.9), (3.10) and (3.11) are the INS error equations when flying wings level over a flat and non-rotating Earth. The error equations are shown in state space notation as,  $\delta \dot{\mathbf{x}} = \mathbf{A} \delta \mathbf{x} + \mathbf{\Gamma} \delta \mathbf{u}$ , where  $\mathbf{A}$  is the error state dynamics matrix, the navigation state's error vector,  $\delta \mathbf{x}$  is

$$\delta \mathbf{x} = [ \delta x \ \delta z \ \delta V_x \ \delta V_z \ \delta \theta ]^T \quad (3.12)$$

and the disturbances,  $\delta \mathbf{u}$ , are the two accelerometers' and the rate gyroscope's biases

$$\delta \mathbf{u} = [ \delta f_x^{(b)} \ \delta f_z^{(b)} \ \delta \omega ]^T \quad (3.13)$$

For this case the trajectory is assumed to be a wings level, constant altitude flight, therefore the nominal variables are  $\theta = 0$ ,  $f_z^{(n)} = g$  and  $f_x^{(n)} = a$ , where  $g$  is the acceleration of gravity and  $a$  is the longitudinal acceleration of the A/C. These variables are non-dimensionalized in order to maintain geometry and remove any issues where the units

may not coincide. They are nondimensionalized as follows

$$\begin{aligned} x &\rightarrow \frac{x}{h} & z &\rightarrow \frac{z}{h} & V_x &\rightarrow \frac{v_x}{v} \\ V_z &\rightarrow \frac{v_z}{v} & t &\rightarrow t \frac{v}{h} & T &\rightarrow T \frac{v}{h} \\ \delta f_x &\rightarrow \frac{\delta f_x}{g} & \delta f_z &\rightarrow \frac{\delta f_z}{g} & \delta \omega &\rightarrow h \frac{\delta \omega}{v} \end{aligned}$$

where  $t$  is the current time,  $T$  is the duration of a measurement epoch and  $h$  is the above ground level altitude. The non-dimensional parameters are

$$g \triangleq \frac{hg}{v^2} \quad \text{and} \quad a \triangleq \frac{ha}{v^2}$$

If, for example,

$$h = 1000[m], \quad v = 100 \left[ \frac{m}{sec} \right], \quad g = 10 \left[ \frac{m}{sec^2} \right]$$

the non-dimensional parameter  $g = 1$ . Therefore, the INS error state equations are

$$\delta \dot{\mathbf{x}} = \begin{bmatrix} 0 & 0 & 1 & 0 & 0 \\ 0 & 0 & 0 & 1 & 0 \\ 0 & 0 & 0 & 0 & g \\ 0 & 0 & 0 & 0 & -a \\ 0 & 0 & 0 & 0 & 0 \end{bmatrix} \delta \mathbf{x} + \begin{bmatrix} 0 & 0 & 0 \\ 0 & 0 & 0 \\ 1 & 0 & 0 \\ 0 & 1 & 0 \\ 0 & 0 & 1 \end{bmatrix} \delta \mathbf{u} \quad (3.14)$$

and with perfect INS alignment

$$\delta \mathbf{x}(0) = \mathbf{0}, \quad 0 \leq t \leq T$$

The nondimensional duration of a measurement session, or epoch, is  $T = 1$ .

It is assumed that the sensor errors are Gaussian distributed, constant biases. This allows the state error vector to be augmented with the vector  $\mathbf{u}$ ; the augmented state is

$$\delta \mathbf{x}_a = \begin{bmatrix} \delta \mathbf{x} \\ \dots \\ \delta \mathbf{u} \end{bmatrix}_{8 \times 1} \quad (3.15)$$

and the  $\mathbf{A}$  matrix is augmented by the  $\mathbf{\Gamma}$  matrix, as shown

$$\mathbf{A}_a = \begin{bmatrix} \mathbf{A} & \mathbf{\Gamma} \\ \mathbf{0}_{3 \times 5} & \mathbf{0}_{3 \times 3} \end{bmatrix}_{8 \times 8} \quad (3.16)$$

When converted to discrete time  $\mathbf{A}_a \rightarrow \mathbf{A}_{ad} = e^{\mathbf{A}_a \Delta t}$ .

$$\mathbf{A}_{ad} = \begin{bmatrix} 1 & 0 & \Delta t & 0 & \frac{g\Delta t^2}{2} & \frac{\Delta t^2}{2} & 0 & \frac{g\Delta t^3}{6} \\ 0 & 1 & 0 & \Delta t & -\frac{a\Delta t^2}{2} & 0 & \frac{\Delta t^2}{2} & -\frac{a\Delta t^3}{6} \\ 0 & 0 & 1 & 0 & g\Delta t & \Delta t & 0 & \frac{g\Delta t^2}{2} \\ 0 & 0 & 0 & 1 & -a\Delta t & 0 & \Delta t & -\frac{a\Delta t^2}{2} \\ 0 & 0 & 0 & 0 & 1 & 0 & 0 & \Delta t \\ 0 & 0 & 0 & 0 & 0 & 1 & 0 & 0 \\ 0 & 0 & 0 & 0 & 0 & 0 & 1 & 0 \\ 0 & 0 & 0 & 0 & 0 & 0 & 0 & 1 \end{bmatrix} \quad (3.17)$$

where  $\Delta t$  is the sampling period. The discrete time state dynamics become

$$\delta \mathbf{x}_a(l+1) = \mathbf{A}_{ad} \delta \mathbf{x}_a(l), \quad l = 0, \dots, N-1 \quad (3.18)$$

where  $l$  is the discrete time step counter and the non-dimensional period between steps is  $\Delta T = \frac{T}{N} = \Delta t \frac{v}{h}$ . Setting  $a$  to zero (assume a constant cruise speed) simplifies the dynamics to

$$\mathbf{A}_{ad} = \begin{bmatrix} 1 & 0 & \Delta t & 0 & \frac{g\Delta t^2}{2} & \frac{\Delta t^2}{2} & 0 & \frac{g\Delta t^3}{6} \\ 0 & 1 & 0 & \Delta t & 0 & 0 & \frac{\Delta t^2}{2} & 0 \\ 0 & 0 & 1 & 0 & g\Delta t & \Delta t & 0 & \frac{g\Delta t^2}{2} \\ 0 & 0 & 0 & 1 & 0 & 0 & \Delta t & 0 \\ 0 & 0 & 0 & 0 & 1 & 0 & 0 & \Delta t \\ 0 & 0 & 0 & 0 & 0 & 1 & 0 & 0 \\ 0 & 0 & 0 & 0 & 0 & 0 & 1 & 0 \\ 0 & 0 & 0 & 0 & 0 & 0 & 0 & 1 \end{bmatrix}$$

This dynamics equation applies as long as the ground features' positions are known.

Assuming the ground features are stationary, but their position is not known, an additional state must be added for each tracked ground feature whose position is estimated. In our two dimensional scenario, if the number of ground features being tracked is  $n$ , then the augmented navigation state is

$$\delta \mathbf{x}_a := \begin{bmatrix} \delta \mathbf{x}_a \\ \vdots \\ \delta x_{p1} \\ \vdots \\ \delta x_{pn} \end{bmatrix}_{(8+n) \times 1} \quad (3.19)$$

and

$$\mathbf{A}_{ad} := \begin{bmatrix} \mathbf{A}_a & \mathbf{0}_{8 \times n} \\ \mathbf{0}_{n \times 8} & \mathbf{I}_{n \times n} \end{bmatrix}_{(8+n) \times (8+n)} \quad (3.20)$$

On one hand, state augmentation reduces the degree of observability, which decreases the strength of INS aiding action. On the other hand, however, the inclusion of additional features to be tracked helps wash out the measurement error.

**3.2.2 Modeling/Calibrating the Free INS.** With the dynamics from Subsection 3.2.1, the values for  $\sigma_a$  and  $\sigma_g$ , the uncertainty in the bias of the accelerometers and gyroscope, respectively, are set such that the free INS is a  $1 \frac{km}{hr}$  navigation system; a non-dimensional hour is 360 non-dimensional seconds. There are  $N = 100$  discrete steps in a non-dimensional second. The calibration is performed by using the solution to the Lyapunov difference equation

$$\mathbf{P}(l+1) = \mathbf{A}_{ad} \mathbf{P}(l) \mathbf{A}_{ad}^T, \quad 0 \leq l \leq 360N - 1 \quad (3.21)$$

with

$$\mathbf{P}(\mathbf{0}) = \begin{bmatrix} \mathbf{0}_{5 \times 5} & \mathbf{0}_{5 \times 1} & \mathbf{0}_{6 \times 1} & \mathbf{0}_{7 \times 1} \\ \mathbf{0}_{1 \times 5} & \sigma_a^2 & \vdots & \vdots \\ \mathbf{0}_{1 \times 6} & \dots & \sigma_a^2 & \vdots \\ \mathbf{0}_{1 \times 7} & \dots & \dots & \sigma_g^2 \end{bmatrix}_{8 \times 8} \quad (3.22)$$

There is a linear relationship between the uncertainty in the A/C's  $x$  position and the uncertainty in the sensors' biases

$$P_{1,1}(360N) = \alpha\sigma_a^2 + \beta\sigma_g^2 \quad (3.23)$$

where the coefficients  $\alpha$  and  $\beta$  are constants. Therefore, Eq. (3.21) was solved for one non-dimensional hour twice to calculate the values of the constants. The first time,  $\sigma_a$  was set to 1 and  $\sigma_g$  was set to 0. The second time,  $\sigma_a$  was set to 0 and  $\sigma_g$  was set to 1. Then assigning the errors in the accelerometers and the error in the gyroscope an equal role in the uncertainty of the A/C's position, the values for the variances of the sensors' biases variances are

$$\sigma_a = \frac{1}{\sqrt{2\alpha}} = 1.0912 \times 10^{-5} \quad (3.24)$$

$$\sigma_g = \frac{1}{\sqrt{2\beta}} = 9.0935 \times 10^{-8} \quad (3.25)$$

*3.2.3 Measurement Model.* Based on the geometry established in Subsection 3.2.1, the foundational relationship between the visual measurements and the ground feature's position is created

$$\tan \xi = \frac{x_f}{f} = \frac{(x_p - x)^{(b)}}{(z_p - z)^{(b)}} \quad (3.26)$$

where  $\xi$  is the angle between the longitudinal body axis and the Line of Sight (LOS) vector, which runs from the origin of the body axis to the ground feature,  $x_f$  is the projection of the ground feature's position onto the camera's focal plane,  $f$  is the focal length of the camera, and  $x_p$  and  $z_p$  are  $x$  and  $z$  coordinates, respectively, of the ground

feature. The relationship of the body coordinates to the navigation is shown by the DCM  $\mathbf{C}_n^b$ , where

$$\mathbf{C}_n^b = \begin{bmatrix} \cos\theta & -\sin\theta \\ \sin\theta & \cos\theta \end{bmatrix} \quad (3.27)$$

thus

$$\begin{aligned} \begin{bmatrix} x_p - x \\ z_p - z \end{bmatrix}^{(b)} &= \mathbf{C}_n^b \begin{bmatrix} x_p - x \\ z_p - z \end{bmatrix}^{(n)} \\ &= \begin{bmatrix} \cos\theta & -\sin\theta \\ \sin\theta & \cos\theta \end{bmatrix} \begin{bmatrix} x_p - x \\ z_p - z \end{bmatrix}^{(n)} \\ &= \begin{bmatrix} (x_p - x)^{(n)} \cos\theta + (z_p - z)^{(n)} \sin\theta \\ (x_p - x)^{(n)} \sin\theta - (z_p - z)^{(n)} \cos\theta \end{bmatrix} \end{aligned} \quad (3.28)$$

The projected position is nondimensionalized such that

$$x_f \rightarrow \frac{x_f}{f}$$

Assuming the ground feature is on the ground, combined with the non-dimensionalization shown above, simplifies Eq. (3.26) to

$$x_f = \frac{(x_p - x)^{(n)} \cos\theta + (z_p - z)^{(n)} \sin\theta}{(x_p - x)^{(n)} \sin\theta - (z_p - z)^{(n)} \cos\theta}$$

It should be noted that for the remainder of this subsection all coordinates will be in the navigation frame. As such, the  $^{(n)}$  will be dropped.

Moving everything to the Left Hand Side (LHS) yields

$$x_f[(x_p - x) \cos\theta + (z_p - z) \sin\theta] + (x_p - x) \sin\theta - (z_p - z) \cos\theta = 0 \quad (3.29)$$

The INS provides the “calculated” navigation state  $[x_c \ z_c \ v_{xc} \ v_{zc} \ \theta_c]^T$ , where  $c$  indicates the calculated value provided by the INS. However, the true values of the states

and measurements are not known. The following perturbations hold

$$\begin{aligned} x_c &= x + \delta x & z_c &= z + \delta z \\ \theta_c &= \theta + \delta \theta & x_{pc} &= x_p + \delta x_p & x_{fm} &= x_f + \delta x_f \end{aligned}$$

where  $_m$  indicates a measured valued. By way of the trigonometric addition formula and small angle approximation, the sin and cos terms simplify to

$$\sin(\theta_c - \delta \theta) = \sin \theta_c - (\sin \theta_c + \cos \theta_c) \delta \theta \quad \cos(\theta_c - \delta \theta) = \cos \theta_c + (\sin \theta_c - \cos \theta_c) \delta \theta$$

Substituting the perturbations into Equation 3.29, yields

$$\begin{aligned} (x_{fm} - \delta x_f) [(\sin \theta_c - (\sin \theta_c + \cos \theta_c) \delta \theta)((x_{pc} - x_c) + \delta x - \delta x_p) - (\cos \theta_c + (\sin \theta_c - \cos \theta_c) \delta \theta)(z_c - \delta z)] \\ - (\cos \theta_c + (\sin \theta_c - \cos \theta_c) \delta \theta)((x_{pc} - x_c) + \delta x - \delta x_p) - (\sin \theta_c - (\sin \theta_c + \cos \theta_c) \delta \theta)(z_c - \delta z) = 0 \end{aligned} \quad (3.30)$$

To simplify the algebra, the LHS will be broken up into components such that

$$A_{comp} = (\sin \theta_c - (\sin \theta_c + \cos \theta_c) \delta \theta)((x_{pc} - x_c) + \delta x - \delta x_p) - (\cos \theta_c + (\sin \theta_c - \cos \theta_c) \delta \theta)(z_c - \delta z) \quad (3.31)$$

$$B_{comp} = -(\cos \theta_c + (\sin \theta_c - \cos \theta_c) \delta \theta)((x_{pc} - x_c) + \delta x - \delta x_p) - (\sin \theta_c - (\sin \theta_c + \cos \theta_c) \delta \theta)(z_c - \delta z) \quad (3.32)$$

such that

$$(x_{fm} - \delta x_f) A_{comp} + B_{comp} = 0 \quad (3.33)$$

The terms within the components need to be distributed out. When two small errors are multiplied together, their product is considered negligible. As such, the component terms become

$$\begin{aligned} A_{comp} &= \sin \theta_c (x_{pc} - x_c) - \cos \theta_c z_c + \delta x \sin \theta_c + \delta z \cos \theta_c \\ &\quad - \delta \theta ((\sin \theta_c + \cos \theta_c)(x_{pc} - x_c) + (\sin \theta_c - \cos \theta_c)z_c) - \delta x_p \sin \theta_c \end{aligned} \quad (3.34)$$

and

$$\begin{aligned} B_{comp} &= -\sin \theta_c z_c - \cos \theta_c (x_{pc} - x_c) - \delta x \cos \theta_c + \delta z \sin \theta_c + \delta x_p \cos \theta_c \\ &\quad + \delta \theta ((\sin \theta_c + \cos \theta_c)z_c) + \delta x_p \cos \theta_c \end{aligned} \quad (3.35)$$

Substituting Eqs. (3.34)-(3.35) into Eq. (3.33) and collecting like error terms yields

$$\begin{aligned}
& x_{fm}(s\theta_c(x_{pc}-x_c) - c\theta_c z_c) - s\theta_c z_c - c\theta_c(x_{pc}-x_c) - \delta x_f(s\theta_c(x_{pc}-x_c) - c\theta_c z_c) \\
& + \delta x(s\theta_c x_{fm} - c\theta_c) + \delta z(s\theta_c + c\theta_c x_{fm}) + \delta x_p(c\theta_c - s\theta_c x_{fm}) \\
& + \delta\theta[(s\theta_c + c\theta_c)z_c - (s\theta_c - c\theta_c)(x_{pc}-x_c) - ((s\theta_c + c\theta_c)(x_{pc}-x_c) + (s\theta_c - c\theta_c)z_c)x_{fm}] = 0
\end{aligned} \tag{3.36}$$

Moving the error terms to the Right Hand Side (RHS) yields

$$\begin{aligned}
& x_{fm}(s\theta_c(x_{pc}-x_c) - c\theta_c z_c) - s\theta_c z_c - c\theta_c(x_{pc}-x_c) = \delta x_f(s\theta_c(x_{pc}-x_c) - c\theta_c z_c) \\
& + \delta x(c\theta_c - s\theta_c x_{fm}) - \delta z(s\theta_c + c\theta_c x_{fm}) - \delta x_p(c\theta_c - s\theta_c x_{fm}) \\
& - \delta\theta[(s\theta_c + c\theta_c)z_c - (s\theta_c - c\theta_c)(x_{pc}-x_c) - ((s\theta_c + c\theta_c)(x_{pc}-x_c) + (s\theta_c - c\theta_c)z_c)x_{fm}]
\end{aligned} \tag{3.37}$$

On the RHS, the nominal value of the states and the measurement are substituted in for the calculated and measured values such that

$$\begin{aligned}
& x_{fm}(c\theta_c z_c - s\theta_c(x_{pc}-x_c)) + (s\theta_c z_c - c\theta_c(x_{pc}-x_c)) = \delta x_f(s\theta(x_p - x) - c\theta z) \\
& + \delta x(c\theta - s\theta x_f) - \delta z(s\theta + c\theta x_f) - \delta x_p(c\theta - s\theta x_f) \\
& - \delta\theta[(s\theta + c\theta)z - (s\theta - c\theta)(x_p - x) - ((s\theta - c\theta)z + (s\theta + c\theta)(x_p - x))x_f]
\end{aligned} \tag{3.38}$$

For the scenario laid out at the beginning of this section,  $z = h$ , which gives it a value of 1 when nondimensionalized according to Subsection 3.2.1,  $\theta = 0$  and  $x_f = -(x_p - x)$ .

Therefore the measurement matrix,  $\mathbf{H}(l)$  for a single unknown ground feature is

$$\mathbf{H}_u(l) = \begin{bmatrix} 1 & x_p - x(l) & 0 & 0 & 2(x_p - x(l)) - (x_p - x(l))^2 - 1 & 0 & 0 & 0 & -1 \end{bmatrix} \tag{3.39}$$

where  $_u$  indicates that the position of the ground feature used is unknown. The nondimensional measurement error is  $\delta x_f$ . However, in order to achieve full aiding [7] two ground features are always used. For the first measurement epoch both ground features have a known position, for the second epoch there is one ground feature position that is known and one that is not, and for the remainder of the measurement epochs both

ground feature positions are unknown. The transition between epochs and the values for  $x(l)$  and  $x_p$  will be discussed more in Subsection 3.2.6.

For the case where both ground points are known,  $\mathbf{H}$  simplifies to

$$\mathbf{H}_{kk}(l) = \begin{bmatrix} 1 & x_{p1} - x(l) & 0 & 0 & 2(x_{p1} - x(l)) - (x_{p1} - x(l))^2 & 0 & 0 & 0 \\ 1 & x_{p2} - x(l) & 0 & 0 & 2(x_{p2} - x(l)) - (x_{p2} - x(l))^2 & 0 & 0 & 0 \end{bmatrix} \quad (3.40)$$

where  $_k$  indicates that the position of the ground feature used is known. When there are two subscripts, as will always be the case, the first subscript is for the ground feature closer to the A/C and the second subscript for the feature further away. When one ground feature position is known and the other is not,  $\mathbf{H}$  becomes

$$\mathbf{H}_{ku}(l) = \begin{bmatrix} 1 & x_{p1} - x(l) & 0 & 0 & 2(x_{p1} - x(l)) - (x_{p1} - x(l))^2 & 0 & 0 & 0 & 0 \\ 1 & x_{p2} - x(l) & 0 & 0 & 2(x_{p2} - x(l)) - (x_{p2} - x(l))^2 & 0 & 0 & 0 & -1 \end{bmatrix} \quad (3.41)$$

Finally for the case where both ground features are unknown,  $\mathbf{H}$  is

$$\mathbf{H}_{uu} = \begin{bmatrix} 1 & x_{p1} - x(l) & 0 & 0 & 2(x_{p1} - x(l)) - (x_{p1} - x(l))^2 & 0 & 0 & 0 & -1 & 0 \\ 1 & x_{p2} - x(l) & 0 & 0 & 2(x_{p2} - x(l)) - (x_{p2} - x(l))^2 & 0 & 0 & 0 & 0 & -1 \end{bmatrix} \quad (3.42)$$

**3.2.4 Initialization.** It is stipulated that, initially, the INS has zero error in the navigation states, that is, the alignment was perfect, and the states representing the biases in the sensors are

$$\delta f_x^{(b)} \sim N(0, \sigma_a^2) \quad \delta f_z^{(b)} \sim N(0, \sigma_a^2) \quad \delta \omega \sim N(0, \sigma_g^2)$$

The  $x$  and  $z$  accelerometers are of the same quality. Thus

$$\delta \mathbf{x}(\mathbf{0}) \sim N(\mathbf{0}, \mathbf{P}(0))$$

with the initial covariance matrix,  $\mathbf{P}(0)$  given by Eq. (3.22).

**3.2.5 Performance of Aided INS.** The cross country flight scenario is shown in Figure 3.2. The A/C is flying wings-level, at a constant speed. It is assumed that the

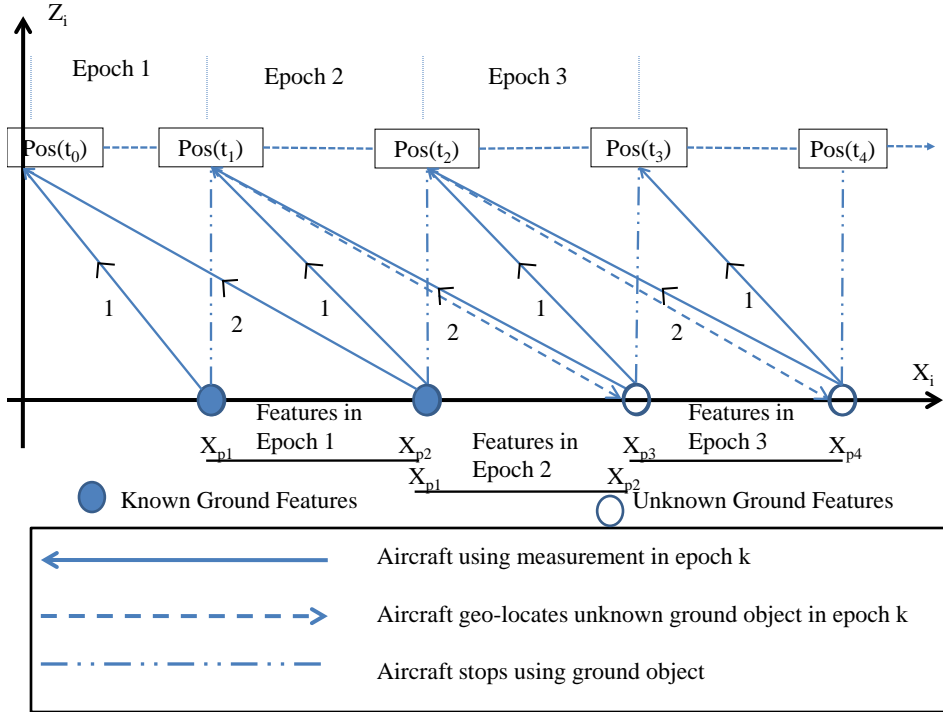


Figure 3.2: Initially the two ground features' position is known, but in the second epoch there is one known and one unknown ground feature, where the unknown feature's position was estimated by the A/C at the end of the first epoch. From epoch 3 onward both ground features' locations are not exactly known.

ground features are equally spaced one kilometer apart, and that the A/C starts one kilometer behind and above the first known ground feature. In the observation matrices

$$x_{f1} = 1 - t$$

$$x_{f2} = 2 - t$$

**3.2.6 Transitioning Between Measurement Epochs.** For the purpose of covariance analysis, and because the features were equally spaced, and it took exactly one measurement epoch for the A/C to fly from directly over one ground feature to directly over the next ground feature, the relative position of the ground features to A/C was the

same at the beginning of each measurement. Therefore the universal positions of the A/C and the ground features are not considered. After non-dimensionalization and discretization the position of the A/C relative to its location at the beginning of a measurement epoch is

$$x(l) = l\Delta t, \quad 0 \leq l \leq N - 1 \quad (3.43)$$

where  $l$  is the discrete time counter within a measurement epoch, and that at the beginning of each epoch  $l$  starts back over at 0. There are 360 epochs to be considered. Each epoch's duration is 1 non-dimensional second and in each epoch  $N = 100$  bearing measurements of a ground feature are taken. With the exception of the first and last ground feature, all the ground features are used for measurements in two time blocks/measurement epochs. Throughout the entirety of the calculations  $x_{p1} = 1$  and  $x_{p2} = 2$ . At the transition point between epochs, the old  $x_{p2}$  becomes the new  $x_{p1}$  and a new  $x_{p2}$  is acquired.

Initially, both ground features used for measurements were known. Therefore, in the first epoch the measurement matrix  $\mathbf{H}_{kk}(l)$ , and the dynamics matrix  $\mathbf{A}_{ad8\times 8}$  were used. In the first epoch, the uncertainty of the states was propagated for one hundred steps using the covariance propagate and update equations of the Kalman filter [6]

$$\mathbf{P}(l + 1)^- = \mathbf{A}_{ad}\mathbf{P}(l)^+\mathbf{A}_d \quad (3.44)$$

$$\mathbf{K} = \mathbf{P}(l + 1)^-\mathbf{H}_{kk}(l)^T \left[ \mathbf{H}_{kk}(l)\mathbf{P}(l + 1)^-\mathbf{H}_{kk}(l)^T + \mathbf{R} \right]^{-1} \quad (3.45)$$

$$\mathbf{P}(l + 1)^+ = (\mathbf{I}_8 - \mathbf{K}\mathbf{H}_{kk}(l))\mathbf{P}(l + 1)^- \quad (3.46)$$

where  $\mathbf{R}$  is the measurement uncertainty caused by ambiguity in the camera pixels

$$\mathbf{R} = \begin{bmatrix} \frac{1}{9} & 0 \\ 0 & \frac{1}{9} \end{bmatrix} \times 10^{-6} \quad (3.47)$$

and the measurement noise

$$\begin{bmatrix} \delta x_{f1} \\ \delta x_{f2} \end{bmatrix} \sim N(0, \mathbf{R})$$

At the conclusion of the first one hundred steps, the first ground feature was dropped from consideration, and a new, unknown ground feature was brought in. Thus the next time block required the use of the new dynamics matrix  $\mathbf{A}_{\text{ad}9 \times 9}$  from Eq. (3.20) and the measurement matrix  $\mathbf{H}_{\text{ku}}(l)$ . The challenging part is to transition the covariance matrix from an  $8 \times 8$  to a  $9 \times 9$  matrix, while including the correct cross-covariance terms. This is done as follows

$$\mathbf{P}(0) = \begin{bmatrix} \mathbf{P}(99)_{8 \times 8} & \mathbf{P}_{(1:8,1)}(99) \\ \mathbf{P}_{(1,1:8)}(99) & \sigma_{\text{new}}^2 \end{bmatrix}_{9 \times 9} \quad (3.48)$$

where  $\sigma_{\text{new}}^2$  is the uncertainty in position of the new ground feature, and it is the uncertainty in the A/C's position at the time the new ground feature is acquired plus the uncertainty of the measurement.

$$\sigma_{\text{new}}^2 = P_{(1,1)}(99) + \sigma_{\xi}^2 \quad (3.49)$$

where  $\sigma_{\xi}^2$  was the uncertainty caused by the error in the LOS angle measurement, and it had a non-dimensional value of  $\frac{4}{9} \times 10^{-6}$ . It is because of the correlation of the errors in the navigation state  $x$  and the new state  $x_{p2}$  that the first row and column from  $\mathbf{P}_{8 \times 8}$  must be transplanted to their respective positions in  $\mathbf{P}_{9 \times 9}$ . Since there is no correlation between the LOS error of the camera and any of the INS navigation or bias states, it is not added to any of the transplanted fields. The covariance matrix is then propagated in the same manner as in the first epoch, following Eqs. (3.44)-(3.46), with the proper substitution of the initial covariance,  $\mathbf{P}(0)_{9 \times 9}$  for  $\mathbf{P}(99)_{8 \times 8}$ , dynamics,  $\mathbf{A}_{\text{ad}9 \times 9}$  for  $\mathbf{A}_{\text{ad}8 \times 8}$ , and measurement matrices,  $\mathbf{H}_{\text{ku}}$  for  $\mathbf{H}_{\text{kk}}$ .

The transition at the beginning of the third epoch from one known/one unknown to two unknown ground features followed the same pattern as incorporating the first unknown ground feature. Now

$$\mathbf{P}(0) = \begin{bmatrix} \mathbf{P}(99)_{9 \times 9} & \mathbf{P}_{(1:9,1)}(99) \\ \mathbf{P}_{(1,1:9)}(99) & \sigma_{\text{new}}^2 \end{bmatrix}_{10 \times 10} \quad (3.50)$$

where

$$\sigma_{new}^2 = P_{(1,1)}(99) + \sigma_\xi^2 \quad (3.51)$$

In the previous epoch, the unknown feature was  $x_{p2}$ , but when it transitioned to  $x_{p1}$  status, all of its cross-covariances went with it. Because  $P_{(9,9)}$  shows the uncertainty of the closest feature to the A/C,  $x_{p1}$ , the entirety of  $\mathbf{P}(99)$  could be directly translated to the upper-diagonal section of the new covariance matrix. Substituting  $\mathbf{H}_{uu}$  for  $\mathbf{H}_{ku}$ , and using the  $\mathbf{A}_{ad}^{10 \times 10}$  dynamics matrix, the covariance was propagated according to Eqs. (3.44)-(3.46). These matrices were used for the remainder of the measurement epochs. The transition becomes more complicated when the A/C completes a time block using two unknown ground features, and begins using a new unknown ground feature. The first step was to remove the ninth row and column of  $\mathbf{P}(99)$ . These values were replaced with the first eight values of the tenth row and column of  $\mathbf{P}(99)$ , as shown

$$\mathbf{P}_{trans} = \begin{bmatrix} \mathbf{P}_{(1:8,1:8)} & \mathbf{P}_{(1:8,10)} \\ \mathbf{P}_{(10,1:8)} & P_{(10,10)} \end{bmatrix}_{9 \times 9} \quad (3.52)$$

This transition matrix was then used to initialize the new state estimation error covariance matrix,  $\mathbf{P}_{10 \times 10}$

$$\mathbf{P}(0) = \begin{bmatrix} \mathbf{P}_{trans} & \mathbf{P}_{trans(1:9,1)} \\ \mathbf{P}_{trans(1,1:9)} & \sigma_{new}^2 \end{bmatrix}_{10 \times 10} \quad (3.53)$$

where

$$\sigma_{new}^2 = P_{(1,1)}(99) + \sigma_\xi^2 \quad (3.54)$$

Starting at epoch 4, the transitions for the remainder of the epochs followed Eqs. (3.52)-(3.54) from epoch 3, because there are no more known ground features.

### 3.3 Three-Dimensional Horizontal Case

*3.3.1 Dynamics.* The navigation frame is the “inertial”  $(X_n, Y_n, Z_n)$  frame and the A/C body axes are  $(X_b, Y_b, Z_b)$ . The A/C’s position is  $(x, y, z)$ , and  $\psi$ , the A/C yaw angle,  $\theta$ ,

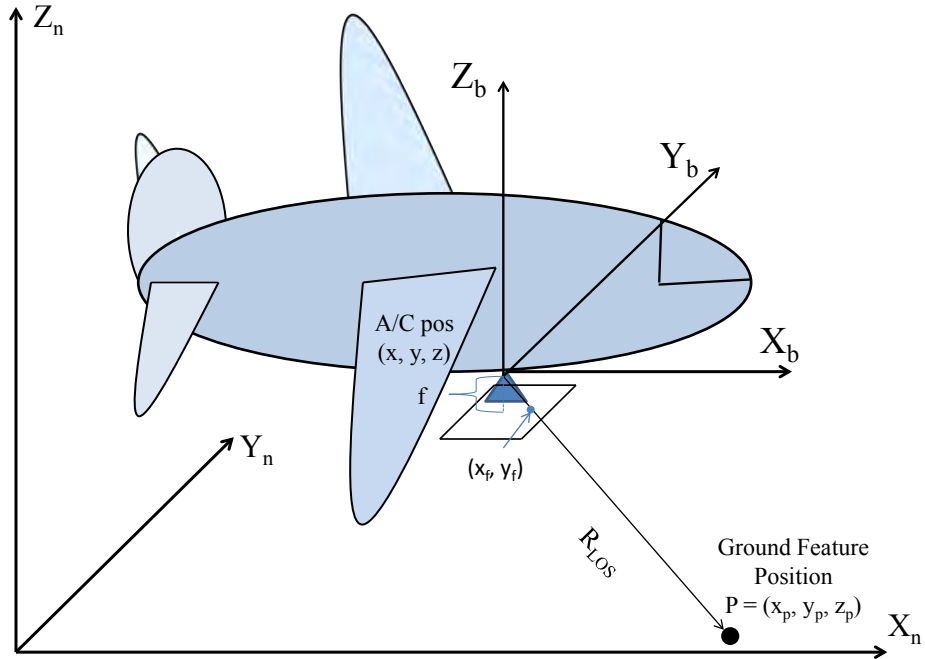


Figure 3.3: The A/C in 3-D space. Notice that the origin of the body frame is located at the camera.

the A/C pitch angle, and  $\phi$  and together they are the A/C's Euler angles. A strapdown [9] INS arrangement is considered. When flying over a non-rotating and flat Earth as shown in Figure 3.3, the dynamics of the INS errors, also known as the error equations, are shown in state space notation as  $\delta\dot{\mathbf{x}} = \mathbf{A}\delta\mathbf{x} + \mathbf{\Gamma}\delta\mathbf{u}$ , where the navigation state's position, velocity and angles error

$$\delta\mathbf{x} = [ \ \delta\mathbf{P} \ \ \delta\mathbf{V} \ \ \delta\mathbf{\Psi} ]^T$$

and the disturbances are the three accelerometers' and the three rate gyroscopes' biases

$$\delta\mathbf{u} = [ \ \delta f_{x_b} \ \ \delta f_{y_b} \ \ \delta f_{z_b} \ \ \delta\omega_x \ \ \delta\omega_y \ \ \delta\omega_z ]^T$$

Concerning the angular errors vector  $\delta\mathbf{\Psi}$ :

$$\delta\mathbf{\Psi} = -\delta\mathbf{C}_b^n\mathbf{C}_n^b \quad (3.55)$$

and

$$\delta\Psi = \delta\Psi \times \quad (3.56)$$

where  $\delta\Psi$  is the skew symmetric matrix formed from the vector  $\delta\Psi$  according to Eq. (3.56).

For small Euler angles  $\psi$ ,  $\theta$ , and  $\phi$ , the DCM

$$\mathbf{C}_b^n(\psi, \theta, \phi) = \begin{bmatrix} 1 & -\psi & \theta \\ \psi & 1 & -\phi \\ -\theta & \phi & 1 \end{bmatrix} \quad (3.57)$$

and therefore its perturbation

$$\delta\mathbf{C}_b^n = \begin{bmatrix} 0 & -\delta\psi & \delta\theta \\ \delta\psi & 0 & -\delta\phi \\ -\delta\theta & \delta\phi & 0 \end{bmatrix} \quad (3.58)$$

For constant altitude flight in the direction of the  $X_n$  axis, the nominal  $\mathbf{C}_n^b = \mathbf{I}_3$ . Thus, using Eq. (3.55) we calculate

$$\delta\Psi = \begin{bmatrix} 0 & \delta\psi & -\delta\theta \\ -\delta\psi & 0 & \delta\phi \\ \delta\theta & -\delta\phi & 0 \end{bmatrix} \quad (3.59)$$

and since  $\delta\Psi = \delta\Psi \times$  we recover the errors in the A/C Euler angles

$$\delta\Psi = [ -\delta\phi \quad -\delta\theta \quad -\delta\psi ]^T \quad (3.60)$$

Hence, the navigation state's error vector is

$$\delta\mathbf{x} = [ \delta x \quad \delta y \quad \delta z \quad \delta v_x \quad \delta v_y \quad \delta v_z \quad -\delta\phi \quad -\delta\theta \quad -\delta\psi ]^T \quad (3.61)$$

The INS error state equations are

$$\delta\dot{\mathbf{x}} = \begin{bmatrix} \mathbf{0}_{3 \times 3} & \mathbf{I}_{3 \times 3} & \mathbf{0}_{3 \times 3} \\ \mathbf{0}_{3 \times 3} & \mathbf{0}_{3 \times 3} & \mathbf{F}_{3 \times 3}^{(n)} \\ \mathbf{0}_{3 \times 3} & \mathbf{0}_{3 \times 3} & \mathbf{0}_{3 \times 3} \end{bmatrix} \delta\mathbf{x} + \begin{bmatrix} \mathbf{0}_{3 \times 3} & \mathbf{0}_{3 \times 3} \\ \mathbf{C}_n^b & \mathbf{0}_{3 \times 3} \\ \mathbf{0}_{3 \times 3} & -\mathbf{C}_n^b \end{bmatrix} \delta\mathbf{u} \quad (3.62)$$

where  $\mathbf{F}^{(n)} = f^{(n)} \times$  is the skew symmetric matrix form of the specific force vector. The nominal specific force components during constant altitude, wings level flight are  $f_x^{(n)} = a$ ,  $f_y^{(n)} = 0$  and  $f_z^{(n)} = -g$ , where  $g$  is the acceleration of gravity and  $a$  is the longitudinal acceleration of the A/C. Therefore

$$f^{(n)} = \begin{bmatrix} f_x^{(n)} \\ f_y^{(n)} \\ f_z^{(n)} \end{bmatrix} = \begin{bmatrix} a \\ 0 \\ g \end{bmatrix} \quad (3.63)$$

Eqs. (3.62) and (3.63) represent the dynamics of navigation state's error,  $(\delta P, \delta V, \delta \Psi)$ , under the assumption that the Earth is flat and non-rotating. The meaning of the angular errors' vector  $\delta \Psi$ , that is, its relationship to the Euler angles' errors, has been determined by the A/C's trajectory, that is, the nominal DCM  $\mathbf{C}_b^n$ .

Having negative angle error states is unorthodox. In order for the navigation state error to be

$$\delta \mathbf{x} = [ \delta x \ \delta y \ \delta z \ \delta v_x \ \delta v_y \ \delta v_z \ \delta \phi \ \delta \theta \ \delta \psi ]^T \quad (3.64)$$

the dynamics Eq. (3.62) is modified as follows

$$\delta \dot{\mathbf{x}} = \begin{bmatrix} \mathbf{0}_{3 \times 3} & \mathbf{I}_{3 \times 3} & \mathbf{0}_{3 \times 3} \\ \mathbf{0}_{3 \times 3} & \mathbf{0}_{3 \times 3} & -\mathbf{F}_{3 \times 3}^{(n)} \\ \mathbf{0}_{3 \times 3} & \mathbf{0}_{3 \times 3} & \mathbf{0}_{3 \times 3} \end{bmatrix} \delta \mathbf{x} + \begin{bmatrix} \mathbf{0}_{3 \times 3} & \mathbf{0}_{3 \times 3} \\ \mathbf{C}_n^b & \mathbf{0}_{3 \times 3} \\ \mathbf{0}_{3 \times 3} & \mathbf{C}_n^b \end{bmatrix} \delta \mathbf{u} \quad (3.65)$$

and with perfect INS alignment,

$$\delta \mathbf{x}(0) = \mathbf{0}$$

Since this is wings level, constant altitude flight, in the direction of the  $X_n$  axis, the nominal navigation variables are

$$\begin{aligned} x &= x_0 + v_x t + \frac{1}{2} a t^2 & y &= 0 & z &= h \\ \phi &= 0 & \theta &= 0 & \psi &= 0 \end{aligned}$$

These variables are non-dimensionalized as follows

$$\begin{aligned}
x &\rightarrow \frac{x}{h}, & y &\rightarrow \frac{y}{h}, & z &\rightarrow \frac{z}{h}, \\
v_x &\rightarrow \frac{v_x}{v}, & v_x &\rightarrow \frac{v_x}{v}, & v_z &\rightarrow \frac{v_z}{v}, \\
\delta f_x &\rightarrow \frac{\delta f_x}{g}, & \delta f_y &\rightarrow \frac{\delta f_y}{g}, & \delta f_z &\rightarrow \frac{\delta f_z}{g}, \\
\delta\omega_x &\rightarrow h \frac{\delta\omega_x}{v}, & \delta\omega_y &\rightarrow h \frac{\delta\omega_y}{v}, & \delta\omega_z &\rightarrow h \frac{\delta\omega_z}{v}, \\
t &\rightarrow t \frac{v}{h}, & T &\rightarrow T \frac{v}{h},
\end{aligned}$$

where  $t$  is the current time, and  $T$  is the length of a measurement epoch. The duration of a nondimensional measurement epoch  $T = 1$ .

The non-dimensional parameters are

$$g \triangleq \frac{hg}{v^2} \quad \text{and} \quad a \triangleq \frac{ha}{v^2}$$

If, for example,

$$h = 1000[m], \quad v = 100 \left[ \frac{m}{sec} \right], \quad g = 10 \left[ \frac{m}{sec^2} \right],$$

the non-dimensional parameter  $g = 1$ .

It is assumed that the sensor errors are constant biases that are Gaussian distributed. This allows the state error vector to be augmented with the vector  $\delta\mathbf{u}$ ; the augmented state is

$$\delta\mathbf{x}_a = \begin{bmatrix} \delta\mathbf{x} \\ \dots \\ \delta\mathbf{u} \end{bmatrix}_{15 \times 1}$$

and the dynamics matrix is augmented by the  $\Gamma$  matrix, as shown

$$\mathbf{A}_a = \begin{bmatrix} \mathbf{A} & \Gamma \\ \mathbf{0}_{6 \times 9} & \mathbf{0}_{6 \times 6} \end{bmatrix}_{15 \times 15}$$

One obtains a dynamic system in “free fall”. When converted to discrete time,

$\mathbf{A}_a \rightarrow \mathbf{A}_{ad} = e^{\mathbf{A}_a \Delta t}$ , where  $\Delta t$  is the sampling interval. The augmented discrete time state dynamics become

$$\delta \mathbf{x}_a(l+1) = \mathbf{A}_{ad} \delta \mathbf{x}_a(l), \quad l = 0, \dots, N-1 \quad (3.66)$$

where  $l$  is the discrete time step counter during a measurement epoch and the non-dimensional time step is  $\Delta T = \frac{T}{N} := \Delta T \frac{v}{h}$ . The discrete-time dynamics matrix can be analytically derived.

This dynamics equation applies as long as the ground features’ positions are known. Assuming the ground features are stationary, but their position is not known, two additional states, the  $x$  and  $y$  horizontal coordinates of the tracked ground features, must be added for each tracked ground feature whose position will be estimated on the fly. If the number of ground features being tracked is  $n$ , then the augmented navigation state is

$$\delta \mathbf{x}_a := \begin{bmatrix} \delta \mathbf{x}_a \\ \vdots \\ \delta x_{p1} \\ \vdots \\ \delta y_{pn} \end{bmatrix}_{(15+2n) \times 1} \quad (3.67)$$

and

$$\mathbf{A}_{ad} := \begin{bmatrix} \mathbf{A}_{ad} & \mathbf{0}_{15 \times 2n} \\ \mathbf{0}_{2n \times 15} & \mathbf{I}_{2n \times 2n} \end{bmatrix}_{(15+2n) \times (15+2n)} \quad (3.68)$$

If, for example, one unknown ground feature is being tracked during a measurement epoch, then the dimension of the augmented navigation state’s error is 17 and if two unknown ground features are being tracked during a measurement epoch then the dimension of the navigation state’s error is 19. On one hand, state augmentation reduces the degree of observability, which decreases the strength of INS aiding action. On the other hand, the inclusion of additional features to be tracked increases the number of measurement equations, which helps wash out the measurement error.

**3.3.2 Modeling/Calibrating the Free INS.** With the dynamics from Subsection 3.3.1, the values for  $\sigma_a$  and  $\sigma_g$ , the uncertainty in the bias of the accelerometers and gyroscopes, respectively, are set such that the free INS is a  $1 \frac{km}{hr}$  navigation system; note that a non-dimensional hour is 360 units long. Since the dynamics are not forced, that is, there is no controlled input, the calibration is performed by using the solution to the Lyapunov difference equation, Eq. (3.21) with

$$\mathbf{P}(\mathbf{0}) = \begin{bmatrix} \mathbf{0}_{9 \times 9} & \mathbf{0} & \mathbf{0} \\ \mathbf{0} & \text{diag}(\sigma_a^2, \sigma_a^2, \sigma_a^2) & \mathbf{0} \\ \mathbf{0} & \mathbf{0} & \text{diag}(\sigma_g^2, \sigma_g^2, \sigma_g^2) \end{bmatrix}_{15 \times 15} \quad (3.69)$$

The Lyapunov difference equation is linear and therefore there is a linear relationship between the uncertainty in the sensors' biases and the ensuing uncertainty in the A/C's  $x$  position:

$$P_{1,1}(360N) = \alpha\sigma_a^2 + \beta\sigma_g^2 \quad (3.70)$$

where the coefficients  $\alpha$  and  $\beta$  are constants. Therefore, Eq. (3.21) was solved for one non-dimensional hour twice to calculate the values of the constants  $\alpha$  and  $\beta$ . The first time,  $\sigma_a$  was set to 1 and  $\sigma_g$  was set to 0. The second time,  $\sigma_a$  was set to 0 and  $\sigma_g$  was set to 1. Then assigning the errors in the accelerometers and gyroscopes an equal role/“guilt” in the uncertainty of the A/C's position at time 360, the values for the variances of the sensors' biases are calculated as

$$\sigma_a = \frac{1}{\sqrt{2\alpha}} = 1.0912 \times 10^{-5} \quad (3.71)$$

$$\sigma_g = \frac{1}{\sqrt{2\beta}} = 9.0935 \times 10^{-8} \quad (3.72)$$

**3.3.3 Measurement Equation.** From the geometry in Figure 3.3 the relationship of the inertial position of the A/C to that of the ground feature  $P$  is

$$\begin{bmatrix} x \\ y \\ z \end{bmatrix} = \begin{bmatrix} x_p \\ y_p \\ z_p \end{bmatrix} - \frac{|R_{LOS}|}{\sqrt{x_f^2 + y_f^2 + f^2}} \mathbf{C}_b^n \begin{bmatrix} x_f \\ y_f \\ -f \end{bmatrix} \quad (3.73)$$

where  $x_p$ ,  $y_p$ , and  $z_p$  are the coordinates of the ground feature in the inertial/navigation frame,  $x_f$  and  $y_f$  are the projections of the ground feature's respective  $x$  and  $y$  coordinates onto the focal plane of the camera and  $f$  is the camera's focal length. For the case when the A/C flies wings level at a constant altitude in the direction of the  $X_n$  axis and the Euler angles are small, the DCM for relating the body frame to the navigation frame is given in Eq. (3.57). The first two equations in the relationship given by Eq. (3.73) are non-linearly dependent on the third. Now, the third equation yields

$$z_p - z = \frac{|R_{LOS}|}{\sqrt{x_f^2 + y_f^2 + f^2}} \begin{bmatrix} 0 & 0 & 1 \end{bmatrix} \mathbf{C}_b^n \begin{bmatrix} x_f \\ y_f \\ -f \end{bmatrix}$$

and thus

$$\frac{|R_{LOS}|}{\sqrt{x_f^2 + y_f^2 + f^2}} = \frac{z_p - z}{\begin{bmatrix} 0 & 0 & 1 \end{bmatrix} \mathbf{C}_b^n \begin{bmatrix} x_f \\ y_f \\ -f \end{bmatrix}} \quad (3.74)$$

Substituting Eq. (3.74) into Eq. (3.73) yields the two measurement equations for the three dimensional case:

$$\begin{bmatrix} x \\ y \end{bmatrix} = \begin{bmatrix} x_p \\ y_p \end{bmatrix} - \frac{z_p - z}{\begin{bmatrix} 0 & 0 & 1 \end{bmatrix} \mathbf{C}_b^n \begin{bmatrix} x_f \\ y_f \\ -f \end{bmatrix}} \begin{bmatrix} 1 & 0 & 0 \\ 0 & 1 & 0 \end{bmatrix} \mathbf{C}_b^n \begin{bmatrix} x_f \\ y_f \\ -f \end{bmatrix}$$

Multiplying out the matrices yields

$$\begin{bmatrix} x \\ y \end{bmatrix} = \begin{bmatrix} x_p \\ y_p \end{bmatrix} - (z_p - z) \frac{1}{-f - \theta x_f + \phi y_f} \begin{bmatrix} x_f - \psi y_f - f\theta \\ y_f + x_f \psi + f\phi \end{bmatrix}$$

and non-dimensionalizing such that

$$x_f \rightarrow \frac{x_f}{f} \quad y_f \rightarrow \frac{y_f}{f}$$

yields

$$\begin{bmatrix} x \\ y \end{bmatrix} = \begin{bmatrix} x_p \\ y_p \end{bmatrix} - (z_p - z) \frac{1}{-1 - \theta x_f + \phi y_f} \begin{bmatrix} x_f - \psi y_f - \theta \\ y_f + x_f \psi + \phi \end{bmatrix}$$

We obtained two separate measurement equations

$$x_p - x = -(z_p - z) \frac{x_f - \psi y_f - \theta}{1 + \theta x_f - \phi y_f} \quad (3.75)$$

$$y_p - y = -(z_p - z) \frac{y_f + x_f \psi + \phi}{1 + \theta x_f - \phi y_f} \quad (3.76)$$

Due to the small angles assumption, the denominator in Eqs. (3.75) and (3.76) can be moved up such that

$$x_p - x \approx -(z_p - z)(x_f - \psi y_f - \theta)(1 - \theta x_f + \phi y_f) \quad (3.77)$$

$$y_p - y \approx -(z_p - z)(y_f + x_f \psi + \phi)(1 - \theta x_f + \phi y_f) \quad (3.78)$$

Since the A/C is using ground features to aid its INS, it can be assumed, without loss of generality, that  $z_p = 0$ . Due to the small values of the angles, when the former fraction is distributed out, the products of the angles are negligible, yielding

$$x_p - x = z[x_f - \theta(1 + x_f^2) + \phi x_f y_f - \psi y_f] \quad (3.79)$$

$$y_p - y = z[y_f - \theta x_f y_f + \phi(1 + y_f^2) + \psi x_f] \quad (3.80)$$

Next, perturb the states and the measurements

$$\begin{aligned}
x &= x_c - \delta x & y &= y_c - \delta y & z &= z_c - \delta z \\
\theta &= \theta_c - \delta \theta & \phi &= \phi_c - \delta \phi & \psi &= \psi_c - \delta \psi \\
x_p &= x_{pc} - \delta x_p & y_p &= y_{pc} - \delta y_p \\
x_f &= (x_{fm} - \delta x_f) & y_f &= (y_{fm} - \delta y_f)
\end{aligned}$$

where the subscript  $c$  indicates calculated values provided by the INS and the subscript  $m$  indicates measured quantities. Inserting the perturbation equations into Eqs. (3.79) and (3.80) yields

$$\begin{aligned}
(x_{pc} - x_c) + \delta x - \delta x_p &= (z_c - \delta z) \left( (x_{fm} - \delta x_f) - (\theta_c - \delta \theta)(1 + (x_{fm} - \delta x_f)^2) \right) \\
&+ (z_c - \delta z) \left( (\phi_c - \delta \phi)(x_{fm} - \delta x_f)(y_{fm} - \delta y_f) - (\psi_c - \delta \psi)(y_{fm} - \delta y_f) \right)
\end{aligned}$$

Again, due to the small error in the measurements, the products of these terms can be neglected.

$$\begin{aligned}
(x_{pc} - x_c) + \delta x - \delta x_p &= \\
(z_c - \delta z) \left( (x_{fm} - \delta x_f) - (\theta_c - \delta \theta)(1 + x_{fm}^2) + (\phi_c - \delta \phi)x_{fm}y_{fm} - (\psi_c - \delta \psi)y_{fm} \right)
\end{aligned}$$

Similarly, in the second measurement equation

$$\begin{aligned}
(y_{pc} - y_c) + \delta y - \delta y_p &= (z_c - \delta z) \left( (y_{fm} - \delta y_f) - (\theta_c - \delta \theta)(x_{fm} - \delta x_f)(y_{fm} - \delta y_f) \right) \\
&+ (z_c - \delta z) \left( (\phi_c - \delta \phi)(1 + (y_{fm} - \delta y_f)^2) + (\psi_c - \delta \psi)(x_{fm} - \delta x_f) \right) \\
&= (z_c - \delta z) \left( (y_{fm} - \delta y_f) - (\theta_c - \delta \theta)x_{fm}y_{fm} + (\phi_c - \delta \phi)(1 + y_{fm}^2) + (\psi_c - \delta \psi)x_{fm} \right)
\end{aligned}$$

Moving all the error terms to the RHS of the equation and all the non-error terms to the LHS yields

$$\begin{aligned}
(x_{pc} - x_c) - z_c(x_{fm} - \theta_c(1 + x_{fm}^2) + \phi_c x_{fm} y_{fm} - \psi_c y_{fm}) &= -\delta x - \delta z(x_{fm} - \theta_c(1 + x_{fm}^2) \\
&+ \phi_c x_{fm} y_{fm} - \psi_c y_{fm}) + \delta \theta(1 + x_{fm}^2)z_c - \delta \phi(x_{fm} y_{fm} z_c) + \delta \psi(y_{fm} z_c) + \delta x_p - \delta x_f z_c
\end{aligned} \tag{3.81}$$

and

$$\begin{aligned}
(y_{pc} - y_c) - z_c(y_{fm} - \theta_c x_{fm} y_{fm} + \phi_c(1 + y_{fm}^2) + \psi_c x_{fm}) = \\
- \delta y - \delta z(y_{fm} - \theta_c x_{fm} y_{fm} + \phi_c(1 + y_{fm}^2) + \psi_c x_{fm}) \\
+ \delta \theta(x_{fm} y_{fm} z_c) - \delta \phi(1 + y_{fm}^2) z_c - \delta \psi(x_{fm} z_c) + \delta y_p - \delta y_f z_c
\end{aligned} \tag{3.82}$$

Finally, non-dimensionalizing such that

$$x_p \rightarrow \frac{x_p}{h} \quad y_p \rightarrow \frac{y_p}{h} \quad z_p \rightarrow \frac{z_p}{h},$$

the nondimensional altitude is  $z = 1$ . In addition, for the purpose of covariance analysis, set all of the calculated values on the RHS equal to the nominal values. This causes all of the angles to go to zero, simplifying the measurement Eqs. (3.81) and (3.82). Also, on the RHS set  $x_{fm} := x_f$  and  $y_{fm} := y_f$ .

$$\begin{aligned}
(x_{pc} - x_c) - z_c(x_{fm} - \theta_c(1 + x_{fm}^2) + \phi_c x_{fm} y_{fm} - \psi_c y_{fm}) = \\
- \delta x - \delta z x_f + \delta \theta(1 + x_f^2) - \delta \phi x_f y_f + \delta \psi y_f + \delta x_p - \delta x_f
\end{aligned} \tag{3.83}$$

and

$$\begin{aligned}
(y_{pc} - y_c) - z_c(y_{fm} - \theta_c x_{fm} y_{fm} + \phi_c(1 + y_{fm}^2) + \psi_c x_{fm}) = \\
- \delta y - \delta z y_f + \delta \theta x_f y_f - \delta \phi(1 + y_f^2) - \delta \psi x_f + \delta y_p - \delta y_f
\end{aligned} \tag{3.84}$$

The time dependent observation matrix  $\mathbf{H}(l)$  for one unknown ground feature is

$$\mathbf{H}_u(l) = \begin{bmatrix} -1 & 0 \\ 0 & -1 \\ -x_f & -y_f \\ 0 & 0 \\ 0 & 0 \\ 0 & 0 \\ -x_f y_f & -(1 + y_f^2) \\ 1 + x_f^2 & x_f y_f \\ y_f & -x_f \\ 0 & 0 \\ 0 & 0 \\ 0 & 0 \\ 0 & 0 \\ 0 & 0 \\ 1 & 0 \\ 0 & 1 \end{bmatrix}^T \quad (3.85)$$

where the subscript  $u$  indicates that the position of the ground feature being tracked is unknown. The nondimensional measurement error is  $[\delta x_f, \delta y_f]^T$ .

For the sake of observability [7] two ground features will be tracked. Therefore, there will be two subscripts. The first will correspond to the ground feature that is closer to the A/C and the second to the ground feature that is further away. If both ground features are

known, the observation matrix is

$$\mathbf{H}_{kk}(l) = \begin{bmatrix} -1 & 0 & -1 & 0 \\ 0 & -1 & 0 & -1 \\ -x_{f1} & -y_{f1} & -x_{f2} & -y_{f2} \\ 0 & 0 & 0 & 0 \\ 0 & 0 & 0 & 0 \\ 0 & 0 & 0 & 0 \\ -x_{f1}y_{f1} & -(1 + y_{f1}^2) & -x_{f2}y_{f2} & -(1 + y_{f2}^2) \\ 1 + x_{f1}^2 & x_{f1}y_{f1} & 1 + x_{f2}^2 & x_{f2}y_{f2} \\ y_{f1} & -x_{f1} & y_{f2} & -x_{f2} \\ 0 & 0 & 0 & 0 \\ 0 & 0 & 0 & 0 \\ 0 & 0 & 0 & 0 \\ 0 & 0 & 0 & 0 \\ 0 & 0 & 0 & 0 \\ 0 & 0 & 0 & 0 \end{bmatrix}^T \quad (3.86)$$

where the subscript  $_k$  indicates that the position of the ground feature is known. When there is one known and one unknown ground feature, the observation matrix is

$$\mathbf{H}_{ku}(l) = \left[ \begin{array}{cccc} -1 & 0 & -1 & 0 \\ 0 & -1 & 0 & -1 \\ -x_{f1} & -y_{f1} & -x_{f2} & -y_{f2} \\ 0 & 0 & 0 & 0 \\ 0 & 0 & 0 & 0 \\ 0 & 0 & 0 & 0 \\ -x_{f1}y_{f1} & -(1 + y_{f1}^2) & -x_{f2}y_{f2} & -(1 + y_{f2}^2) \\ 1 + x_{f1}^2 & x_{f1}y_{f1} & 1 + x_{f2}^2 & x_{f2}y_{f2} \\ y_{f1} & -x_{f1} & y_{f2} & -x_{f2} \\ 0 & 0 & 0 & 0 \\ 0 & 0 & 0 & 0 \\ 0 & 0 & 0 & 0 \\ 0 & 0 & 0 & 0 \\ 0 & 0 & 0 & 0 \\ 0 & 0 & 1 & 0 \\ 0 & 0 & 0 & 1 \end{array} \right]^T \quad (3.87)$$

Finally, when neither ground feature's position is known, the observation matrix

$$\mathbf{H}_{uu}(l) = \begin{bmatrix} -1 & 0 & -1 & 0 \\ 0 & -1 & 0 & -1 \\ -x_{f1} & -y_{f1} & -x_{f2} & -y_{f2} \\ 0 & 0 & 0 & 0 \\ 0 & 0 & 0 & 0 \\ 0 & 0 & 0 & 0 \\ -x_{f1}y_{f1} & -(1 + y_{f1}^2) & -x_{f2}y_{f2} & -(1 + y_{f2}^2) \\ 1 + x_{f1}^2 & x_{f1}y_{f1} & 1 + x_{f2}^2 & x_{f2}y_{f2} \\ y_{f1} & -x_{f1} & y_{f2} & -x_{f2} \\ 0 & 0 & 0 & 0 \\ 0 & 0 & 0 & 0 \\ 0 & 0 & 0 & 0 \\ 0 & 0 & 0 & 0 \\ 0 & 0 & 0 & 0 \\ 1 & 0 & 0 & 0 \\ 0 & 1 & 0 & 0 \\ 0 & 0 & 1 & 0 \\ 0 & 0 & 0 & 1 \end{bmatrix}^T \quad (3.88)$$

**3.3.4 Performance of Aided INS.** The cross country flight scenario is shown in Figure 3.2. The A/C is flying wings-level, at a constant speed. It is assumed that the ground features are equally spaced one kilometer apart, and that the A/C starts one kilometer behind and above the first known ground feature. It is also assumed that the

ground features lay on the A/C's ground track. In the observation matrices

$$x_{f1}(t) = 1 - t$$

$$x_{f2}(t) = 2 - t$$

$$y_{f1}(t) = y_{f2}(t) = 0$$

*3.3.5 Initialization.* It is stipulated that, initially, the INS has zero error in the navigation states, that is, the INS alignment was perfect, and the states representing the biases in the sensors are

$$\begin{aligned} \delta f_x^{(b)} &\sim N(0, \sigma_a^2) & \delta f_y^{(b)} &\sim N(0, \sigma_a^2) & \delta f_z^{(b)} &\sim N(0, \sigma_a^2) \\ \delta \omega_x &\sim N(0, \sigma_g^2) & \delta \omega_y &\sim N(0, \sigma_g^2) & \delta \omega_z &\sim N(0, \sigma_g^2) \end{aligned}$$

The  $x$ ,  $y$  and  $z$  accelerometers are of the same quality; also the  $x$ ,  $y$  and  $z$  gyroscopes are of the same quality. Thus

$$\delta \mathbf{x}(\mathbf{0}) \sim N(\mathbf{0}, \mathbf{P}(0))$$

with the initial covariance matrix  $\mathbf{P}(0)$  given by Eq. (3.69).

*3.3.6 Transitioning Between Measurement Epochs.* For the purpose of covariance analysis, and because the features were equally spaced and it took exactly one time block for the A/C to fly from directly over one ground feature to directly over the next ground feature, the relative position of the ground features to the A/C was the same at the beginning of each time block/measurement epoch. Therefore the absolute positions of the A/C and the ground features are not considered. After non-dimensionalization, the position of the A/C relative to its location at the beginning of a measurement epoch is

$$x(l) = l\Delta t, \quad y(l) = 0, \quad 0 \leq l \leq N - 1 \quad (3.89)$$

Recall that  $l$  is the discrete time counter within a measurement epoch, and that at the beginning of each epoch  $l$  starts back over at 0. There are 360 epochs to be considered.

Each epoch's duration,  $T$ , is 1 non-dimensional second and in each epoch  $N = 100$  bearing measurements of a ground feature are taken. With the exception of the first and last ground feature, all the ground features are used for measurements in two consecutive time blocks/measurement epochs. Throughout the entirety of the calculations  $x_{p1} = 1$  and  $x_{p2} = 2$ . The lateral positions of the ground features are 0. At the transition point between epochs, the old  $x_{p2}$  and  $y_{p2}$  becomes the new  $x_{p1}$  and  $y_{p1}$ , respectively, and a new ground feature is acquired.

Initially, the positions of both tracked ground features were assumed known. Therefore, in epoch 1 the observation matrix  $\mathbf{H}_{kk}(l)$ , and the dynamics matrix  $\mathbf{A}_{ad15\times15}$  were used. In the first epoch, the uncertainty of the states was propagated for one hundred steps using the covariance propagate and update equations, Eqs.(3.44)-(3.46), substituting in the correct values for the dynamics, observation and identity matrices. where  $\mathbf{R}$  is the measurement uncertainty caused by one pixel in the camera's focal plane

$$\begin{bmatrix} \delta x_{f1} \\ \delta y_{f1} \\ \delta x_{f2} \\ \delta y_{f2} \end{bmatrix} \sim N(\mathbf{0}, \mathbf{R})$$

We assume a 9 Megapixel camera with an aspect ratio of 1 and therefore the nondimensional

$$\mathbf{R} = \begin{bmatrix} \frac{1}{9} & 0 & 0 & 0 \\ 0 & \frac{1}{9} & 0 & 0 \\ 0 & 0 & \frac{1}{9} & 0 \\ 0 & 0 & 0 & \frac{1}{9} \end{bmatrix} \times 10^{-6}$$

At the conclusion of the first one hundred steps/the first measurement epoch, the first ground feature was dropped from consideration, and a new, unknown ground feature was brought in. Thus the next time block required the use of the augmented dynamics matrix  $\mathbf{A}_{ad17\times17}$  from Eq. (3.68) and the observation matrix  $\mathbf{H}_{ku}(l)$ .

The challenging part is to transition the covariance matrix  $\mathbf{P}$  from an  $15 \times 15$  to a  $17 \times 17$  matrix, while including the correct cross-covariance terms. This is done as follows: when transitioning from two known ground features to one known/one unknown ground feature, the new initial covariance matrix is

$$\mathbf{P}(0) = \begin{bmatrix} \mathbf{P}(99)_{15 \times 15} & \mathbf{P}(99)_{(1:15,1)} & \mathbf{P}(99)_{(1:15,2)} \\ \mathbf{P}(99)_{(1,1:15)} & \sigma_{x_{new}}^2 & P(99)_{1,2} \\ \mathbf{P}(99)_{(2,1:15)} & P(99)_{1,2} & \sigma_{y_{new}}^2 \end{bmatrix}_{17 \times 17} \quad (3.90)$$

where  $\sigma_{x_{new}}^2$  is the uncertainty in the  $x$  position of the new ground feature, and it is the uncertainty in the A/C's  $x$  position at the time the new ground feature is acquired plus the uncertainty brought about by the optical measurement:

$$\sigma_{x_{new}}^2 = P_{(1,1)}(99) + \sigma_{\xi}^2 \quad (3.91)$$

Similarly,  $\sigma_{y_{new}}^2$  is the uncertainty in the  $y$  position of the new ground feature, and it is the uncertainty in the A/C's  $y$  position at the time the new ground feature is acquired plus the uncertainty brought about by the optical measurement:

$$\sigma_{y_{new}}^2 = P_{(2,2)}(99) + \sigma_{\mu}^2 \quad (3.92)$$

where  $\sigma_{\xi}^2$  and  $\sigma_{\mu}^2$  are the uncertainties caused by the error in the LOS angle measurements, and they each have a non-dimensional value of  $\frac{4}{9} \times 10^{-6}$ . It is because of the correlation of the errors in the A/C navigation state  $x$  and the new ground feature's position state  $x_{p2}$  that the first row and column from  $\mathbf{P}_{15 \times 15}$  must be transplanted to their respective positions in  $\mathbf{P}_{17 \times 17}$ . Since there is no correlation between the LOS error of the camera and any of the INS navigation or bias states, it is not added to any of the transplanted fields. The same holds true for the navigation state  $y$  and the new state  $y_{p2}$ . The covariance matrix is then propagated in the same manner as in the first epoch, following Eqs. (3.44)-(3.46), with the proper substitution of the initial covariance,  $\mathbf{P}(0)_{17 \times 17}$  for  $\mathbf{P}(99)_{15 \times 15}$ , dynamics,  $\mathbf{A}_{ad17 \times 17}$  (found using Eq. 3.68) for  $\mathbf{A}_{ad15 \times 15}$ , and observation matrices,  $\mathbf{H}_{ku}$  for  $\mathbf{H}_{kk}$ .

The transition at the beginning of the third epoch from one known/one unknown to two unknown ground features follows the same pattern as incorporating the first unknown ground feature. Now

$$\mathbf{P}(0) = \begin{bmatrix} \mathbf{P}(99)_{17 \times 17} & \mathbf{P}(99)_{(1:17,1)} & \mathbf{P}(99)_{(1:17,2)} \\ \mathbf{P}(99)_{(1,1:17)} & \sigma_{xnew}^2 & P(99)_{1,2} \\ \mathbf{P}(99)_{(2,1:17)} & P(99)_{1,2} & \sigma_{ynew}^2 \end{bmatrix}_{19 \times 19} \quad (3.93)$$

where  $\sigma_{xnew}^2$  and  $\sigma_{ynew}^2$  are calculated according to Eqs. (3.91) and (3.92).

In the previous epoch, the unknown feature's position was  $(x_{p2}, y_{p2})$ , but when it transitioned to being the closer ground feature, all of its cross-covariances went with it. Because  $P_{(16,16)}$  and  $P_{17,17}$  show the uncertainty of the closest feature to the A/C, the entirety of  $\mathbf{P}(99)$  could be directly translated to the upper-diagonal section of the new covariance matrix. Substituting  $\mathbf{H}_{uu}$  for  $\mathbf{H}_{ku}$ , and using the  $\mathbf{A}_{ad}{}_{19 \times 19}$  dynamics matrix, the covariance was propagated according to Eqs. (3.44)-(3.46). These matrices were used for the remainder of the measurement epochs.

The transition becomes more complicated when the A/C completes a time block using two unknown ground features, and begins using a new unknown ground feature. A transition matrix is required

$$\mathbf{P} = \begin{bmatrix} \mathbf{P}(99)_{15 \times 15} & \mathbf{P}(99)_{(1:15,18)} & \mathbf{P}(99)_{(1:16,19)} \\ \mathbf{P}(99)_{(18,1:15)} & P(99)_{18,18} & \vdots \\ \mathbf{P}(99)_{(19,1:16)} & \dots & P(99)_{19,19} \end{bmatrix}_{17 \times 17} \quad (3.94)$$

This transition matrix was then used to initialize the new state estimation error covariance matrix,  $\mathbf{P}_{19 \times 19}$ :

$$\mathbf{P}(0) = \begin{bmatrix} \mathbf{P} & \mathbf{P}_{(1:17,1)} & \mathbf{P}_{(1:17,2)} \\ \mathbf{P}_{(1,1:17)} & \sigma_{xnew}^2 & P_{(1,2)} \\ \mathbf{P}_{(2,1:17)} & P_{(1,2)} & \sigma_{ynew}^2 \end{bmatrix}_{19 \times 19} \quad (3.95)$$

where  $\sigma_{xnew}^2$  and  $\sigma_{ynew}^2$  are calculated according to Eqs. (3.91) and (3.92). Starting at epoch 4, the transitions for the remainder of the epochs followed Eqs. (3.94)-(3.95) from epoch 3, because there are no more known ground features.

### 3.4 Three Dimensional Vertical Case

The inertial and body frames are same as for horizontal case laid out in Subsection 3.3.1. When flying towards a flat, non-rotating Earth the reference frame relationship is shown in Figure 3.4. For this case the body axes have been rotated away from the body fixed frame in order for them to remain aligned with the navigation axes. This was done to maintain the established linear mathematics model. To keep the body axes aligned such that the  $X_b$  axis is the longitudinal axis, one must use the nonlinear dynamics model found in Appendix D and the nonlinear measurement model found in Section E.2. For this case it is assumed that  $v(0) = 0$ .

*3.4.1 Dynamics.* The dynamics model is the same as the horizontal case, shown in Eq. (3.65). The primary difference is that the nominal specific force components during a perfect vertical drop will be time varying. Until the munition reaches terminal velocity all of the nominal specific forces are zero. Therefore

$$f^{(n)} = \begin{bmatrix} f_x^{(n)} \\ f_y^{(n)} \\ f_z^{(n)} \end{bmatrix} = \begin{bmatrix} 0 \\ 0 \\ 0 \end{bmatrix} \quad \forall 0 \leq t < t_{term} \quad (3.96)$$

Once the munition reaches terminal velocity, at  $t_{term}$ , the accelerometers will detect nominal specific forces such that  $f_x^{(n)} = a_x$ ,  $f_y^{(n)} = a_y$ , and  $f_z^{(n)} = g$  where  $g$  is the acceleration of gravity and  $a_x$  and  $a_y$  are the acceleration components of the munition along its  $X_b$  and  $Y_b$  axes. Since a purely vertical drop is considered,  $a_x = a_y = 0$ .

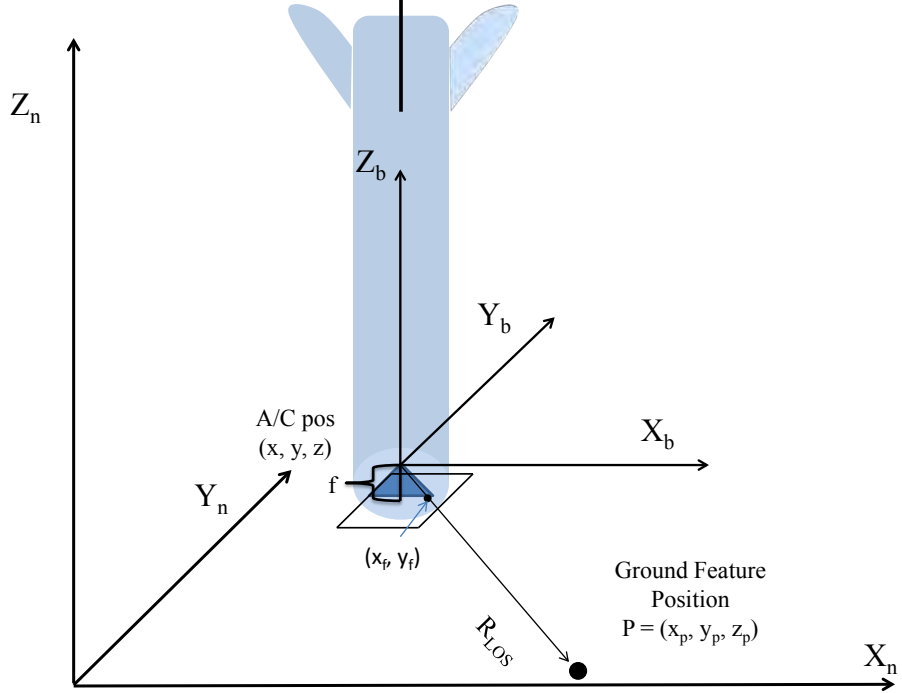


Figure 3.4: The munition falling in 3-D space. Notice that the origin of the body frame is located at the camera.

Therefore,

$$f^{(n)} = \begin{bmatrix} f_x^{(n)} \\ f_y^{(n)} \\ f_z^{(n)} \end{bmatrix} = \begin{bmatrix} 0 \\ 0 \\ g \end{bmatrix} \quad \forall \quad t_{term} \leq t \leq T \quad (3.97)$$

Eqs. (3.65, 3.96, 3.97) represent the time-varying dynamics of navigation state's error.

Since this is a vertical drop and the nominal trajectory is such that the body axes are aligned with the navigation axes, the time history of the nominal navigation variables is  $x = 0$ ,  $y = 0$ , and

$$z(t) = \begin{cases} h_{rel} - \frac{g}{2}t^2 & \forall \quad 0 \leq t < t_{term} \\ h_{term} + v_{term}t_{term} - v_{term}t & \forall \quad t_{term} \leq t \leq T \end{cases}$$

$\phi = \theta = \psi = 0$ , where  $h_{term}$  and  $v_{term}$  are the altitude and velocity of the munition when the munition reaches terminal velocity. These variables are non-dimensionalized as follows

$$\begin{aligned} t &\rightarrow t \frac{v}{h}, & T &\rightarrow T \frac{v}{h} \\ h_{term} &\rightarrow \frac{h_{term}}{h} & v_{term} &\rightarrow \frac{v_{term}}{v}, \end{aligned}$$

where  $h$  and  $v$  are a typical altitude and velocity when flying wings-level,  $t$  is the current time, and  $T = 7$  is the nondimensional fall duration.

The remainder of the dynamics model is identical to that of Subsection 3.3.3.

**3.4.2 Modeling/Calibrating the Free INS.** With the dynamics from Subsection 3.3.1, the values for  $\sigma_a$  and  $\sigma_g$ , the uncertainty in the bias of the accelerometers and gyroscopes, respectively, are set such that during wings level horizontal flight the free INS is a  $100 \frac{km}{hr}$  navigation system; note that a non-dimensional hour is 360 units long. Since the dynamics are not forced, that is, there is no controlled input, the calibration is performed by using the solution to the Lyapunov difference equation, Eq. (3.21) with  $\mathbf{P}(\mathbf{0})$  from Eq. (3.69)

The Lyapunov difference equation is linear and therefore there is a linear relationship between the uncertainty in the sensors' biases and the ensuing uncertainty in the munition's  $x$  position:

$$P_{1,1}(360N) = \alpha\sigma_a^2 + \beta\sigma_g^2$$

where the coefficients  $\alpha$  and  $\beta$  are constants. Therefore, Eq. (3.21) was solved for one non-dimensional hour twice to calculate the values of the constants  $\alpha$  and  $\beta$ . The first time,  $\sigma_a$  was set to 1 and  $\sigma_g$  was set to 0. The second time,  $\sigma_a$  was set to 0 and  $\sigma_g$  was set to 1. Then assigning the errors in the accelerometers and gyroscopes an equal role/“guilt” in the uncertainty of the munition's position at time 360, the values for the variances of the

sensors' biases are calculated as

$$\sigma_a = \frac{1}{\sqrt{2\alpha}} = 1.0912 \times 10^{-3} \quad (3.98)$$

$$\sigma_g = \frac{1}{\sqrt{2\beta}} = 9.0935 \times 10^{-6} \quad (3.99)$$

*3.4.3 Measurement Model.* Because the body reference frame is aligned with the navigation, the measurement model developed in Eqs. (3.73)-(3.82) holds true.

Nondimensionalizing such that

$$x_p \rightarrow \frac{x_p}{h} \quad y_p \rightarrow \frac{y_p}{h} \quad z_p \rightarrow \frac{z_p}{h},$$

the nondimensional altitude is  $z_c = z_l$ . In addition, for the purpose of covariance analysis, set all of the calculated values on the RHS equal to the nominal values. This causes all of the angles to go to zero, simplifying the measurement Eqs. (3.81) and (3.82). Also, on the RHS set  $x_{fm} := x_f$  and  $y_{fm} := y_f$ .

$$\begin{aligned} (x_{pc} - x_c) - z_c(x_{fm} - \theta_c(1 + x_{fm}^2) + \phi_c x_{fm} y_{fm} - \psi_c y_{fm}) = \\ - \delta x - \delta z x_f + \delta \theta(1 + x_f^2) z_l - \delta \phi x_f y_f z_l + \delta \psi y_f z_l + \delta x_p - \delta x_f z_l \end{aligned} \quad (3.100)$$

and

$$\begin{aligned} (y_{pc} - y_c) - z_c(y_{fm} - \theta_c x_{fm} y_{fm} + \phi_c(1 + y_{fm}^2) + \psi_c x_{fm}) = \\ - \delta y - \delta z y_f + \delta \theta x_f y_f z_l - \delta \phi(1 + y_f^2) z_l - \delta \psi x_f z_l + \delta y_p - \delta y_f z_l \end{aligned} \quad (3.101)$$

The time dependent observation matrix  $\mathbf{H}(l)$  for one unknown ground feature is

$$\mathbf{H}_u(l) = \begin{bmatrix} -1 & 0 \\ 0 & -1 \\ -x_f & -y_f \\ 0 & 0 \\ 0 & 0 \\ 0 & 0 \\ -x_f y_f z_l & -(1 + y_f^2) z_l \\ (1 + x_f^2) z_l & x_f y_f z_l \\ y_f z_l & -x_f z_l \\ 0 & 0 \\ 0 & 0 \\ 0 & 0 \\ 0 & 0 \\ 0 & 0 \\ 1 & 0 \\ 0 & 1 \end{bmatrix}^T \quad (3.102)$$

where the subscript  $u$  indicates that the position of the ground object being tracked is unknown. The nondimensional measurement error is  $[\delta x_f, \delta y_f]^T$ .

For the sake of observability [7] two ground objects will be tracked. The observation matrix for tracking two unknown ground features

$$\mathbf{H}_{uu}(l) = \left[ \begin{array}{cccc}
 -1 & 0 & -1 & 0 \\
 0 & -1 & 0 & -1 \\
 -x_{f1} & -y_{f1} & -x_{f2} & -y_{f2} \\
 0 & 0 & 0 & 0 \\
 0 & 0 & 0 & 0 \\
 0 & 0 & 0 & 0 \\
 -x_{f1}y_{f1}z_l & -(1+y_{f1}^2)z_l & -x_{f2}y_{f2}z_l & -(1+y_{f2}^2)z_l \\
 (1+x_{f1}^2)z_l & x_{f1}y_{f1}z_l & (1+x_{f2}^2)z_l & x_{f2}y_{f2}z_l \\
 y_{f1}z_l & -x_{f1}z_l & y_{f2}z_l & -x_{f2}z_l \\
 0 & 0 & 0 & 0 \\
 0 & 0 & 0 & 0 \\
 0 & 0 & 0 & 0 \\
 0 & 0 & 0 & 0 \\
 0 & 0 & 0 & 0 \\
 1 & 0 & 0 & 0 \\
 0 & 1 & 0 & 0 \\
 0 & 0 & 1 & 0 \\
 0 & 0 & 0 & 1
 \end{array} \right]^T \quad (3.103)$$

**3.4.4 Performance of Aided INS.** The munition is in a free fall, that is,  $v_z(0) = 0$  and its acceleration is  $-g$  along the  $Z_n$  axis until it reaches terminal velocity. The nominal vertical drop is such that  $h_{rel} = 7500$  [m]. The terminal  $v_{term} = 100 \frac{m}{s}$  so that the free fall is 10 seconds and the duration of the vertical drop is 80 seconds. The nominal trajectory is

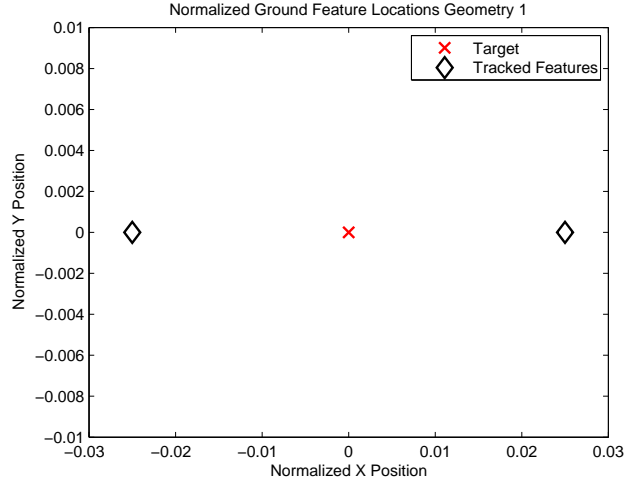


Figure 3.5: The locations of the tracked ground features in the first geometry.

$x(t) = 0, y(t) = 0$  and

$$z(t) = \begin{cases} 7500 - 5t^2 & \forall 0 \leq t < t_{term} \\ 7000 - 100(t - t_{term}) & \forall t_{term} \leq t \leq T \end{cases}$$

Once the terminal velocity has been reached there is no further acceleration and the vertical speed is constant. Two ground feature geometries were considered. The first is shown in Figure 3.5. For this geometry, in the observation matrix

$$x_{f1}(l) = \frac{x_{p1}}{z_l} = \frac{.025}{z_l}$$

$$x_{f2}(l) = \frac{x_{p2}}{z_l} = \frac{-.025}{z_l}$$

$$y_{f1}(l) = y_{f2}(l) = 0, \quad l = 0, \dots, N-1$$

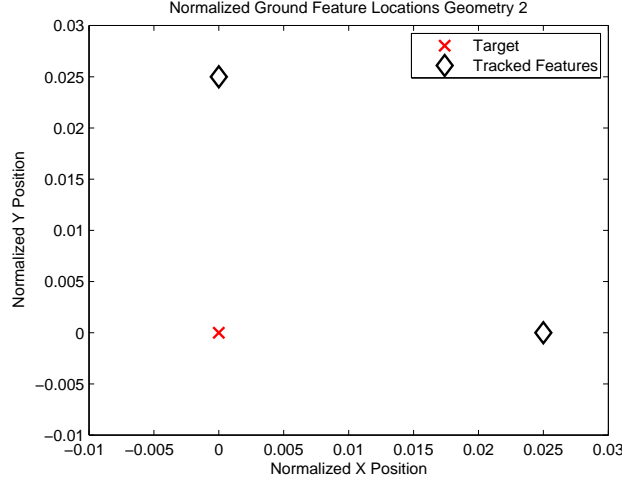


Figure 3.6: The locations of the tracked ground features in the second geometry.

The second geometry is shown in Figure 3.6. For this geometry, in the observation matrix

$$\begin{aligned}
 x_{f1}(l) &= \frac{x_{p1}}{z_l} = \frac{.025}{z_l} \\
 x_{f2}(l) &= y_{f1}(l) = 0 \\
 y_{f2}(l) &= \frac{y_{p2}}{z_l} = \frac{.025}{z_l}, \quad l = 0, \dots, N-1
 \end{aligned}$$

**3.4.5 Initialization.** It is stipulated that initially, the INS has zero error in the navigation states, that is, the INS alignment was perfect, and the states representing the biases in the sensors are

$$\begin{array}{lll}
 \delta f_x^{(b)} \sim N(0, \sigma_a^2) & \delta f_y^{(b)} \sim N(0, \sigma_a^2) & \delta f_z^{(b)} \sim N(0, \sigma_a^2) \\
 \delta \omega_x \sim N(0, \sigma_g^2) & \delta \omega_y \sim N(0, \sigma_g^2) & \delta \omega_z \sim N(0, \sigma_g^2)
 \end{array}$$

The  $x$ ,  $y$  and  $z$  accelerometers are of the same quality, and also the  $x$ ,  $y$  and  $z$  gyroscopes are of the same quality. Thus

$$\delta \mathbf{x}(\mathbf{0}) \sim N(\mathbf{0}, \mathbf{P}(0))$$

with the initial covariance matrix  $\mathbf{P}(0)$  given by Eq. (3.69).

**3.4.6 Transitioning Between Measurement Epochs.** In the pure free fall case, there are three measurement epochs. The first is while the munition is accelerating toward the earth. The duration of the first epoch is one nondimensional second. There is  $N = 100$  discrete steps per nondimensional second.

Therefore, in epoch 1 the observation matrix  $\mathbf{H}_{uu}(l)$ , and the dynamics matrix  $\mathbf{A}_{ad15 \times 15}$  based on the nominal accelerometer values from Eq. (3.96) were used. In the first epoch, the uncertainty of the states were propagated for one hundred steps using the covariance propagate and update equations of the Kalman filter, Eqs. (3.44)(3.46), where  $\mathbf{R}$  is the measurement uncertainty caused by one pixel in the camera's focal plane

$$\begin{bmatrix} \delta x_{f1} \\ \delta y_{f1} \\ \delta x_{f2} \\ \delta y_{f2} \end{bmatrix} \sim N(\mathbf{0}, \mathbf{R})$$

We assume a 9 Megapixel camera with an aspect ratio of 1. However, recall from Eqs. (3.100) and (3.101) that the measurement error terms on the RHS are multiplied by the time-varying altitude  $z_l$ . Therefore, the nondimensional

$$\mathbf{R} = z_l^2 \begin{bmatrix} \frac{1}{9} & 0 & 0 & 0 \\ 0 & \frac{1}{9} & 0 & 0 \\ 0 & 0 & \frac{1}{9} & 0 \\ 0 & 0 & 0 & \frac{1}{9} \end{bmatrix} \times 10^{-6} \quad (3.104)$$

where  $z_l$  is squared to match  $\mathbf{R}$ . If  $\mathbf{R}$  was standard deviation of the noise instead of the variance then  $z_l$  would not need to be squared.

At the conclusion of the first one hundred steps/the first measurement epoch the munition reached terminal velocity. Thus the next time block required the use of the dynamics matrix  $\mathbf{A}_{ad15 \times 15}$  to be based on the nominal accelerometer values from

Eq. (3.97). The second measurement epoch was 6 nondimensional seconds long. Without any further transitions, Eqs. (3.44)-(3.46) were repeated for  $101 \leq l \leq 700$ , using the updated dynamics matrix.

We assumed a camera Field of View (FOV) of 50 milliradians. Based on the geometry set forth in Figure 3.5, the ground features leave the camera FOV when the munition is 1000 meters above the ground,  $h_{final}$ . Thus the third and final measurement epoch started when the munition reached  $h_{final}$  in 70 seconds. In the final 10 seconds of its flight the INS is not aided, and one reverts to a free INS. As such the calculations using the KF equations, (3.44)-(3.46), were terminated and the calculation for the free INS, Eq. (3.21), was used for the last 10 seconds.

This process was completed for both geometries listed at the beginning of Subsection 3.4.4.

## 4 Covariance Analysis Results

### 4.1 Introduction

This chapter is broken up into the three sections: Section 4.2 covers the two dimensional case, Section 4.3 shows the case where the A/C was flying horizontally, and Section 4.4 discusses the case where a munition is in vertical free fall, for both of the geometries considered. All three sections will start with baseline plots showing the development of the standard deviations of the position estimates from the unaided INS. This information will then be followed by plots of the aided INS. Plots showing the remainder of the navigation states, for both the unaided and aided INS schemes are found in Appendices A-C.

### 4.2 Two Dimensional Results

Initially the standard deviation of the navigation states of the unaided INS were plotted as a baseline. As expected, the standard deviation of the  $x$  position was 1 kilometer after one hour. The standard deviations for the  $x$  and  $z$  positions are shown in Figure 4.1. There was a significant degree of aiding achieved with this scheme, shown in Figure 4.2. After an hour of flight the standard deviation in the  $x$  position is only five meters, an improvement of 99.5% off of the unaided system. If one multiplies the position standard deviations produced by the unaided INS scheme, the area of uncertainty is calculated

$$\sigma_{area} = \sigma_x(360N) \times \sigma_z(360N) = .7071 [km^2] \quad (4.1)$$

That means that the A/C is likely to be somewhere inside a square with that area. That being said, if the same process is applied to the aided scheme

$$\sigma_{area} = \sigma_x(360N) \times \sigma_z(360N) = 1.8771 \times 10^{-7} [km^2] \quad (4.2)$$

There is an eight order of magnitude improvement in the uncertainty of the position estimate of the aided case over the unaided case!

But the  $x$  position was not the only navigation state that was aided. The other four states showed an order of magnitude reduction in uncertainty as well, shown in Figures A.1-A.4. A side-by-side comparison of the navigation state vector standard deviations is shown in Table 4.1.

In the best tradition of SLAM, the aiding action factored into the uncertainty of the ground objects' position as well. Notice that in Figure A.5 the ground objects' position standard deviation trends similarly as the  $x$  position standard deviation. A closer inspection of the ground objects' position uncertainty in Figure A.6 shows how at the beginning of each epoch there is a spike for  $x_{p2}$ . This is due to the initialization error from the LOS angle error of the camera. There is a jump in the position uncertainty of  $x_{p1}$  as well, but it is far less drastic than for  $x_{p2}$ , but that is because the position uncertainty of  $x_{p2}$  at the end of an epoch becomes the position uncertainty of  $x_{p1}$  at the beginning of the next epoch.

Table 4.1: The peak/final standard deviation values for the unaided navigation states. Also included are the peak and final standard deviations for aided navigation states for the two-dimensional case.

Standard Deviation	Unaided Final Value	Aided Peak Value	Aided Final Value
$\sigma_x$	1 [km]	4.7 [m]	4.7 [m]
$\sigma_z$	.7071 [km]	.1 [m]	.04 [m]
$\sigma_{Vx}$	$7 \times 10^{-3}$ [m/s]	$8.21 \times 10^{-5}$ [m/s]	$4.0 \times 10^{-5}$ [m/s]
$\sigma_{Vz}$	$4 \times 10^{-3}$ [m/s]	$3.9 \times 10^{-5}$ [m/s]	$2.2 \times 10^{-7}$ [m/s]
$\sigma_\theta$	$3.27 \times 10^{-5}$ [rad]	$3.31 \times 10^{-6}$ [rad]	$2.44 \times 10^{-7}$ [rad]

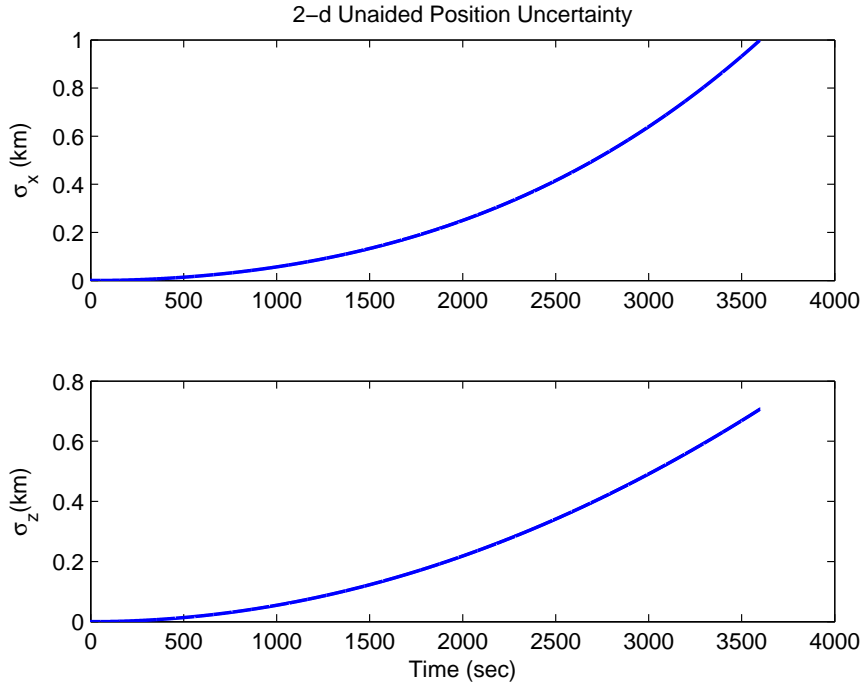


Figure 4.1: The 2-d standard deviation of the position states in the unaided, free INS

### 4.3 Horizontal Three Dimensions

The results for the three dimensional calculations showed strong correlation to the two dimensional case, though more insight was offered to the attitude navigation states. As expected the unaided INS had a standard deviation for the  $x$  and  $y$  positions of 1 kilometer each, shown in Figure 4.3 with the improvement produced by the aiding scheme shown in Figure 4.4. Once again the horizontal position uncertainties dropped to a little below five meters. If we multiply the position standard deviations produced by the unaided INS scheme, we calculate a volume of uncertainty

$$\sigma_{vol} = \sigma_x(360N) \times \sigma_y(360N) \times \sigma_z(360N) = .7071[km^3] \quad (4.3)$$

That means that the A/C is very likely to be somewhere inside a box with that volume.

That being said, if the same process is applied to the aided scheme

$$\sigma_{vol} = \sigma_x(360N) \times \sigma_y(360N) \times \sigma_z(360N) = 7.4177 \times 10^{-10}[km^3] \quad (4.4)$$

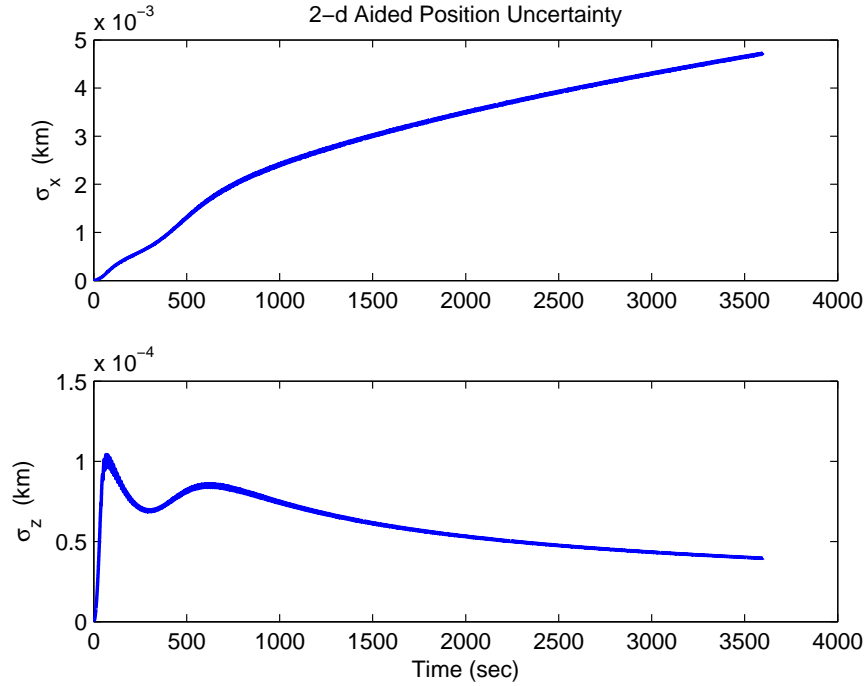


Figure 4.2: The 2-d standard deviation of the position states in the aided INS

There is an eleven order of magnitude improvement in the uncertainty of the position estimate of the aided case over the unaided case! Five of the other six navigation states showed an order of magnitude improvement as well, seen by comparing the peak and final navigation states' standard deviations shown in Table 4.2. The temporal development of the standard deviations of the velocity and attitude states is shown in Figures B.1-B.4.

Once again, there is a relationship between the uncertainty of the A/C position estimate and the ground features' position uncertainty. As shown in Figures B.5 and B.6 the  $x$  and  $y$  position standard deviations of the ground features trend similarly to the  $x$  and  $y$  position standard deviations of the A/C.

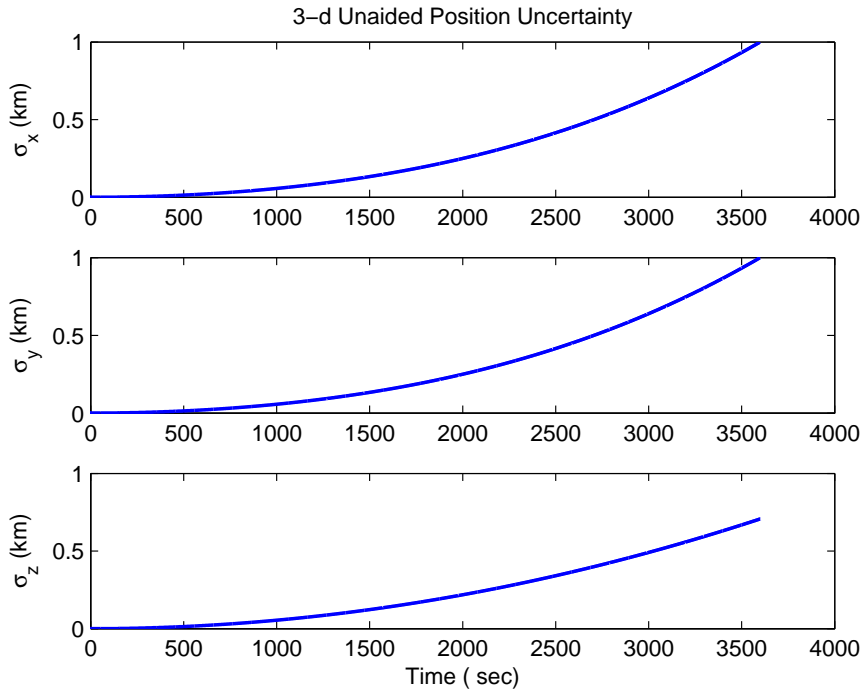


Figure 4.3: The 3-d standard deviation of the position states in the unaided, free INS

#### 4.4 Vertical Three Dimensions

Once again there was a considerable decrease in the uncertainty of the position estimate from the unaided case, Figure 4.5, to the two aided schemes, Figures 4.6 and 4.7. The final standard deviations of the unaided  $x$ ,  $y$ , and  $z$  positions are about 35 meters. For the first geometry, the horizontal position estimates had standard deviations of about 12 centimeters, with the  $z$  standard deviation ending around 4.3333 meters. The second geometry produced  $x$ ,  $y$  and  $z$  standard deviations of 12 centimeters, 17 centimeters and 1 micrometer respectively. This shows that by removing the symmetry in the ground feature geometry the uncertainty of the altitude state drops greatly. To put this in another perspective, the unaided volume of uncertainty is  $4.1 \times 10^4 \text{ m}^3$  and the aided volume of uncertainty for the second geometry is  $2.05 \times 10^{-8} \text{ m}^3$ .

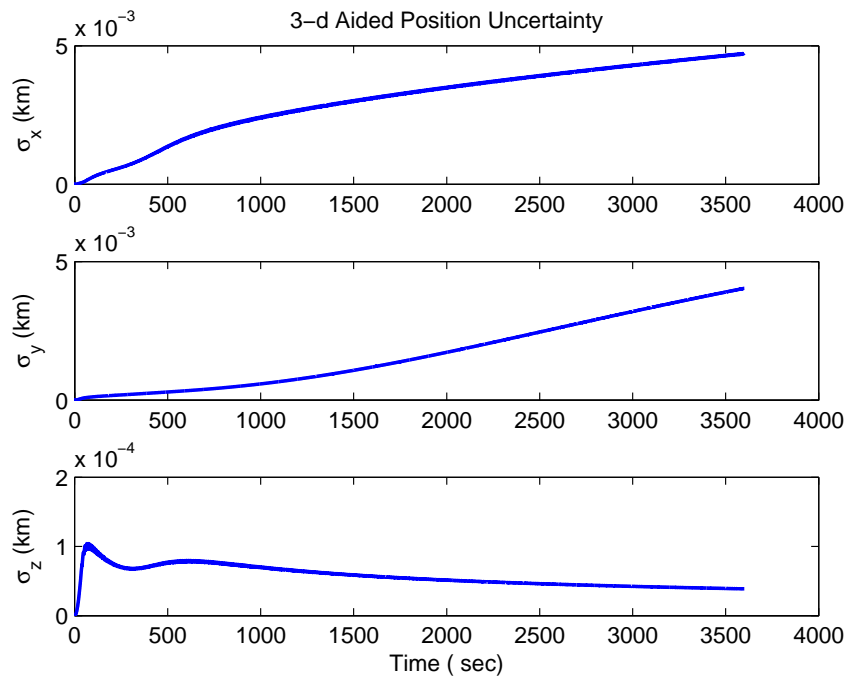


Figure 4.4: The 3-d standard deviation of the position states in the aided INS

The temporal development of the unaided standard deviation for the velocity and attitude states is shown in Figures C.1-C.2. The temporal development of the aided standard deviations for both geometries is shown in Figures C.3-C.10. The peak and final standard deviations for the first geometry are listed in Table 4.3

Table 4.2: The peak/final standard deviation values for the unaided navigation states. Also included are the peak and final standard deviations for aided navigation states for the three-dimensional horizontal case.

Standard Deviation	Unaided Final Value	Aided Peak Value	Aided Final Value
$\sigma_x$	1 [km]	4.7 [m]	4.7 [m]
$\sigma_y$	1 [km]	4.0 [m]	4.0 [m]
$\sigma_z$	.7071 [km]	0.10 [m]	0.0389 [m]
$\sigma_{Vx}$	$7 \times 10^{-3}$ [m/s]	$8.21 \times 10^{-5}$ [m/s]	$3.93 \times 10^{-5}$ [m/s]
$\sigma_{Vy}$	$7 \times 10^{-3}$ [m/s]	$3.06 \times 10^{-5}$ [m/s]	$2.29 \times 10^{-5}$ [m/s]
$\sigma_{Vz}$	$4 \times 10^{-3}$ [m/s]	$3.9 \times 10^{-5}$ [m/s]	$2.16 \times 10^{-7}$ [m/s]
$\sigma_\phi$	$3.27 \times 10^{-5}$ [rad]	$2.40 \times 10^{-6}$ [rad]	$1.07 \times 10^{-7}$ [rad]
$\sigma_\theta$	$3.27 \times 10^{-5}$ [rad]	$3.16 \times 10^{-6}$ [rad]	$2.39 \times 10^{-7}$ [rad]
$\sigma_\psi$	$3.27 \times 10^{-5}$ [rad]	$2.23 \times 10^{-5}$ [rad]	$2.23 \times 10^{-5}$ [rad]

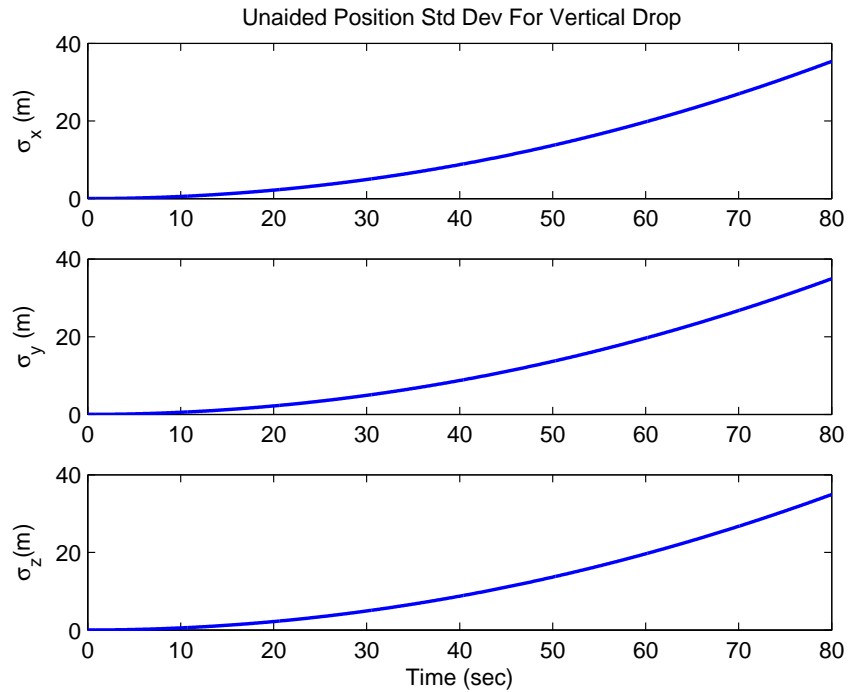


Figure 4.5: The 3-d standard deviation of the position states in the unaided, free, INS for the vertical drop

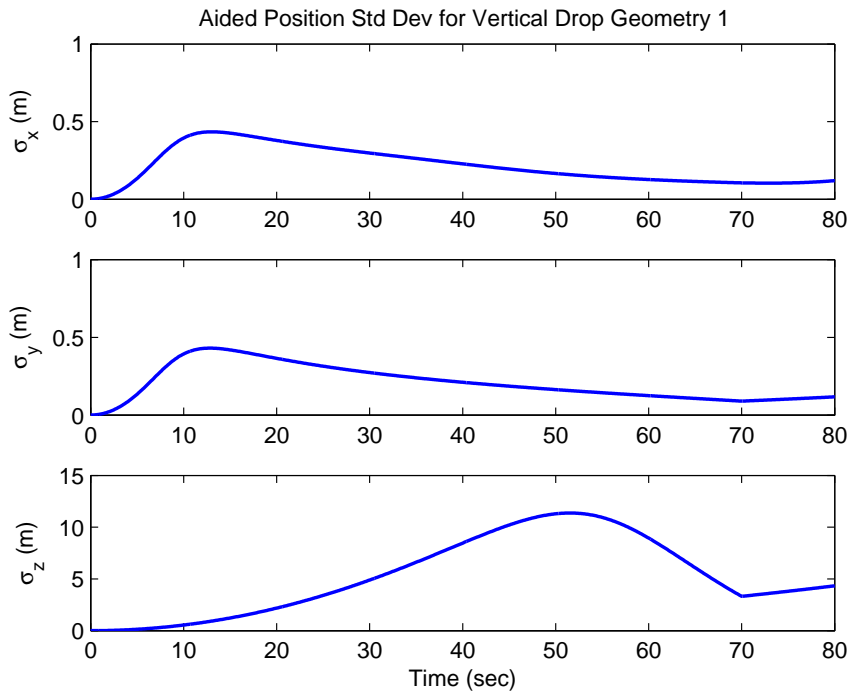


Figure 4.6: The development of the standard deviation of the position errors in the aided INS for geometry 1 for the vertical drop.

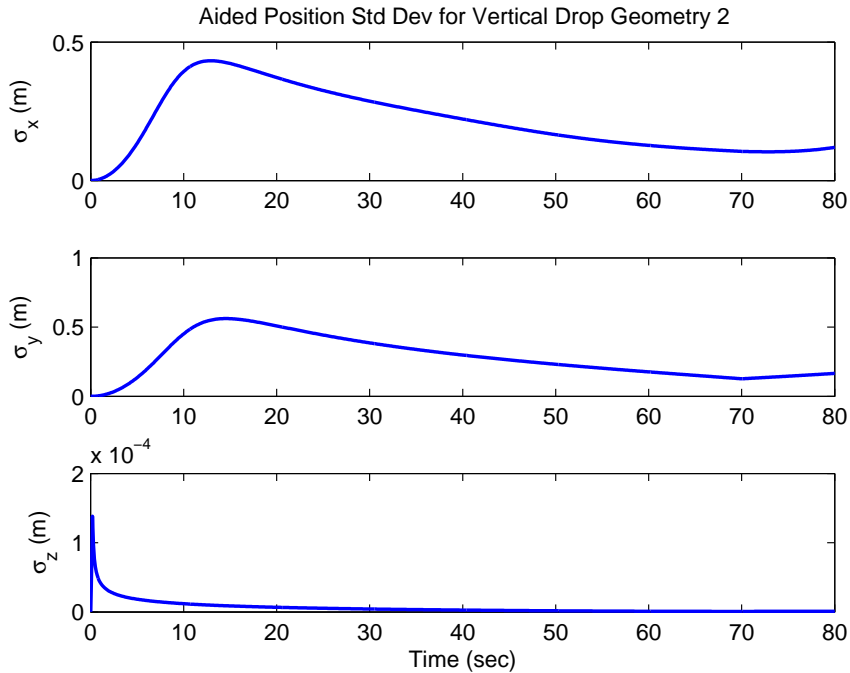


Figure 4.7: The development of the standard deviation of the position errors in the aided INS for geometry 2 for the vertical drop.

Table 4.3: The peak/final standard deviation values for the unaided navigation states. Also included are the peak and final standard deviations for aided navigation states for the vertical three-dimensional case using the first geometry shown in Section 3.4.

Standard Deviation	Unaided Final Value	Aided Peak Value	Aided Final Value
$\sigma_x$	35.4 [m]	43.4 [cm]	11.97 [cm]
$\sigma_y$	34.9 [m]	43.0 [cm]	11.70 [cm]
$\sigma_z$	34.9 [m]	11.4 [m]	4.33 [m]
$\sigma_{Vx}$	.899 [m/s]	.079 [m/s]	.011 [m/s]
$\sigma_{Vy}$	.873 [m/s]	.079 [m/s]	.0029 [m/s]
$\sigma_{Vz}$	.873 [m/s]	.458 [m/s]	.11 [m/s]
$\sigma_\phi$	$7.27 \times 10^{-5}$ [rad]	$7.27 \times 10^{-5}$ [rad]	$7.27 \times 10^{-5}$ [rad]
$\sigma_\theta$	$7.27 \times 10^{-5}$ [rad]	$2.74 \times 10^{-5}$ [rad]	$.937 \times 10^{-5}$ [rad]
$\sigma_\psi$	$7.27 \times 10^{-5}$ [rad]	$7.27 \times 10^{-5}$ [rad]	$7.27 \times 10^{-5}$ [rad]

Table 4.4: The peak/final standard deviation values for the unaided navigation states. Also included are the peak and final standard deviations for aided navigation states for the vertical three-dimensional case using the second geometry shown in Section 3.4.

Standard Deviation	Unaided Final Value	Aided Peak Value	Aided Final Value
$\sigma_x$	35.4 [m]	43.2 [cm]	11.97 [cm]
$\sigma_y$	34.9 [m]	56.1 [cm]	16.55 [cm]
$\sigma_z$	34.9 [m]	.14 [mm]	1.0365 [micron]
$\sigma_{Vx}$	.899 [m/s]	.079 [m/s]	.011 [m/s]
$\sigma_{Vy}$	.873 [m/s]	.091 [m/s]	.0041 [m/s]
$\sigma_{Vz}$	.873 [m/s]	.0014 [m/s]	25.91 [nm/s]
$\sigma_\phi$	$7.27 \times 10^{-5}$ [rad]	$2.17 \times 10^{-5}$ [rad]	$.929 \times 10^{-5}$ [rad]
$\sigma_\theta$	$7.27 \times 10^{-5}$ [rad]	$2.17 \times 10^{-5}$ [rad]	$.929 \times 10^{-5}$ [rad]
$\sigma_\psi$	$7.27 \times 10^{-5}$ [rad]	$7.27 \times 10^{-5}$ [rad]	$7.27 \times 10^{-5}$ [rad]

## 5 Conclusion

### 5.1 Conclusions

Demonstrating INS aiding action using vision while loitering in the vicinity of a ground feature is a possibility, but then one does not go places. The “bootstrapping” method for INS aiding during cross country navigation, that is, using bearing measurements of ground features as they come into view, shows that an aircraft can use its own position to geolocate a ground object, then use that geolocation to strongly aid its own INS and repeat the process as long as necessary. While the errors in the horizontal position will continue to grow unbounded, the rate of growth was cut by 99.5%. If one considers the volume of position uncertainty for the unaided INS is  $.7071 \text{ km}^3$ , from Eq. (4.3), and contrasts that with the position uncertainty volume of the optical tracking aided INS,  $7.4177 \times 10^{-10} \text{ km}^3$ , it is clearly shown that despite the negative connotation of “bootstrapping”, it is a mechanism that makes INS aiding using vision practical for long range flight.

It is also clearly shown that using visual bearings-only measurements greatly reduces the uncertainty in the INS provided navigation state estimate during a vertical drop. This improvement will allow for more accurate guidance of the munition, and therefore a greater chance of the munition hitting its target. This is achieved using a passive means and autonomous guidance.

### 5.2 Follow-On Topics

There are still many ways this research can be expanded upon to take it from the realm of the academic to the operational realm. Consider the following

- Perform an error state analysis. Find out how often the estimates actually fall within  $1\sigma$  of the truth information.

- Consider a maneuvering A/C where the A/C Euler angles cannot be assumed small. There are few instances where a military A/C will be able to fly a straight course to the target. The A/C will need to avoid densely covered air defense areas, when possible. This dictates a maneuver, and sometimes, multiple drastic maneuvers.
- Consider a long range munition on a ballistic terminal trajectory. This would provide an effective means of combining the horizontal and vertical three dimensional cases.
- Transition from a flat, non-rotating Earth to spherical rotating Earth. The higher quality navigation systems will be able to detect the rotation of the Earth, which can introduce further errors into the system.
- Close the guidance-control loop to maneuver the munition towards the target.

## Appendix A: 2-D Standard Deviation Plots

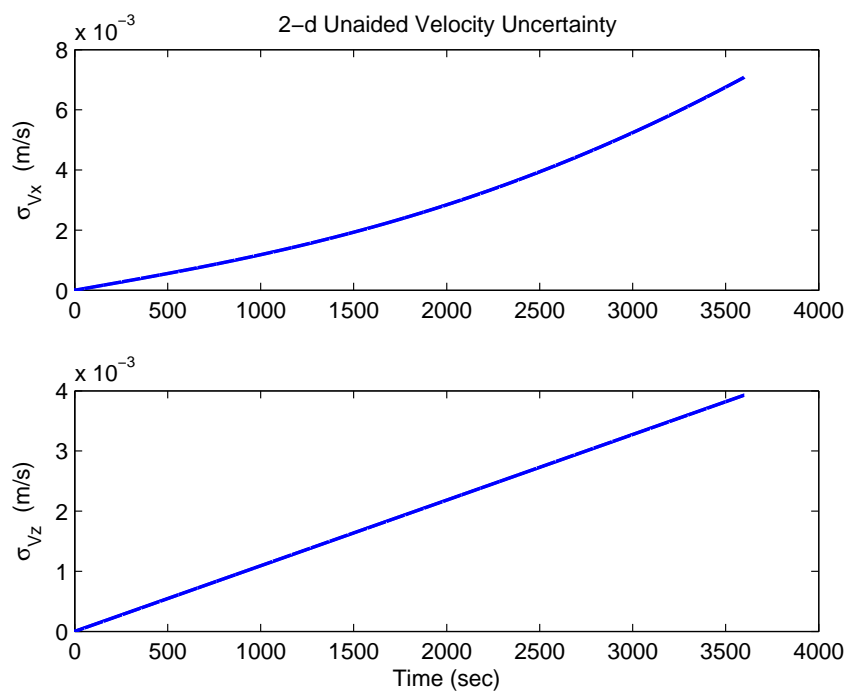


Figure A.1: The 2-d standard deviation of the velocity states in the unaided, free INS

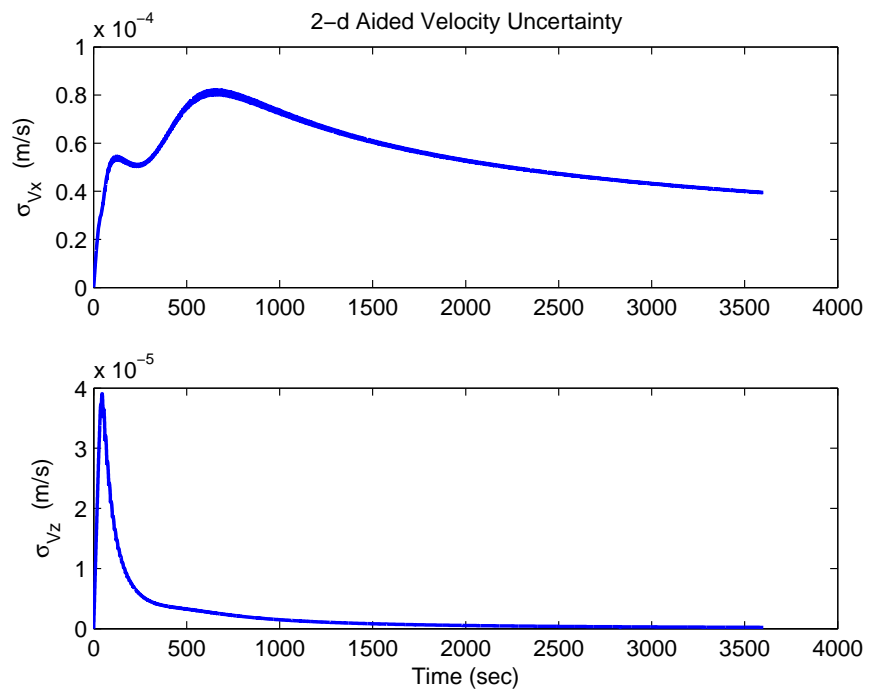


Figure A.2: The 2-d standard deviation of the velocity states in the aided INS

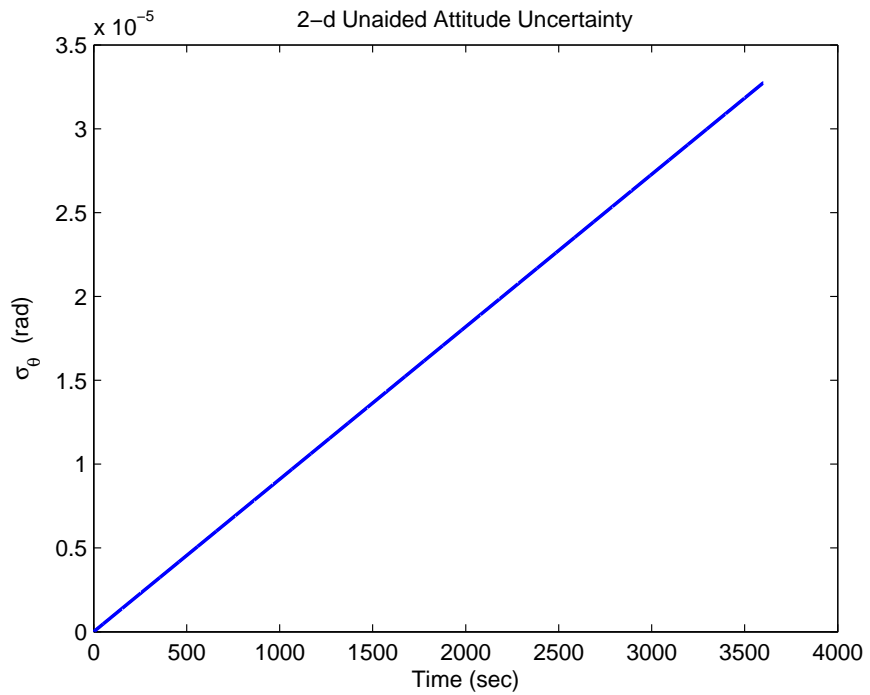


Figure A.3: The 2-d standard deviation of the attitude state in the unaided, free INS

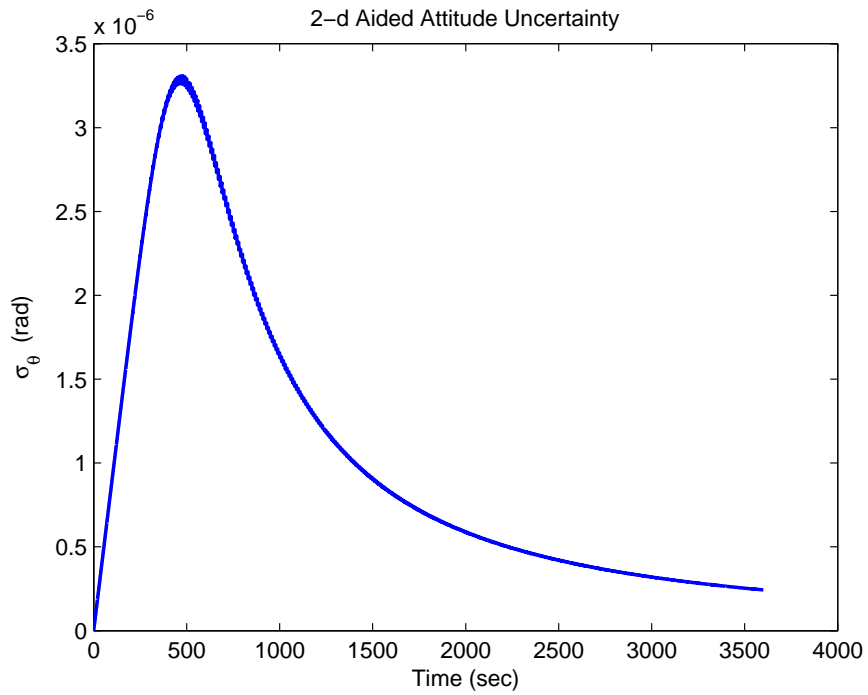


Figure A.4: The 2-d standard deviation of the attitude state in the aided INS

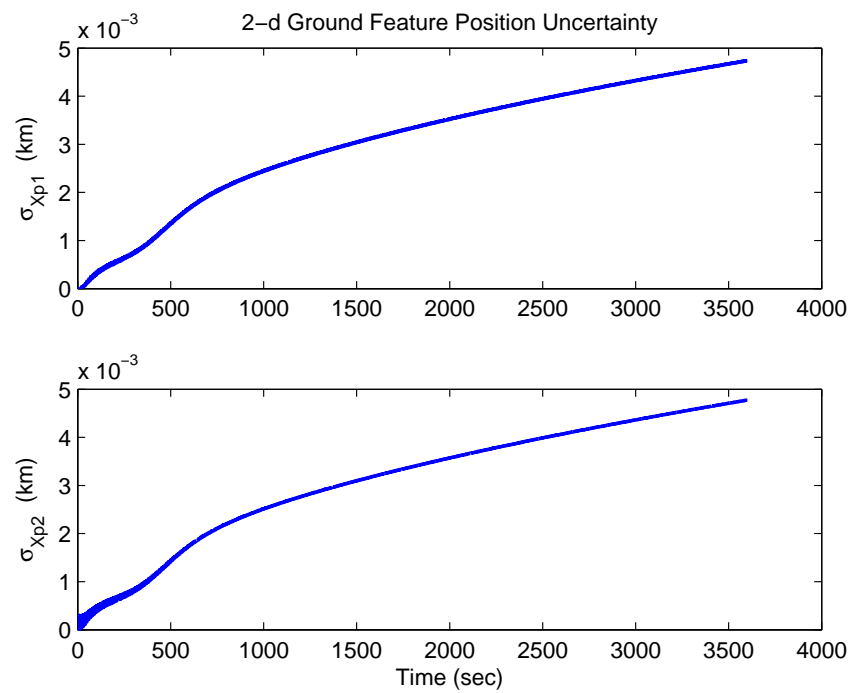


Figure A.5: The standard deviation of the tracked ground objects' position, over 1 hour

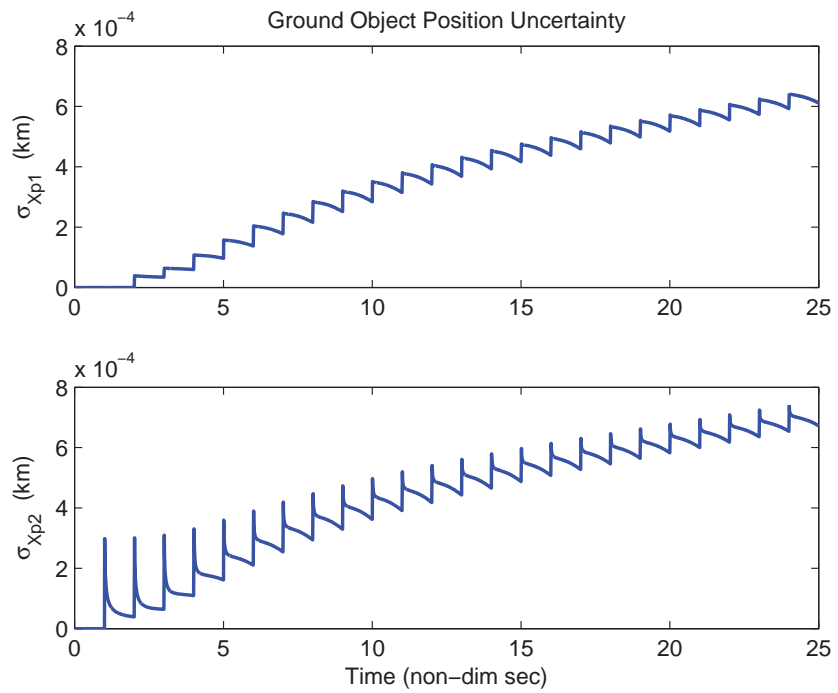


Figure A.6: The standard deviation of the tracked ground objects' position, over 250 seconds

## Appendix B: 3-D Horizontal Plots

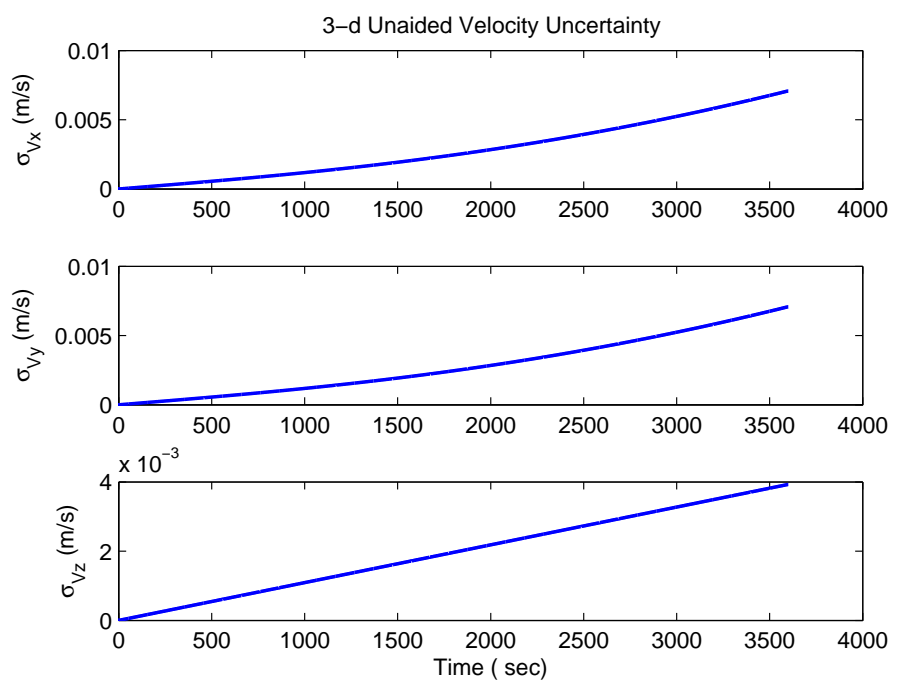


Figure B.1: The 3-d standard deviation of the velocity states in the unaided, free INS

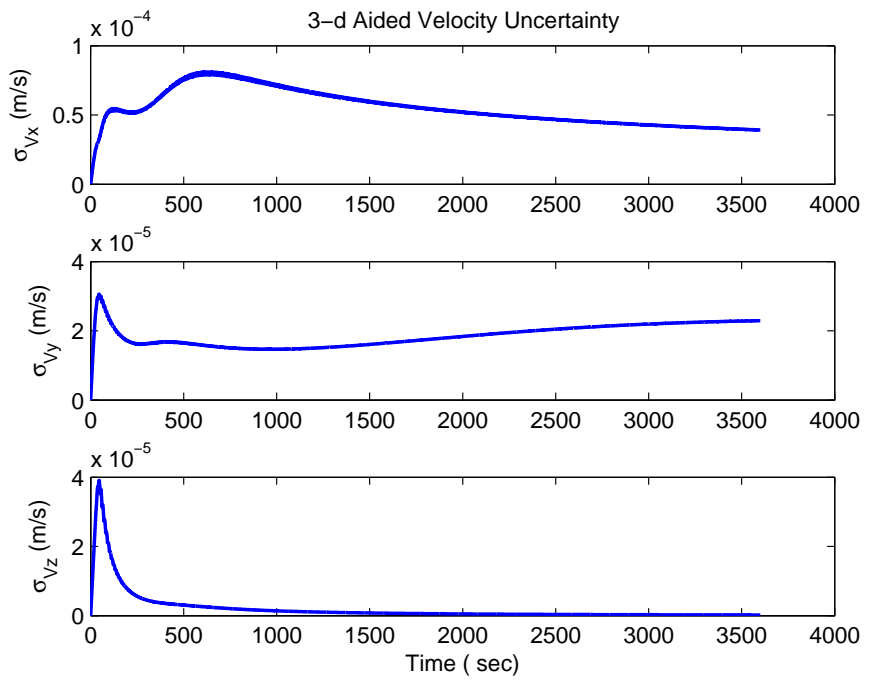


Figure B.2: The 3-d standard deviation of the velocity states in the aided INS

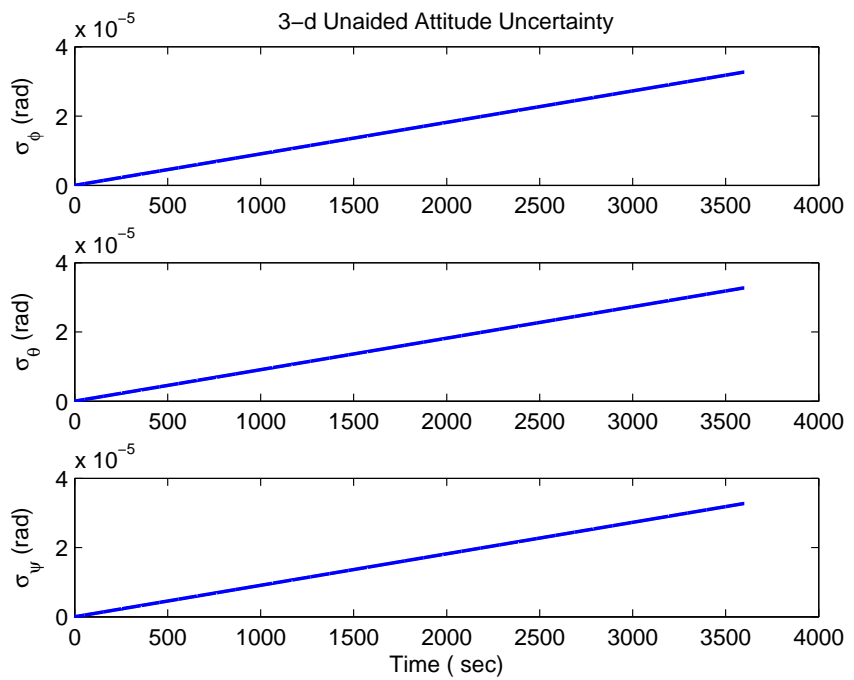


Figure B.3: The 3-d standard deviation of the attitude state in the unaided, free INS

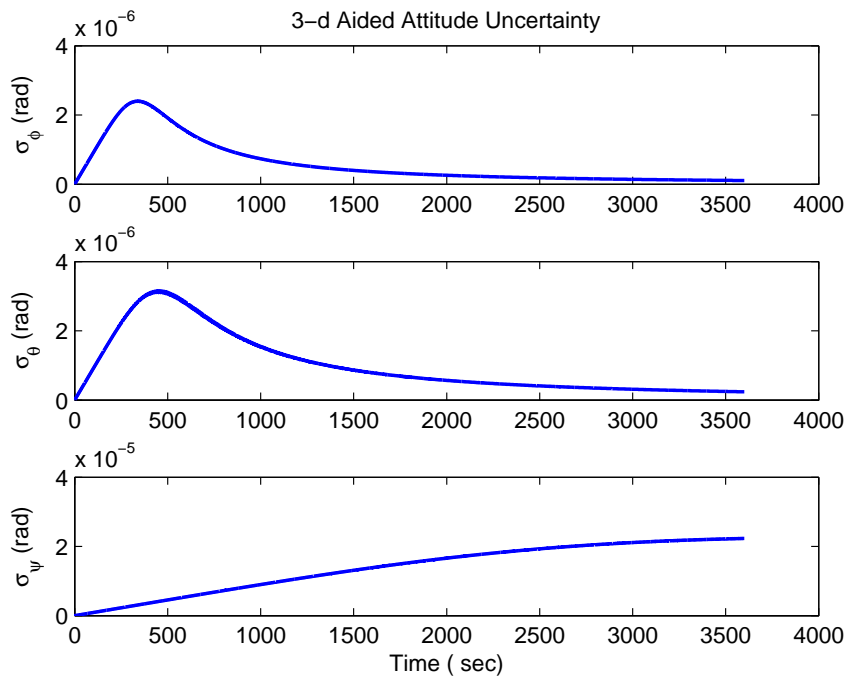


Figure B.4: The 3-d standard deviation of the attitude state in the aided INS

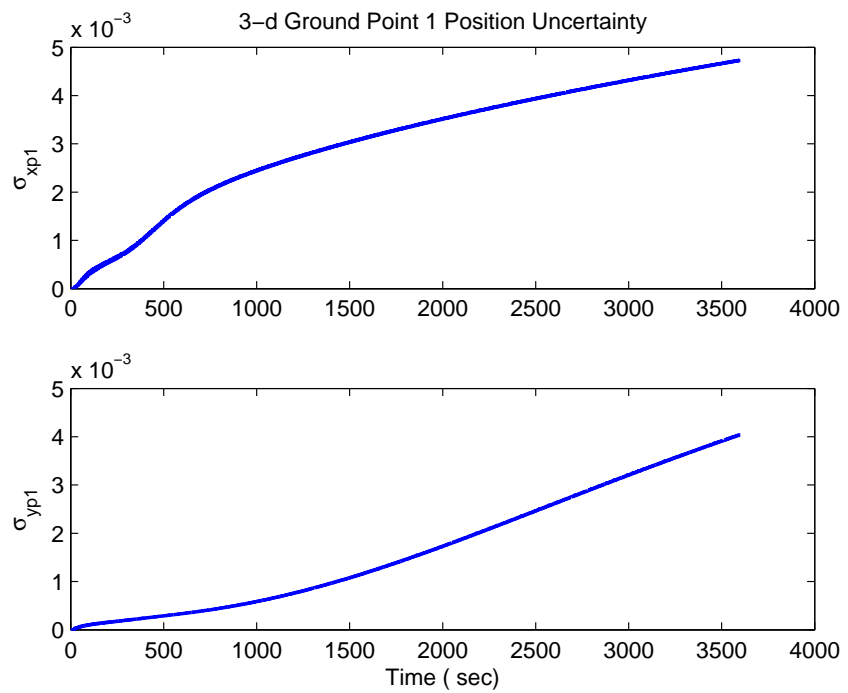


Figure B.5: The standard deviation of the closer tracked ground object's position

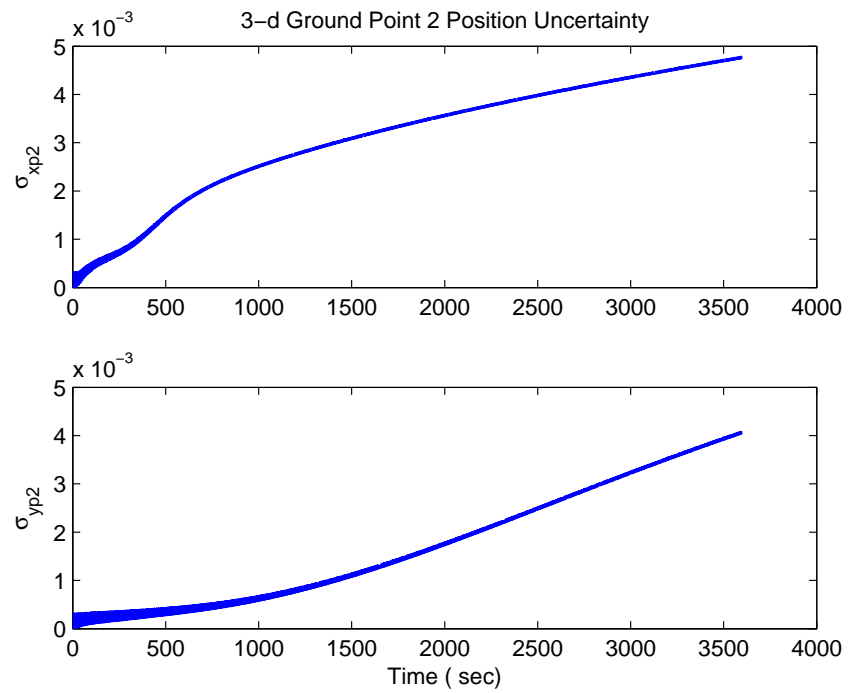


Figure B.6: The standard deviation of the further tracked ground object's position

## Appendix C: 3-D Vertical Plots

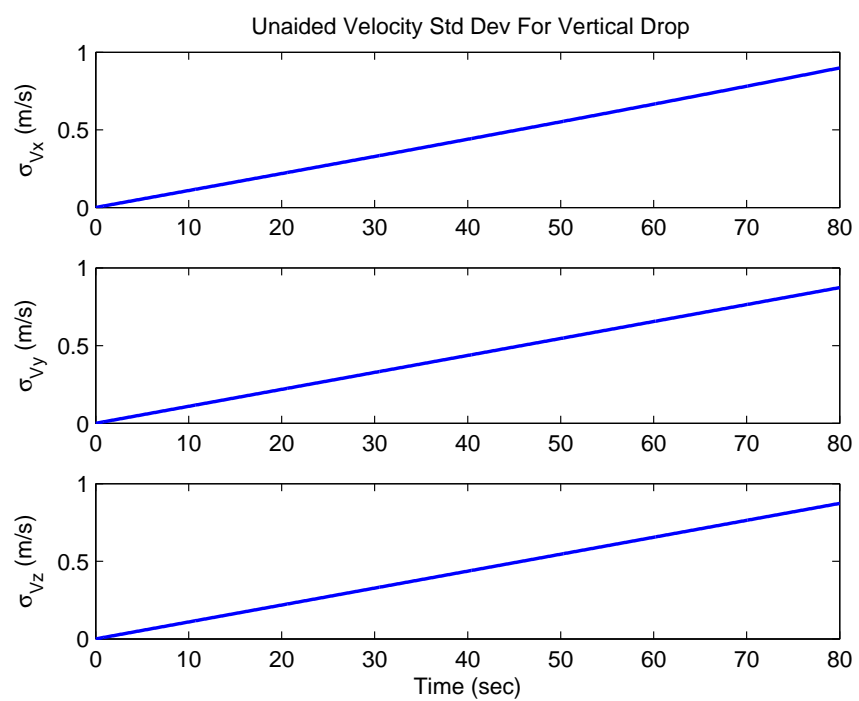


Figure C.1: The development of the standard deviation of the velocity errors in the unaided, free INS for the vertical drop.

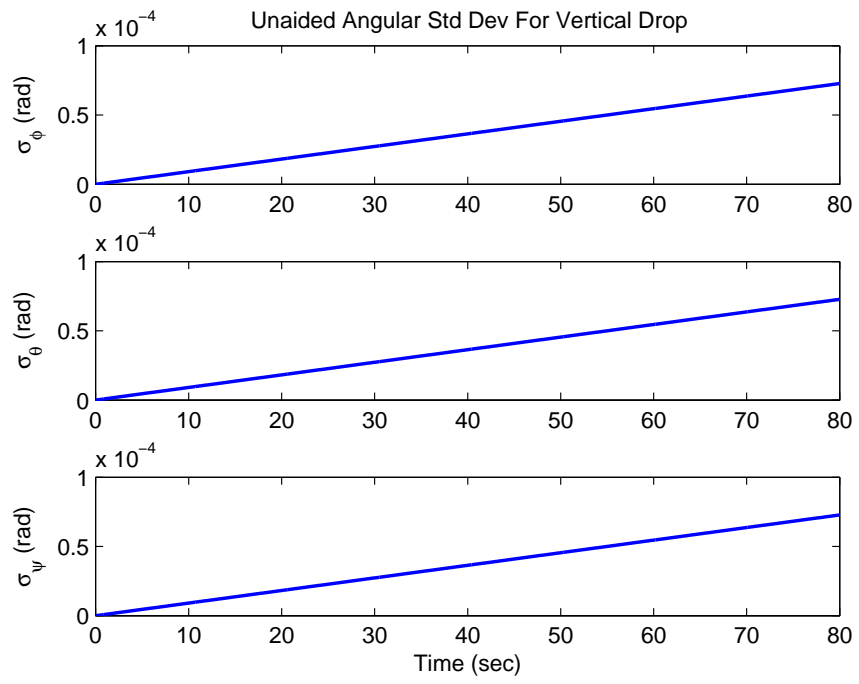


Figure C.2: The development of the standard deviation of the angle errors in the unaided, free INS for the vertical drop.

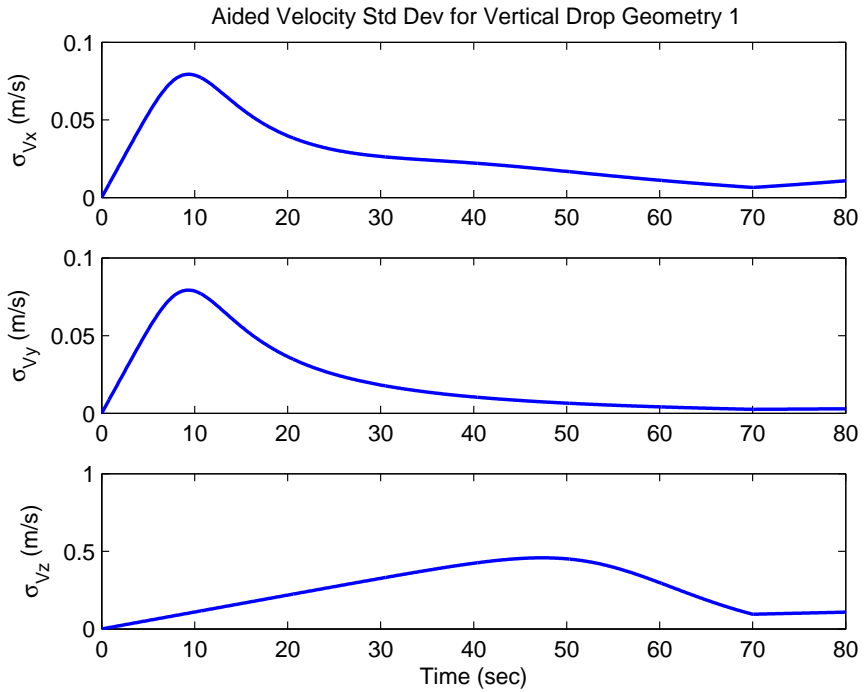


Figure C.3: The development of the standard deviation of the velocity errors in the aided INS for geometry 1 for the vertical drop.

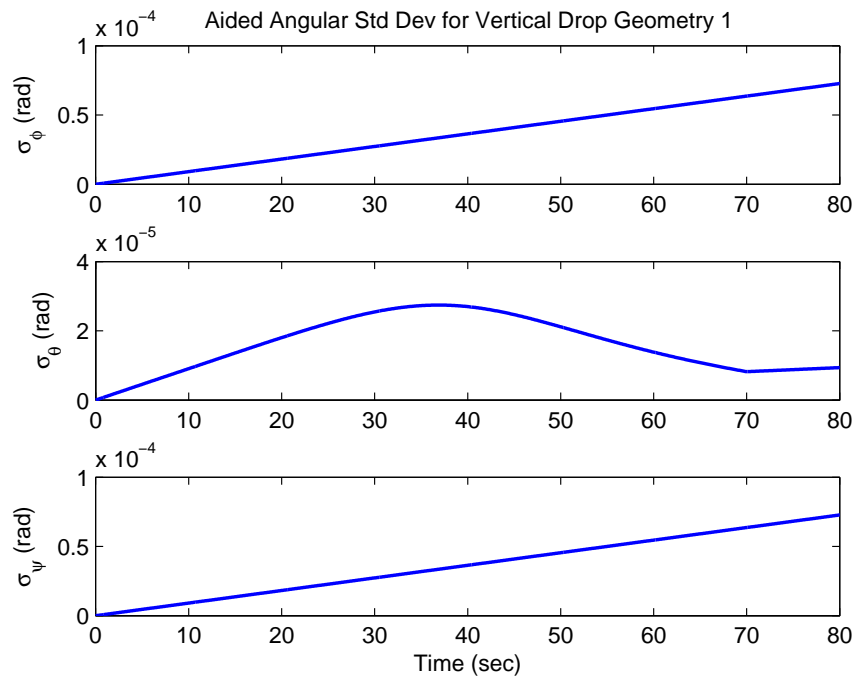


Figure C.4: The development of the standard deviation of the angle errors in the aided INS for geometry 1 for the vertical drop.

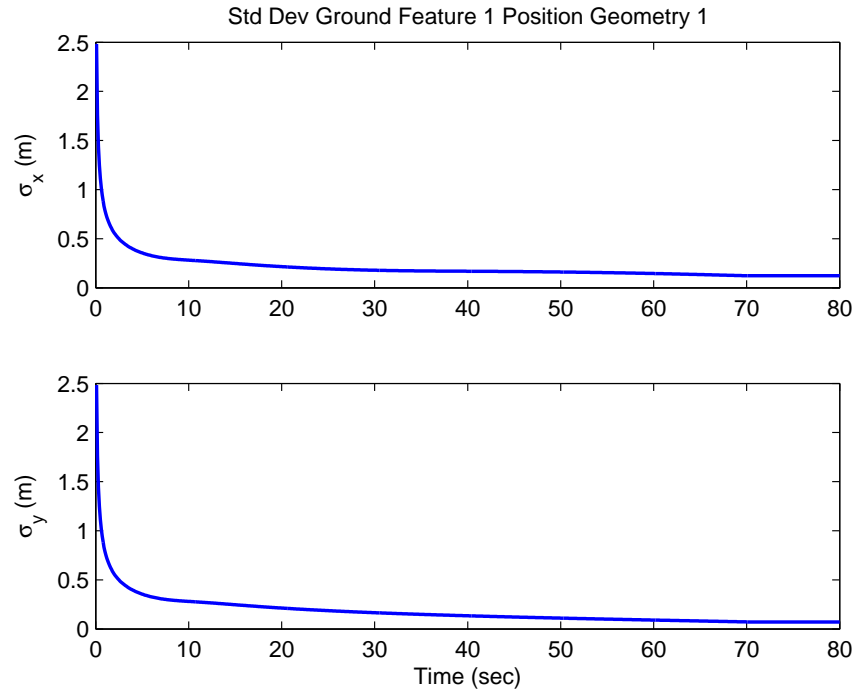


Figure C.5: The development of the standard deviation of the first ground object's position for geometry 1 for the vertical drop.

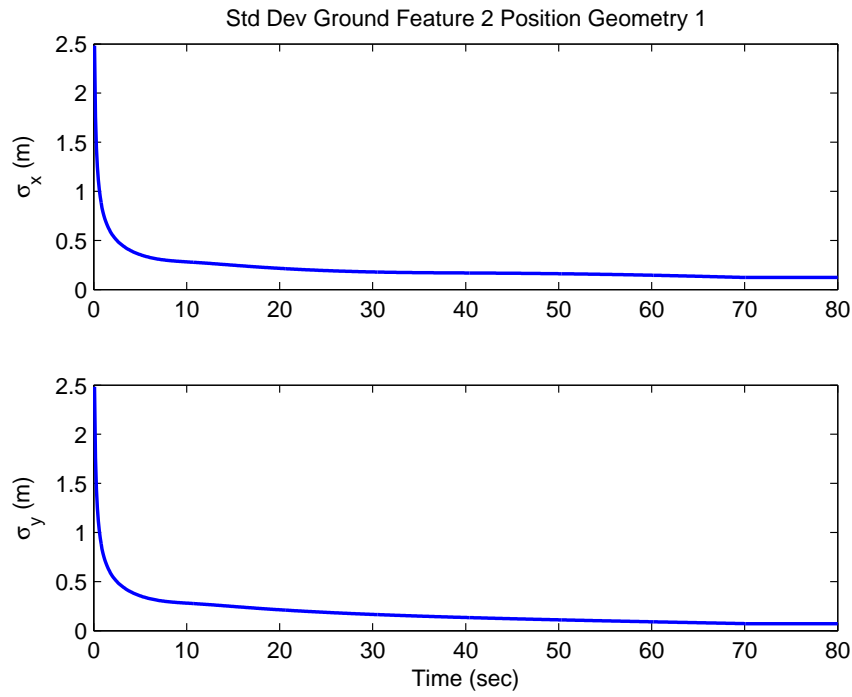


Figure C.6: The development of the standard deviation of the second ground object's position for geometry 1 for the vertical drop.

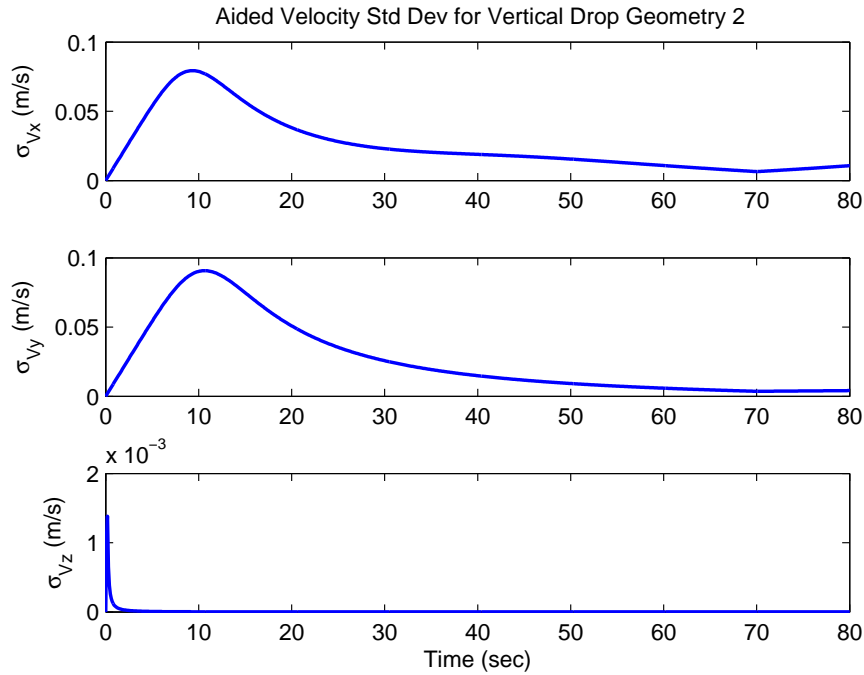


Figure C.7: The development of the standard deviation of the velocity errors in the aided INS for geometry 2 for the vertical drop.

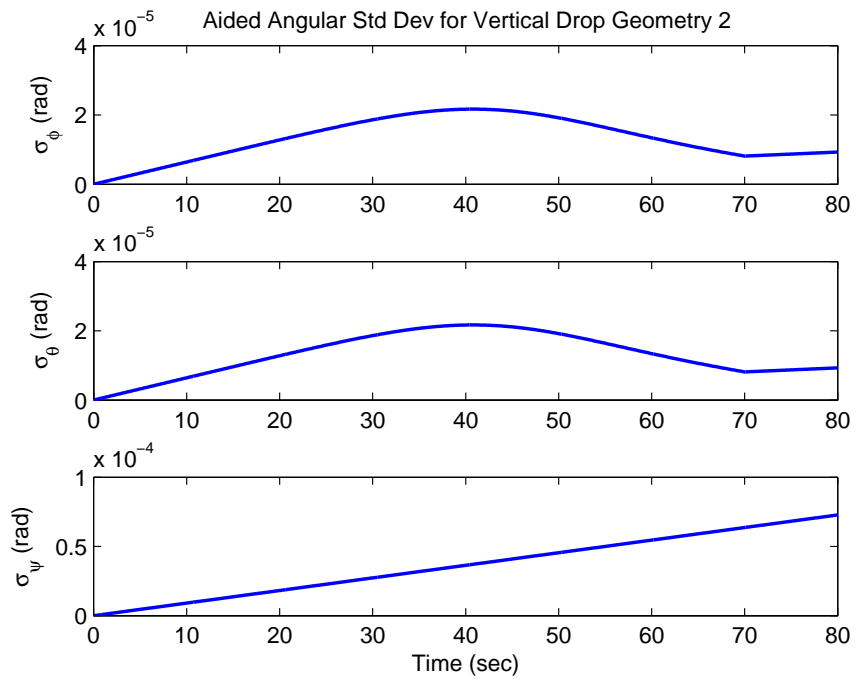


Figure C.8: The development of the standard deviation of the angle errors in the aided INS for geometry 2 for the vertical drop.

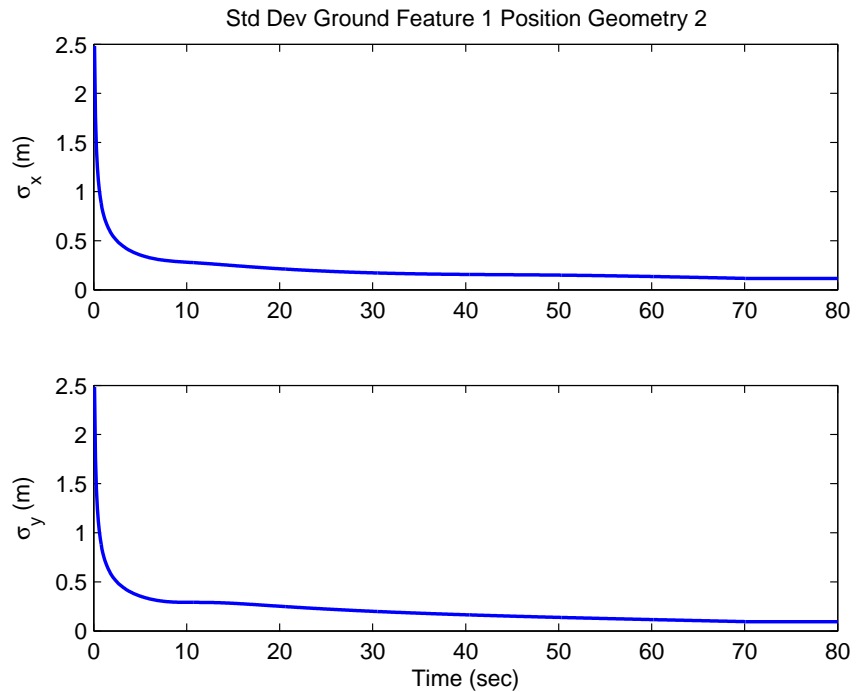


Figure C.9: The development of the standard deviation of the first ground object's position for geometry 2 for the vertical drop.

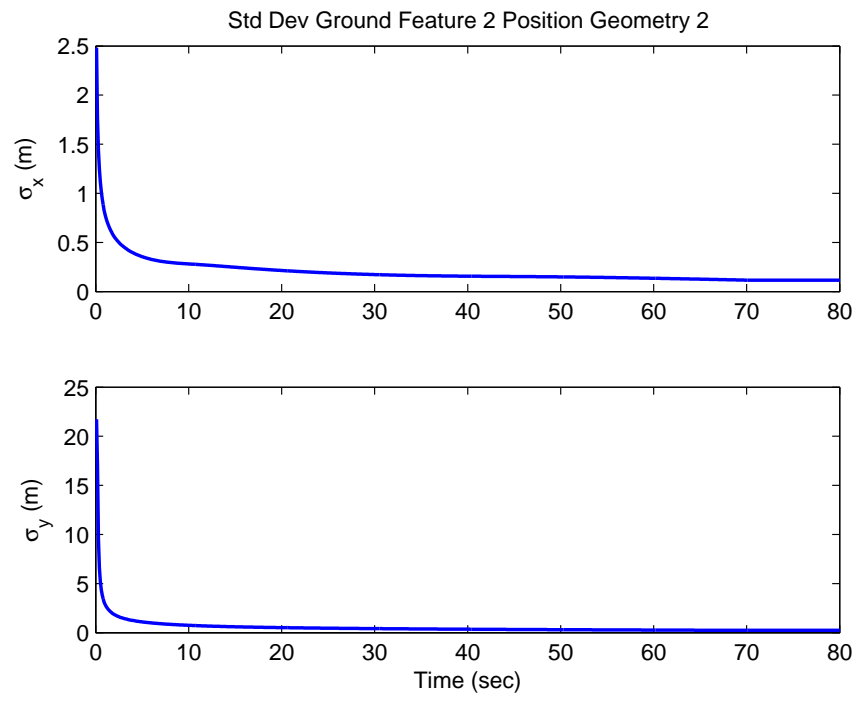


Figure C.10: The development of the standard deviation of the second ground object's position for geometry 2 for the vertical drop.

## Appendix D: General Form Dynamics

The following is the derivation of the state error equations for the case when the Euler angles are not small. It will allow for aircraft maneuvers. The assumptions about a flat and non-rotating Earth are still used.

The DCM relating the accelerometer measurements in the body frame to the specific forces in the navigation frame [9] is

$$\mathbf{C}_b^n = \begin{bmatrix} c\theta c\psi & s\theta s\phi c\psi - c\phi s\psi & c\phi s\theta c\psi + s\phi s\psi \\ c\theta s\psi & s\theta s\phi s\psi + c\phi c\psi & c\phi s\theta s\psi - s\phi c\psi \\ -s\theta & s\phi c\theta & c\theta c\phi \end{bmatrix} \quad (D.1)$$

such that

$$\begin{bmatrix} F_{x_i} \\ F_{y_i} \\ F_{z_i} \end{bmatrix} = \begin{bmatrix} c\theta c\psi & s\theta s\phi c\psi - c\phi s\psi & c\phi s\theta c\psi + s\phi s\psi \\ c\theta s\psi & s\theta s\phi s\psi + c\phi c\psi & c\phi s\theta s\psi - s\phi c\psi \\ -s\theta & s\phi c\theta & c\theta c\phi \end{bmatrix} \begin{bmatrix} f_{x_b} \\ f_{y_b} \\ f_{z_b} \end{bmatrix} \quad (D.2)$$

$$F_{x_i} = (c\theta c\psi)f_{x_b} + (s\theta s\phi c\psi - c\phi s\psi)f_{y_b} + (c\phi s\theta c\psi + s\phi s\psi)f_{z_b} \quad (D.3)$$

$$F_{y_i} = (c\theta s\psi)f_{x_b} + (s\theta s\phi s\psi + c\phi c\psi)f_{y_b} + (c\phi s\theta s\psi - s\phi c\psi)f_{z_b} \quad (D.4)$$

$$F_{z_i} = (-s\theta)f_{x_b} + (s\phi c\theta)f_{y_b} + (c\theta c\phi)f_{z_b} \quad (D.5)$$

However, the sensors have inherent uncertainty in them. As such, Eqs. (D.3)-(D.5) must be perturbed using the First Order Taylor Series Expansion (FOTSE).

$$\begin{aligned} \delta F_{x_i} = & \delta\phi((s\theta c\phi c\psi + s\phi s\psi)f_{y_b} + (c\phi s\psi - s\phi s\theta c\psi)f_{z_b}) \\ & + \delta\theta(-s\theta c\psi f_{x_b} + c\theta s\phi c\psi f_{y_b} + c\theta c\phi c\psi f_{z_b}) \\ & + \delta\psi(-s\psi c\theta f_{x_b} - (s\theta s\phi s\psi + c\theta c\psi)f_{y_b} + (s\phi c\psi - c\phi s\theta s\psi)f_{z_b}) \\ & + \delta f_{x_b}(c\theta c\psi) + \delta f_{y_b}(s\theta s\phi c\psi - c\phi s\psi) + \delta f_{z_b}(c\phi s\theta c\psi + s\phi s\psi) \end{aligned} \quad (D.6)$$

$$\begin{aligned}
\delta F_{yi} = & \delta\phi((s\theta c\phi s\psi - s\phi c\psi)f_{yb} - (s\theta s\phi s\psi + c\phi c\psi)f_{zb}) \\
& + \delta\theta(-s\theta s\psi f_{xb} + c\theta s\phi s\psi f_{yb} + c\theta c\phi s\psi f_{zb}) \\
& + \delta\psi(c\theta c\psi f_{xb} + (s\theta s\phi c\psi - c\phi s\psi)f_{yb} + (s\theta c\phi c\psi + s\phi s\psi)f_{zb}) \\
& + \delta f_{xb}(c\theta s\psi) + \delta f_{yb}(s\theta s\phi s\psi + c\phi c\psi) + \delta f_{zb}(c\phi s\theta s\psi - s\phi c\psi)
\end{aligned} \tag{D.7}$$

and

$$\begin{aligned}
\delta F_{zi} = & \delta\phi(c\theta c\phi f_{yb} - s\phi c\theta f_{zb}) + \delta\theta(-c\theta f_{xb} - s\theta s\phi f_{yb} - s\theta c\phi f_{zb}) \\
& - \delta f_{xb}(s\theta) + \delta f_{yb}(s\phi c\theta) + \delta f_{zb}(c\theta c\phi)
\end{aligned} \tag{D.8}$$

are the results of the FOTSE. The errors in the specific forces are related to the error states by

$$\begin{aligned}
\dot{\delta v}_x &= \delta F_{xi} & \dot{\delta v}_y &= \delta F_{yi} & \dot{\delta v}_z &= \delta F_{zi} \\
\dot{\delta x} &= \delta v_x & \dot{\delta y} &= \delta v_y & \dot{\delta z} &= \delta v_z
\end{aligned}$$

Due to the overwhelming complexity of the dynamics, the **A** matrix will be assembled piecemeal. If a component of the matrix is not listed, it has a value of zero.

$$\mathbf{A}(1:3, 4:7) = \mathbf{I} \tag{D.9}$$

$$\mathbf{A}(4:6, 7) = \begin{bmatrix} (s\theta c\phi c\psi + s\phi s\psi)f_{yb} + (c\phi s\psi - s\phi s\theta c\theta)f_{zb} \\ (s\theta c\phi s\psi - s\phi c\psi)f_{yb} - (s\theta s\phi s\psi + c\phi c\psi)f_{zb} \\ c\theta c\phi f_{yb} - s\phi c\theta f_{zb} \end{bmatrix} \tag{D.10}$$

$$\mathbf{A}(4:6, 8) = \begin{bmatrix} -s\theta c\psi f_{xb} + c\theta s\phi c\psi f_{yb} + c\theta c\phi c\psi f_{zb} \\ -s\theta s\psi f_{xb} + c\theta s\phi s\psi f_{yb} + c\theta c\phi s\psi f_{zb} \\ -c\theta f_{xb} - s\theta s\phi f_{yb} - s\theta c\phi f_{zb} \end{bmatrix} \tag{D.11}$$

$$\mathbf{A}(4:5, 9) = \begin{bmatrix} -s\psi c\theta f_{xb} - (s\theta s\phi s\psi + c\theta c\psi)f_{yb} + (s\phi c\psi - c\phi s\theta s\psi)f_{zb} \\ c\theta c\psi f_{xb} + (s\theta s\phi c\psi - c\phi s\phi)f_{yb} + (s\theta c\phi c\psi + s\phi s\psi)f_{zb} \end{bmatrix} \tag{D.12}$$

The disturbance matrix,  $\Gamma$ , while complicated, is still simple enough that it can be listed in its entirety

$$\Gamma = \begin{bmatrix} 0 & 0 & 0 & 0 & 0 & 0 \\ 0 & 0 & 0 & 0 & 0 & 0 \\ 0 & 0 & 0 & 0 & 0 & 0 \\ c\theta c\psi & (s\theta s\phi c\psi - c\phi s\psi) & (s\phi s\psi + s\theta c\phi c\psi) & 0 & 0 & 0 \\ c\theta s\psi & (c\phi c\psi + s\theta s\phi s\psi) & (s\theta s\psi c\phi - s\phi c\psi) & 0 & 0 & 0 \\ -s\theta & s\phi c\theta & c\theta c\phi & 0 & 0 & 0 \\ 0 & 0 & 0 & 1 & 0 & 0 \\ 0 & 0 & 0 & 0 & 1 & 0 \\ 0 & 0 & 0 & 0 & 0 & 1 \end{bmatrix} \quad (D.13)$$

## Appendix E: General Form Measurement Model

### E.1 Measurement for Primarily Horizontal Flight

For the case when the camera is located on the underside of an aircraft, where the focal plane is orthogonal to the negative vertical axis. When the aircraft's Euler angles cannot be assumed small, the nonlinear DCM from the navigation frame to the body frame is

$$\mathbf{C}_n^b = \begin{bmatrix} c\theta c\psi & c\theta s\psi & -s\theta \\ s\theta s\phi c\psi - c\phi s\psi & s\theta s\phi s\psi + c\phi c\psi & s\phi c\theta \\ c\phi s\theta c\psi + s\phi s\psi & c\phi s\theta s\psi - s\phi c\psi & c\theta c\phi \end{bmatrix} \quad (E.1)$$

and the relationship between the navigation frame and the body frame is

$$\begin{bmatrix} x_p - x \\ y_p - y \\ z_p - z \end{bmatrix}^{(b)} = \mathbf{C}_n^b \begin{bmatrix} x_p - x \\ y_p - y \\ z_p - z \end{bmatrix}^{(n)} \quad (E.2)$$

The angles  $\xi$ , the angle from the  $x^{(b)}$  axis to the tracked ground feature, and  $\mu$ , the angle from the  $y^{(b)}$  axis to the tracked ground feature, provide the relationship basis for the measurement equations.

$$\tan \xi = \frac{x_f}{f} = \frac{(x_p - x)^{(b)}}{(z_p - z)^{(b)}} \quad (E.3)$$

$$\tan \mu = \frac{y_f}{f} = \frac{(y_p - y)^{(b)}}{(z_p - z)^{(b)}} \quad (E.4)$$

The  $x$  measurement will be shown first. The nondimensionalized  $x_f$ ,

$$x_f = \frac{c\theta c\psi(x_p - x) + c\theta s\psi(y_p - y) + s\theta(z)}{(c\phi s\theta c\psi + s\phi s\psi)(x_p - x) + (c\phi s\theta s\psi - s\phi c\psi)(y_p - y) - c\theta c\phi(z)} \quad (E.5)$$

Moving everything to the LHS of the equation produces

$$\begin{aligned} x_f((c\phi s\theta c\psi + s\phi s\psi)(x_p - x) + (c\phi s\theta s\psi - s\phi c\psi)(y_p - y) - c\theta c\phi(z)) \\ - c\theta c\psi(x_p - x) - c\theta s\psi(y_p - y) - s\theta(z) = 0 \end{aligned} \quad (E.6)$$

Due to the sheer complexity of the equation, it is broken up into the following components

$$A = \cos\phi \sin\theta \cos\psi + \sin\phi \sin\psi \quad (\text{E.7})$$

$$B = \cos\phi \sin\theta \sin\psi - \sin\phi \cos\psi \quad (\text{E.8})$$

$$C = \sin\theta \cos\phi \quad (\text{E.9})$$

$$D = \sin\theta \sin\phi \quad (\text{E.10})$$

$$E = \cos\theta \sin\psi \quad (\text{E.11})$$

$$F = (x_p - x) \quad (\text{E.12})$$

$$G = (y_p - y) \quad (\text{E.13})$$

such that

$$(x_{fm} - \delta x_f)(AF + BG + Cz_c) - DF - EG + \sin\theta_c z_c = 0$$

The states and measurements must then be perturbed to account for uncertainty from the INS and measurements.

$$\theta = \theta_c - \delta\theta \quad \phi = \phi_c - \delta\phi \quad \psi = \psi_c - \delta\psi$$

$$x = x_c - \delta x \quad y = y_c - \delta y \quad z = z_c - \delta z$$

$$x_p = x_{pc} - \delta x_p \quad y_p = y_{pc} - \delta y_p \quad x_f = x_{fm} - \delta x_f$$

Based on the angle addition rule and the small angle assumption of the error terms, the trigonometric terms have the following relationships

$$\sin(\theta_c - \delta\theta) = \sin\theta_c - (\cos\theta_c + \sin\theta_c)\delta\theta \quad \cos(\theta_c - \delta\theta) = \cos\theta_c + (\sin\theta_c - \cos\theta_c)\delta\theta$$

$$\sin(\phi_c - \delta\phi) = \sin\phi_c - (\cos\phi_c + \sin\phi_c)\delta\phi \quad \cos(\phi_c - \delta\phi) = \cos\phi_c + (\sin\phi_c - \cos\phi_c)\delta\phi$$

$$\sin(\psi_c - \delta\psi) = \sin\psi_c - (\cos\psi_c + \sin\psi_c)\delta\psi \quad \cos(\psi_c - \delta\psi) = \cos\psi_c + (\sin\psi_c - \cos\psi_c)\delta\psi$$

Substituting the perturbed trigonometric terms into the component terms from Eqs. (E.7)-(E.11), distributing the terms, and collecting like error terms yields

$$\begin{aligned}
A &= (c\phi_c + (s\phi_c - c\phi_c)\delta\phi)(s\theta_c - (s\theta_c + c\theta_c)\delta\theta)(c\psi_c + (s\psi_c - c\psi_c)\delta\psi) \\
&\quad + (s\phi_c - (s\phi_c + c\phi_c)\delta\phi)(s\psi_c - (s\psi_c + c\psi_c)\delta\psi) \\
&= (s\theta_c c\phi_c + (s\phi_c - c\phi_c)s\theta_c \delta\phi - (s\theta_c + c\theta_c)c\phi_c \delta\theta)(c\psi_c + (s\psi_c - c\psi_c)\delta\psi) \\
&\quad + s\phi_c s\psi_c - s\phi_c(s\psi_c + c\psi_c)\delta\psi - s\psi_c(s\phi_c + c\phi_c)\delta\phi \\
&= s\theta_c c\phi_c c\psi_c + s\theta_c c\psi_c(s\phi_c - c\phi_c)\delta\phi - c\phi_c c\psi_c(s\theta_c + c\theta_c)\delta\theta + (s\psi_c - c\psi_c)s\theta_c c\phi_c \delta\psi \\
&\quad + s\phi_c s\psi_c - s\phi_c(s\psi_c + c\psi_c)\delta\psi - s\psi_c(s\phi_c + c\phi_c)\delta\phi \\
A &= (s\theta_c c\phi_c c\psi_c + s\phi_c s\psi_c) - \delta\theta(c\phi_c c\psi_c(s\theta_c + c\theta_c)) \\
&\quad + \delta\phi(s\theta_c c\psi_c(s\phi_c - c\phi_c) - s\psi_c(s\phi_c + c\phi_c)) + \delta\psi((s\psi_c - c\psi_c)s\theta_c c\phi_c - s\phi_c(s\psi_c + c\psi_c))
\end{aligned} \tag{E.14}$$

$$\begin{aligned}
B &= (c\phi_c + (s\phi_c - c\phi_c)\delta\phi)(s\theta_c - (s\theta_c + c\theta_c)\delta\theta)(s\psi_c - (s\psi_c + c\psi_c)\delta\psi) \\
&\quad - (s\phi_c - (s\phi_c + c\phi_c)\delta\phi)(c\psi_c + (s\psi_c - c\psi_c)\delta\psi) \\
&= (s\theta_c c\phi_c - c\phi_c(s\theta_c + c\theta_c)\delta\theta + s\theta_c(s\phi_c - c\phi_c)\delta\phi)(s\psi_c - (s\psi_c + c\psi_c)\delta\psi) \\
&\quad - s\phi_c c\psi_c - s\phi_c(s\psi_c - c\psi_c)\delta\psi + c\psi_c(s\phi_c + c\phi_c)\delta\phi \\
&= s\theta_c s\psi_c c\phi_c - s\theta_c c\phi_c(s\psi_c + c\psi_c)\delta\psi - s\psi_c c\phi_c(s\theta_c + c\theta_c)\delta\theta + s\theta_c s\psi_c(s\phi_c - c\phi_c)\delta\phi \\
&\quad - s\phi_c c\psi_c - s\phi_c(s\psi_c - c\psi_c)\delta\psi + c\psi_c(s\phi_c + c\phi_c)\delta\phi \\
B &= (s\theta_c s\psi_c c\phi_c - s\phi_c c\psi_c) - \delta\theta(s\psi_c c\phi_c(s\theta_c + c\theta_c)) \\
&\quad + \delta\phi(s\theta_c s\psi_c(s\phi_c - c\phi_c) + c\psi_c(s\phi_c + c\phi_c)) - \delta\psi(s\theta_c c\phi_c(s\psi_c + c\psi_c) + s\phi_c(s\psi_c - c\psi_c))
\end{aligned} \tag{E.15}$$

$$\begin{aligned}
C &= (c\theta_c + (s\theta_c - c\theta_c)\delta\theta)(c\phi_c + (s\phi_c - c\phi_c)\delta\phi) \\
&= c\theta_c c\phi_c + c\theta_c(s\phi_c - c\phi_c)\delta\phi + c\phi_c(s\theta_c - c\theta_c)\delta\theta
\end{aligned} \tag{E.16}$$

$$\begin{aligned}
D &= (c\theta_c + (s\theta_c - c\theta_c)\delta\theta)(c\psi_c + (s\psi_c - c\psi_c)\delta\psi) \\
&= c\theta_c c\psi_c + c\theta_c(s\psi_c - c\psi_c)\delta\psi + c\psi_c(s\theta_c - c\theta_c)\delta\theta
\end{aligned} \tag{E.17}$$

and

$$\begin{aligned}
E &= (s\psi_c - (s\psi_c + c\psi_c)\delta\psi)(c\theta_c + (s\theta_c - c\theta_c)\delta\theta) \\
&= s\psi_c c\theta_c + s\psi_c (s\theta_c - c\theta_c)\delta\theta - c\theta_c (s\psi_c + c\psi_c)\delta\psi
\end{aligned} \tag{E.18}$$

Notice that the error terms that were multiplied together were neglected. The perturbations were then substituted into Eqs. (E.12) and (E.13) producing

$$F = (x_{pc} - x_c) - \delta x_p + \delta x \tag{E.19}$$

and

$$G = (y_{pc} - y_c) + \delta y - \delta y_p \tag{E.20}$$

Next, we started to merge the components by distributing their terms, again whenever error terms were multiplied together, they were neglected due to how small they are.

$$\begin{aligned}
AF &= (s\theta_c c\phi_c c\psi_c + s\phi_c s\psi_c)(x_{pc} - x_c) + \delta x (s\theta_c c\phi_c c\psi_c + s\phi_c s\psi_c) \\
&\quad - \delta\theta (c\phi_c c\psi_c (s\theta_c + c\theta_c))(x_{pc} - x_c) \\
&\quad + \delta\psi ((s\psi_c - c\psi_c) s\theta_c c\phi_c - s\phi_c (s\psi_c + c\psi_c))(x_{pc} - x_c) \\
&\quad + \delta\phi (s\theta_c c\psi_c (s\phi_c - c\phi_c) - s\psi_c (s\phi_c + c\phi_c))(x_{pc} - x_c) - \delta x_p (s\theta_c c\phi_c c\psi_c + s\phi_c s\psi_c)
\end{aligned} \tag{E.21}$$

$$\begin{aligned}
BG &= (s\theta_c s\psi_c c\phi_c - s\phi_c c\psi_c)(y_{pc} - y_c) - \delta\theta (s\psi_c c\phi_c (s\theta_c + c\theta_c))(y_{pc} - y_c) \\
&\quad + \delta\phi (s\theta_c s\psi_c (s\phi_c - c\phi_c) + c\psi_c (s\phi_c + c\phi_c))(y_{pc} - y_c) \\
&\quad - \delta\psi (s\theta_c c\phi_c (s\psi_c + c\psi_c) + s\phi_c (s\psi_c - c\psi_c))(y_{pc} - y_c)
\end{aligned} \tag{E.22}$$

$$+ \delta y (s\theta_c s\psi_c c\phi_c - s\phi_c c\psi_c) - \delta y_p (s\theta_c s\psi_c c\phi_c - s\phi_c c\psi_c)$$

$$Cz = -(c\theta_c c\phi_c z_c + \delta\phi c\theta_c (s\phi_c - c\phi_c) z_c + \delta\theta c\phi_c (s\theta_c - c\theta_c) z_c - \delta z c\theta_c c\phi_c) \tag{E.23}$$

The merged terms are collected, such that

$$Q = AF + BG + Cz \tag{E.24}$$

and the result  $Q$  is then multiplied by the measurement term.

$$\begin{aligned}
x_f Q = & (x_{fm} - \delta x_f) \left( (\sin \theta_c \cos \phi_c \cos \psi_c + \sin \phi_c \sin \psi_c)(x_{pc} - x_c) \right. \\
& + (\sin \theta_c \sin \psi_c \cos \phi_c - \sin \phi_c \cos \psi_c)(y_{pc} - y_c) - \cos \theta_c \cos \phi_c z_c \Big) \\
& + \delta x (\sin \theta_c \cos \phi_c \cos \psi_c + \sin \phi_c \sin \psi_c) x_f + \delta y (\sin \theta_c \sin \psi_c \cos \phi_c - \sin \phi_c \cos \psi_c) x_f + \delta z \cos \theta_c \cos \phi_c x_f \\
& - \delta \theta \left( (\cos \phi_c \cos \psi_c (\sin \theta_c + \cos \theta_c))(x_{pc} - x_c) + \sin \psi_c \cos \phi_c (\sin \theta_c + \cos \theta_c)(y_{pc} - y_c) + \cos \phi_c (\sin \theta_c - \cos \theta_c) z_c \right) x_f \\
& + \delta \phi \left( (\sin \theta_c \cos \psi_c (\sin \phi_c - \cos \phi_c) - \sin \psi_c (\sin \phi_c + \cos \phi_c))(x_{pc} - x_c) - \cos \theta_c (\sin \phi_c - \cos \phi_c) z_c \right. \\
& + (\sin \theta_c \sin \psi_c (\sin \phi_c - \cos \phi_c) + \cos \psi_c (\sin \phi_c + \cos \phi_c))(y_{pc} - y_c) \Big) x_f \\
& + \delta \psi \left( ((\sin \psi_c - \cos \psi_c) \sin \theta_c \cos \phi_c - \sin \phi_c (\sin \psi_c + \cos \psi_c))(x_{pc} - x_c) \right. \\
& - (\sin \theta_c \cos \phi_c (\sin \psi_c + \cos \psi_c) + \sin \phi_c (\sin \psi_c - \cos \psi_c))(y_{pc} - y_c) \Big) x_f \\
& - \delta x_p (\sin \theta_c \cos \phi_c \cos \psi_c + \sin \phi_c \sin \psi_c) x_f - \delta y_p (\sin \theta_c \sin \psi_c \cos \phi_c - \sin \phi_c \cos \psi_c) x_f
\end{aligned} \tag{E.25}$$

the remainder of the components were merged

$$-DF = -c\theta_c c\psi_c(x_{pc} - x_c) - \delta x c\theta_c c\psi_c - \delta\theta c\psi_c(s\theta_c - c\theta_c)(x_{pc} - x_c) - \delta\psi c\theta_c(s\psi_c - c\psi_c)(x_{pc} - x_c) + \delta x_p c\theta_c c\psi_c \quad (E.26)$$

$$\begin{aligned}
-EG = & -s\psi_c \cos\theta_c (y_{pc} - y_c) - \delta y \sin\psi_c \cos\theta_c - \delta\theta \sin\psi_c (\sin\theta_c - \cos\theta_c) (y_{pc} - y_c) \\
& + \delta\psi \cos\theta_c (\sin\psi_c + \cos\psi_c) (y_{pc} - y_c) + \delta y_p \sin\psi_c \cos\theta_c
\end{aligned} \tag{E.27}$$

$$z \sin \theta = -\sin \theta_c z_c + \delta \theta (\sin \theta_c + \cos \theta_c) z_c + \delta z \sin \theta_c \quad (E.28)$$

and collected, such that

$$\begin{aligned}
O &= -DF - EG + z \sin \theta \\
&= -\cos \theta_c \cos \psi_c (x_{pc} - x_c) - \sin \psi_c \cos \theta_c (y_{pc} - y_c) - \sin \theta_c z_c - \delta x \cos \theta_c \cos \psi_c - \delta y \sin \psi_c \cos \theta_c + \delta z \sin \theta_c \\
&\quad - \delta \theta ((\sin \theta_c + \cos \theta_c) z_c + \cos \psi_c (\sin \theta_c - \cos \theta_c) (x_{pc} - x_c) + \sin \psi_c (\sin \theta_c - \cos \theta_c) (y_{pc} - y_c)) \\
&\quad - \delta \psi (\cos \theta_c (\sin \psi_c - \cos \psi_c) (x_{pc} - x_c) - \cos \theta_c (\sin \psi_c + \cos \psi_c) (y_{pc} - y_c)) + \delta x_p \cos \theta_c \cos \psi_c + \delta y_p \sin \psi_c \cos \theta_c
\end{aligned} \tag{E.29}$$

Moving all of the error terms to the RHS of the equation yields the  $x$  measurement equation for the primarily horizontal case

$$\begin{aligned}
& x_{fm} \left( (s\theta_c c\phi_c c\psi_c + s\phi_c s\psi_c)(x_{pc} - x_c) + (s\theta_c s\psi_c c\phi_c - s\phi_c c\psi_c)(y_{pc} - y_c) - c\theta_c c\phi_c z_c \right) \\
& - c\theta_c c\psi_c (x_{pc} - x_c) - s\psi_c c\theta_c (y_{pc} - y_c) - s\theta_c z_c = \delta x \left( c\theta_c c\psi_c - (s\theta_c c\phi_c c\psi_c + s\phi_c s\psi_c) x_f \right) \\
& - \delta y \left( (s\theta_c s\psi_c c\phi_c - s\phi_c c\psi_c) x_f - s\psi_c c\theta_c \right) - \delta z (s\theta_c + c\theta_c c\phi_c x_f) \\
& + \delta \theta \left[ (c\psi_c (s\theta_c - c\theta_c)(x_{pc} - x_c) + s\psi_c (s\theta_c - c\theta_c)(y_{pc} - y_c) - (s\theta_c + c\theta_c) z_c) + \right. \\
& \left. \left( (c\phi_c c\psi_c (s\theta_c + c\theta_c))(x_{pc} - x_c) + s\psi_c c\phi_c (s\theta_c + c\theta_c)(y_{pc} - y_c) + c\phi_c (s\theta_c - c\theta_c) z_c \right) x_f \right] \\
& - \delta \phi \left( (s\theta_c c\psi_c (s\phi_c - c\phi_c) - s\psi_c (s\phi_c + c\phi_c))(x_{pc} - x_c) - c\theta_c (s\phi_c - c\phi_c) z_c \right. \\
& \left. + (s\theta_c s\psi_c (s\phi_c - c\phi_c) + c\psi_c (s\phi_c + c\phi_c))(y_{pc} - y_c) \right) x_f \\
& + \delta \psi \left[ c\theta_c (s\psi_c - c\psi_c)(x_{pc} - x_c) - c\theta_c (s\psi_c + c\psi_c)(y_{pc} - y_c) \right. \\
& \left. - \left( ((s\psi_c - c\psi_c) s\theta_c c\phi_c - s\phi_c (s\psi_c + c\psi_c))(x_{pc} - x_c) \right. \right. \\
& \left. \left. - (s\theta_c c\phi_c (s\psi_c + c\psi_c) + s\phi_c (s\psi_c - c\psi_c))(y_{pc} - y_c) \right) x_f \right] \\
& + \delta x_p \left( (s\theta_c c\phi_c c\psi_c + s\phi_c s\psi_c) x_f - c\theta_c c\psi_c \right) - \delta y_p \left( s\psi_c c\theta_c - (s\theta_c s\psi_c c\phi_c - s\phi_c c\psi_c) x_f \right) \\
& + \delta x_f \left( (s\theta_c c\phi_c c\psi_c + s\phi_c s\psi_c)(x_{pc} - x_c) + (s\theta_c s\psi_c c\phi_c - s\phi_c c\psi_c)(y_{pc} - y_c) - c\theta_c c\phi_c z_c \right) \\
& \tag{E.30}
\end{aligned}$$

where  $x_f$  is determined by plugging the nominal values for the A/C Euler angles into Eq. (E.5).

The process then had to be repeated for the  $y$  measurement.

$$y_f = \frac{(x_p - x)(s\theta s\phi c\psi - c\phi s\psi) + (y_p - y)(s\theta s\phi s\psi + c\phi c\psi) - z(s\phi c\theta)}{(c\phi s\theta c\psi + s\phi s\psi)(x_p - x) + (c\phi s\theta s\psi - s\phi c\psi)(y_p - y) - c\theta c\phi(z)} \tag{E.31}$$

Moving everything to the LHS of the equation

$$\begin{aligned}
& y_f ((c\phi s\theta c\psi + s\phi s\psi)(x_p - x) + (c\phi s\theta s\psi - s\phi c\psi)(y_p - y) - c\theta c\phi(z)) \\
& - (x_p - x)(s\theta s\phi c\psi - c\phi s\psi) - (y_p - y)(s\theta s\phi s\psi + c\phi c\psi) + z(s\phi c\theta) = 0
\end{aligned} \tag{E.32}$$

Since the denominator in Eq. (E.31) is the same as in Eq. (E.5), many of the components are the same as in the  $x$  measurement. The unique components are

$$I = s\theta s\phi c\psi - c\phi s\psi$$

$$J = s\theta s\phi s\psi + c\phi c\psi$$

$$L = s\phi c\theta$$

Substituting in the perturbations, distributing the terms, and collecting like error terms yields

$$\begin{aligned}
I &= (s\theta_c - (s\theta_c + c\theta_c)\delta\theta)(s\phi_c - (s\phi_c + c\phi_c)\delta\phi)(c\psi_c + (s\psi_c - c\psi_c)\delta\psi) \\
&\quad - (c\phi_c + (s\phi_c - c\phi_c)\delta\phi)(s\psi_c - (s\psi_c + c\psi_c)\delta\psi) \\
&= (s\theta_c s\phi_c - s\theta_c (s\phi_c + c\phi_c)\delta\phi - s\phi_c (s\theta_c + c\theta_c)\delta\theta)(c\psi_c + (s\psi_c - c\psi_c)\delta\psi) \\
&\quad - s\psi_c c\phi_c + c\phi_c (s\psi_c + c\psi_c)\delta\psi - s\psi_c (s\phi_c - c\phi_c)\delta\phi \\
&= s\theta_c s\phi_c c\psi_c + s\theta_c s\phi_c (s\psi_c - c\psi_c)\delta\psi - s\theta_c c\psi_c (s\phi_c + c\phi_c)\delta\phi - s\phi_c c\psi_c (s\theta_c + c\theta_c)\delta\theta \\
&\quad - s\psi_c c\phi_c + c\phi_c (s\psi_c + c\psi_c)\delta\psi - s\psi_c (s\phi_c - c\phi_c)\delta\phi \\
I &= (s\theta_c s\phi_c c\psi_c - s\psi_c c\phi_c) - \delta\theta s\phi_c c\psi_c (s\theta_c + c\theta_c) \\
&\quad - \delta\phi (s\psi_c (s\phi_c - c\phi_c) + s\theta_c c\psi_c (s\phi_c + c\phi_c)) + \delta\psi (c\phi_c (s\psi_c + c\psi_c) + s\theta_c s\phi_c (s\psi_c - c\psi_c))
\end{aligned} \tag{E.33}$$

$$\begin{aligned}
J &= (\sin\theta_c - (\sin\theta_c + \cos\theta_c)\delta\theta)(\sin\phi_c - (\sin\phi_c + \cos\phi_c)\delta\phi)(\sin\psi_c - (\sin\psi_c + \cos\psi_c)\delta\psi) \\
&\quad + (\cos\phi_c + (\sin\phi_c - \cos\phi_c)\delta\phi)(\cos\psi_c + (\sin\psi_c - \cos\psi_c)\delta\psi) \\
&= (\sin\theta_c \sin\phi_c - \sin\theta_c (\sin\phi_c + \cos\phi_c)\delta\phi - \sin\phi_c (\sin\theta_c + \cos\theta_c)\delta\theta)(\sin\psi_c - (\sin\psi_c + \cos\psi_c)\delta\psi) \\
&\quad + \cos\phi_c \cos\psi_c + \cos\phi_c (\sin\psi_c - \cos\psi_c)\delta\psi + \cos\psi_c (\sin\phi_c - \cos\phi_c)\delta\phi \\
&= \sin\theta_c \sin\phi_c \sin\psi_c - \sin\theta_c \sin\phi_c (\sin\psi_c + \cos\psi_c)\delta\psi - \sin\theta_c \sin\psi_c (\sin\phi_c + \cos\phi_c)\delta\phi - \sin\phi_c \sin\psi_c (\sin\theta_c + \cos\theta_c)\delta\theta \\
&\quad + \cos\phi_c \cos\psi_c + \cos\phi_c (\sin\psi_c - \cos\psi_c)\delta\psi + \cos\psi_c (\sin\phi_c - \cos\phi_c)\delta\phi \\
J &= (\sin\theta_c \sin\phi_c \sin\psi_c + \cos\phi_c \cos\psi_c) - \delta\theta(\sin\phi_c \sin\psi_c (\sin\theta_c + \cos\theta_c)) \\
&\quad - \delta\phi(\sin\theta_c \sin\psi_c (\sin\phi_c + \cos\phi_c) - \cos\psi_c (\sin\phi_c - \cos\phi_c)) + \delta\psi(\cos\phi_c (\sin\psi_c - \cos\psi_c) - \sin\theta_c \sin\phi_c (\sin\psi_c + \cos\psi_c)) \\
\end{aligned} \tag{E.34}$$

and

$$\begin{aligned}
L &= (\sin\phi_c - (\sin\phi_c + \cos\phi_c)\delta\phi)(\cos\theta_c + (\sin\theta_c - \cos\theta_c)\delta\theta) \\
&= \sin\phi_c \cos\theta_c + \sin\phi_c (\sin\theta_c - \cos\theta_c)\delta\theta - \cos\theta_c (\sin\phi_c + \cos\phi_c)\delta\phi
\end{aligned} \tag{E.35}$$

Merging the noncommon components yields

$$\begin{aligned}
-IF &= -(\sin\theta_c \sin\phi_c \cos\psi_c - \sin\psi_c \cos\phi_c)(x_{pc} - x_c) + \delta\theta \sin\phi_c \cos\psi_c (\sin\theta_c + \cos\theta_c)(x_{pc} - x_c) \\
&\quad + \delta\phi(\sin\psi_c (\sin\phi_c - \cos\phi_c) + \sin\theta_c \cos\psi_c (\sin\phi_c + \cos\phi_c))(x_{pc} - x_c) \\
&\quad - \delta\psi(\cos\phi_c (\sin\psi_c + \cos\psi_c) + \sin\theta_c \sin\phi_c (\sin\psi_c - \cos\psi_c))(x_{pc} - x_c) \\
&\quad - \delta x(\sin\theta_c \sin\phi_c \cos\psi_c - \sin\psi_c \cos\phi_c) + \delta x_p(\sin\theta_c \sin\phi_c \cos\psi_c - \sin\psi_c \cos\phi_c)
\end{aligned} \tag{E.36}$$

$$\begin{aligned}
-JG &= -(\sin\theta_c \sin\phi_c \sin\psi_c + \cos\phi_c \cos\psi_c)(y_{pc} - y_c) + \delta\theta(\sin\phi_c \sin\psi_c (\sin\theta_c + \cos\theta_c))(y_{pc} - y_c) \\
&\quad + \delta\phi(\sin\theta_c \sin\psi_c (\sin\phi_c + \cos\phi_c) - \cos\psi_c (\sin\phi_c - \cos\phi_c))(y_{pc} - y_c) \\
&\quad - \delta\psi(\cos\phi_c (\sin\psi_c - \cos\psi_c) - \sin\theta_c \sin\phi_c (\sin\psi_c + \cos\psi_c))(y_{pc} - y_c) \\
&\quad - \delta y(\sin\theta_c \sin\phi_c \sin\psi_c + \cos\phi_c \cos\psi_c) + \delta y_p(\sin\theta_c \sin\phi_c \sin\psi_c + \cos\phi_c \cos\psi_c)
\end{aligned} \tag{E.37}$$

and

$$-Lz = \sin\phi_c \cos\theta_c z_c + \delta\theta \sin\phi_c (\sin\theta_c - \cos\theta_c)z_c - \delta\phi \cos\theta_c (\sin\phi_c + \cos\phi_c)z_c - \sin\phi_c \cos\theta_c \delta z \tag{E.38}$$

## Collecting the merged components

$$\begin{aligned}
R &= -IF - JG - LZ \\
&= -(s\theta_c s\phi_c c\psi_c - s\psi_c c\phi_c)(x_{pc} - x_c) - (s\theta_c s\phi_c s\psi_c + c\phi_c c\psi_c)(y_{pc} - y_c) - s\phi_c c\theta_c z_c \\
&\quad - \delta x(s\theta_c s\phi_c c\psi_c - s\psi_c c\phi_c) - \delta y(s\theta_c s\phi_c s\psi_c + c\phi_c c\psi_c) - \delta z s\phi_c c\theta_c \\
&\quad + \delta\theta \left( s\phi_c c\psi_c (s\theta_c + c\theta_c)(x_{pc} - x_c) + (s\phi_c s\psi_c (s\theta_c + c\theta_c))(y_{pc} - y_c) + s\phi_c (s\theta_c - c\theta_c)z_c \right) \\
&\quad + \delta\phi \left[ (s\psi_c (s\phi_c - c\phi_c) + s\theta_c c\psi_c (s\phi_c + c\phi_c))(x_{pc} - x_c) \right. \\
&\quad \left. + (s\theta_c s\psi_c (s\phi_c + c\phi_c) - c\psi_c (s\phi_c - c\phi_c))(y_{pc} - y_c) - c\theta_c (s\phi_c + c\phi_c)z_c \right] \\
&\quad - \delta\psi \left( (c\phi_c (s\psi_c + c\psi_c) + s\theta_c s\phi_c (s\psi_c - c\psi_c))(x_{pc} - x_c) \right. \\
&\quad \left. + (c\phi_c (s\psi_c - c\psi_c) - s\theta_c s\phi_c (s\psi_c + c\psi_c))(y_{pc} - y_c) \right) \\
&\quad + \delta x_p(s\theta_c s\phi_c c\psi_c - s\psi_c c\phi_c) + \delta y_p(s\theta_c s\phi_c s\psi_c + c\phi_c c\psi_c)
\end{aligned} \tag{E.39}$$

The common terms, represented in the  $Q$  need to be multiplied by the y measurement term

$$\begin{aligned}
y_f Q = & (y_{fm} - \delta y_f) \left( (s\theta_c c\phi_c c\psi_c + s\phi_c s\psi_c)(x_{pc} - x_c) \right. \\
& + (s\theta_c s\psi_c c\phi_c - s\phi_c c\psi_c)(y_{pc} - y_c) - c\theta_c c\phi_c z_c \Big) \\
& + \delta x (s\theta_c c\phi_c c\psi_c + s\phi_c s\psi_c) y_f + \delta y (s\theta_c s\psi_c c\phi_c - s\phi_c c\psi_c) y_f + \delta z c\theta_c c\phi_c y_f \\
& - \delta \theta \left( (c\phi_c c\psi_c (s\theta_c + c\theta_c))(x_{pc} - x_c) + s\psi_c c\phi_c (s\theta_c + c\theta_c)(y_{pc} - y_c) + c\phi_c (s\theta_c - c\theta_c) z_c \right) y_f \\
& + \delta \phi \left( (s\theta_c c\psi_c (s\phi_c - c\phi_c) - s\psi_c (s\phi_c + c\phi_c))(x_{pc} - x_c) - c\theta_c (s\phi_c - c\phi_c) z_c \right. \\
& + (s\theta_c s\psi_c (s\phi_c - c\phi_c) + c\psi_c (s\phi_c + c\phi_c))(y_{pc} - y_c) \Big) y_f \\
& + \delta \psi \left( ((s\psi_c - c\psi_c) s\theta_c c\phi_c - s\phi_c (s\psi_c + c\psi_c))(x_{pc} - x_c) \right. \\
& - (s\theta_c c\phi_c (s\psi_c + c\psi_c) + s\phi_c (s\psi_c - c\psi_c))(y_{pc} - y_c) \Big) y_f \\
& - \delta x_p (s\theta_c c\phi_c c\psi_c + s\phi_c s\psi_c) y_f - \delta y_p (s\theta_c s\psi_c c\phi_c - s\phi_c c\psi_c) y_f
\end{aligned} \tag{E.40}$$

Merging  $R$  and  $Q$ , and moving all the error terms to the RHS, produces the  $y$  measurement equation for primarily horizontal case

$$\begin{aligned}
y_{fm} & \left( (s\theta_c c\phi_c c\psi_c + s\phi_c s\psi_c)(x_{pc} - x_c) + (s\theta_c s\psi_c c\phi_c - s\phi_c c\psi_c)(y_{pc} - y_c) - c\theta_c c\phi_c z_c \right) \\
& - (s\theta_c s\phi_c c\psi_c - s\psi_c c\phi_c)(x_{pc} - x_c) - (s\theta_c s\phi_c s\psi_c + c\phi_c c\psi_c)(y_{pc} - y_c) + s\phi_c c\theta_c z_c = \\
& \delta x \left( s\theta_c s\phi_c c\psi_c - s\psi_c c\phi_c - (s\theta_c c\phi_c c\psi_c + s\phi_c s\psi_c) y_f \right) \\
& - \delta y \left( (s\theta_c s\psi_c c\phi_c - s\phi_c c\psi_c) y_f - s\theta_c s\phi_c s\psi_c - c\phi_c c\psi_c \right) - \delta z \left( (c\theta_c c\phi_c y_f) - s\phi_c c\theta_c \right) \\
& + \delta \theta \left[ \left( (c\phi_c c\psi_c (s\theta_c + c\theta_c))(x_{pc} - x_c) + s\psi_c c\phi_c (s\theta_c + c\theta_c)(y_{pc} - y_c) + c\phi_c (s\theta_c - c\theta_c) z_c \right) y_f \right. \\
& \left. - \left( s\phi_c c\psi_c (s\theta_c + c\theta_c)(x_{pc} - x_c) + (s\phi_c s\psi_c (s\theta_c + c\theta_c))(y_{pc} - y_c) + s\phi_c (s\theta_c - c\theta_c) z_c \right) \right] \\
& - \delta \phi \left[ \left( (s\theta_c c\psi_c (s\phi_c - c\phi_c) - s\psi_c (s\phi_c + c\phi_c))(x_{pc} - x_c) - c\theta_c (s\phi_c - c\phi_c) z_c \right. \right. \\
& \left. \left. + (s\theta_c s\psi_c (s\phi_c - c\phi_c) + c\psi_c (s\phi_c + c\phi_c))(y_{pc} - y_c) \right) y_f \right. \\
& \left. + (s\psi_c (s\phi_c - c\phi_c) + s\theta_c c\psi_c (s\phi_c + c\phi_c))(x_{pc} - x_c) \right. \\
& \left. + (s\theta_c s\psi_c (s\phi_c + c\phi_c) - c\psi_c (s\phi_c - c\phi_c))(y_{pc} - y_c) - c\theta_c (s\phi_c + c\phi_c) z_c \right] \\
& + \delta \psi \left[ \left( (c\phi_c (s\psi_c + c\psi_c) + s\theta_c s\phi_c (s\psi_c - c\psi_c))(x_{pc} - x_c) \right. \right. \\
& \left. \left. + (c\phi_c (s\psi_c - c\psi_c) - s\theta_c s\phi_c (s\psi_c + c\psi_c))(y_{pc} - y_c) \right) \right. \\
& \left. - \left( (s\psi_c - c\psi_c) s\theta_c c\phi_c - s\phi_c (s\psi_c + c\psi_c))(x_{pc} - x_c) \right. \right. \\
& \left. \left. - (s\theta_c c\phi_c (s\psi_c + c\psi_c) + s\phi_c (s\psi_c - c\psi_c))(y_{pc} - y_c) \right) y_f \right] \\
& + \delta x_p \left( (s\theta_c c\phi_c c\psi_c + s\phi_c s\psi_c) y_f - (s\theta_c s\phi_c c\psi_c - s\psi_c c\phi_c) \right) \\
& - \delta y_p \left( (s\theta_c s\phi_c s\psi_c + c\phi_c c\psi_c) - (s\theta_c s\psi_c c\phi_c - s\phi_c c\psi_c) y_f \right) \\
& + \delta y_f \left( (s\theta_c c\phi_c c\psi_c + s\phi_c s\psi_c)(x_{pc} - x_c) + (s\theta_c s\psi_c c\phi_c - s\phi_c c\psi_c)(y_{pc} - y_c) - c\theta_c c\phi_c z_c \right) \tag{E.41}
\end{aligned}$$

where  $y_f$  is found by substituting the nominal values for the A/C Euler angles into Eq. (E.31).

## E.2 Measurement for Primarily Vertical Flight

For the munitions case where the camera is assumed in the nose of the munition with the focal plane orthogonal to the longitudinal axis. The new measurements will be in the  $z^{(b)}$  and  $y^{(b)}$  frame of reference

$$\tan \xi = \frac{z_f}{f} = \frac{(z_p - z)^{(b)}}{(x_p - x)^{(b)}} \quad (\text{E.42})$$

where  $z_f$  is the projection  $z^{(b)}$  coordinate of the ground feature onto the camera focal plane. Since  $z_f$  equals the reciprocal  $x_f$  from Eq. (E.5), all of the component terms are the same. All that needs to be done for this measurement is change the values in Eq. (E.30) that are multiplied by the measurement term. If a term was previously multiplied by  $x_f$  it will not be multiplied by  $z_f$ , but if it was not, then it will be multiplied by  $z_f$ . Also, the sign previously connected with the measurement term accompanies the transfer of the

measurement term. Therefore the  $z$  measurement equation

$$\begin{aligned}
& z_{fm} \left( c\theta_c c\psi_c (x_{pc} - x_c) + s\psi_c c\theta_c (y_{pc} - y_c) - s\theta_c z_c \right) + \\
& (s\theta_c c\phi_c c\psi_c + s\phi_c s\psi_c)(x_{pc} - x_c) + (s\theta_c s\psi_c c\phi_c - s\phi_c c\psi_c)(y_{pc} - y_c) + c\theta_c c\phi_c z_c = \\
& \delta x \left( (s\theta_c c\phi_c c\psi_c + s\phi_c s\psi_c) - c\theta_c c\psi_c z_f \right) - \delta y \left( s\psi_c c\theta_c z_f - (s\theta_c s\psi_c c\phi_c - s\phi_c c\psi_c) \right) \\
& + \delta z (s\theta_c z_f + c\theta_c c\phi_c) + \delta \theta \left[ ((s\theta_c + c\theta_c)z_c + c\psi_c(s\theta_c - c\theta_c)(x_{pc} - x_c) + s\psi_c(s\theta_c - c\theta_c)(y_{pc} - y_c))z_f + \right. \\
& \left. (c\phi_c c\psi_c(s\theta_c + c\theta_c))(x_{pc} - x_c) + s\psi_c c\phi_c(s\theta_c + c\theta_c)(y_{pc} - y_c) - c\phi_c(s\theta_c - c\theta_c)z_c \right] \\
& - \delta \phi \left( (s\theta_c c\psi_c(s\phi_c - c\phi_c) - s\psi_c(s\phi_c + c\phi_c))(x_{pc} - x_c) + c\theta_c(s\phi_c - c\phi_c)z_c \right. \\
& \left. + (s\theta_c s\psi_c(s\phi_c - c\phi_c) + c\psi_c(s\phi_c + c\phi_c))(y_{pc} - y_c) \right) \\
& + \delta \psi \left[ ((s\psi_c - c\psi_c)s\theta_c c\phi_c - s\phi_c(s\psi_c + c\psi_c))(x_{pc} - x_c) - (s\theta_c c\phi_c(s\psi_c + c\psi_c) + s\phi_c(s\psi_c - c\psi_c))(y_{pc} - y_c) \right. \\
& \left. - (c\theta_c(s\psi_c - c\psi_c)(x_{pc} - x_c) - c\theta_c(s\psi_c + c\psi_c)(y_{pc} - y_c))z_f \right] \\
& + \delta x_p \left( c\theta_c c\psi_c z_f - (s\theta_c c\phi_c c\psi_c + s\phi_c s\psi_c) \right) - \delta y_p \left( (s\theta_c s\psi_c c\phi_c - s\phi_c c\psi_c) - s\psi_c c\theta_c z_f \right) \\
& + \delta z_f \left( c\theta_c c\psi_c (x_{pc} - x_c) + s\psi_c c\theta_c (y_{pc} - y_c) - s\theta_c z_c \right)
\end{aligned} \tag{E.43}$$

where  $z_f$  is found by substituting the nominal values for the A/C Euler angles into the reciprocal of the RHS of Eq. (E.5).

The  $y$  measurement based on  $f$  being along the longitudinal axis will take more work

$$\begin{aligned}
\tan \mu &= \frac{y_{xf}}{f} = \frac{(y_p - y)^{(b)}}{(x_p - x)^{(b)}} \\
&= \frac{(s\theta s\phi c\psi - c\phi s\psi)(x_p - x)^{(n)} + (s\theta s\phi s\psi + c\phi c\psi)(y_p - y)^{(n)} + s\phi c\theta(z_p - z)^{(n)}}{c\theta c\psi(x_p - x)^{(n)} + c\theta s\psi(y_p - y)^{(n)} - s\theta(z_p - z)^{(n)}}
\end{aligned} \tag{E.44}$$

where  $y_{xf}$  is the y measurement term for the vertical case. Breaking Eq. (E.44) into previously defined components

$$\begin{aligned}
& y_{xf}(DF + EG - s\theta z) \\
&= (y_{xf} - \delta y_{xf})(c\theta_c c\psi_c(x_{pc} - x_c) + \delta x c\theta_c c\psi_c + \delta\theta c\psi_c(s\theta_c - c\theta_c)(x_{pc} - x_c) \\
&\quad + \delta\psi c\theta_c(s\psi_c - c\psi_c)(x_{pc} - x_c) - \delta x_p c\theta_c c\psi_c + s\psi_c c\theta_c(y_{pc} - y_c) \\
&\quad + \delta y s\psi_c c\theta_c + \delta\theta s\psi_c(s\theta_c - c\theta_c)(y_{pc} - y_c) - \delta\psi c\theta_c(s\psi_c + c\psi_c)(y_{pc} - y_c) - \delta y_p s\psi_c c\theta_c \\
&\quad - s\theta_c z_c + \delta\theta(s\theta_c + c\theta_c)z_c + \delta z s\theta_c) \\
&= (y_{xf} - \delta y_{xf})(c\theta_c c\psi_c(x_{pc} - x_c) + s\psi_c c\theta_c(y_{pc} - y_c) - s\theta_c z_c) + \delta x(c\theta_c c\psi_c y_{xf}) \\
&\quad + \delta y(s\psi_c c\theta_c y_{xf}) + \delta z(s\theta_c y_{xf}) \\
&\quad + \delta\theta(c\psi_c(s\theta_c - c\theta_c)(x_{pc} - x_c) + s\psi_c(s\theta_c - c\theta_c)(y_{pc} - y_c) + (s\theta_c + c\theta_c)z_c)y_{xf} \\
&\quad + \delta\psi(c\theta_c(s\psi_c - c\psi_c)(x_{pc} - x_c) - c\theta_c(s\psi_c + c\psi_c)(y_{pc} - y_c))y_{xf} \\
&\quad - \delta x_p(c\theta_c c\psi_c y_{xf}) - \delta y_p(s\psi_c c\theta_c y_{xf})
\end{aligned} \tag{E.45}$$

and

$$\begin{aligned}
R &= -IF - JG - LZ \\
&= -(s\theta_c s\phi_c c\psi_c - s\psi_c c\phi_c)(x_{pc} - x_c) - (s\theta_c s\phi_c s\psi_c + c\phi_c c\psi_c)(y_{pc} - y_c) - s\phi_c c\theta_c z_c \\
&\quad - \delta x(s\theta_c s\phi_c c\psi_c - s\psi_c c\phi_c) - \delta y(s\theta_c s\phi_c s\psi_c + c\phi_c c\psi_c) + \delta z s\phi_c c\theta_c \\
&\quad + \delta\theta(s\phi_c c\psi_c(s\theta_c + c\theta_c)(x_{pc} - x_c) + (s\phi_c s\psi_c(s\theta_c + c\theta_c))(y_{pc} - y_c) - s\phi_c(s\theta_c - c\theta_c)z_c) \\
&\quad + \delta\phi(s\psi_c(s\phi_c - c\phi_c) + s\theta_c c\psi_c(s\phi_c + c\phi_c))(x_{pc} - x_c) \\
&\quad + (s\theta_c s\psi_c(s\phi_c + c\phi_c) - c\psi_c(s\phi_c - c\phi_c))(y_{pc} - y_c) + c\theta_c(s\phi_c + c\phi_c)z_c \\
&\quad - \delta\psi(c\phi_c(s\psi_c - c\psi_c) - s\theta_c s\phi_c(s\psi_c + c\psi_c))(y_{pc} - y_c) \\
&\quad + (c\phi_c(s\psi_c + c\psi_c) + s\theta_c s\phi_c(s\psi_c - c\psi_c))(x_{pc} - x_c) \\
&\quad + \delta x_p(s\theta_c s\phi_c c\psi_c - s\psi_c c\phi_c) + \delta y_p(s\theta_c s\phi_c s\psi_c + c\phi_c c\psi_c)
\end{aligned} \tag{E.46}$$

Finally, collecting the like terms and moving the error terms to the RHS, yields the  $y$  measurement equation for the primarily vertical case

$$\begin{aligned}
& y_{xf}(\mathbf{c}\theta_c \mathbf{c}\psi_c(x_{pc}-x_c) + \mathbf{s}\psi_c \mathbf{c}\theta_c(y_{pc}-y_c) - \mathbf{s}\theta_c z_c) \\
& - (\mathbf{s}\theta_c \mathbf{s}\phi_c \mathbf{c}\psi_c - \mathbf{s}\psi_c \mathbf{c}\phi_c)(x_{pc}-x_c) - (\mathbf{s}\theta_c \mathbf{s}\phi_c \mathbf{s}\psi_c + \mathbf{c}\phi_c \mathbf{c}\psi_c)(y_{pc}-y_c) - \mathbf{s}\phi_c \mathbf{c}\theta_c z_c = \\
& \delta x(\mathbf{s}\theta_c \mathbf{s}\phi_c \mathbf{c}\psi_c - \mathbf{s}\psi_c \mathbf{c}\phi_c - \mathbf{c}\theta_c \mathbf{c}\psi_c y_{xf}) + \delta y(\mathbf{s}\theta_c \mathbf{s}\phi_c \mathbf{s}\psi_c + \mathbf{c}\phi_c \mathbf{c}\psi_c - \mathbf{s}\psi_c \mathbf{c}\theta_c y_{xf}) \\
& - \delta z(\mathbf{s}\theta_c y_{xf} + \mathbf{s}\phi_c \mathbf{c}\theta_c) - \delta\phi[(\mathbf{s}\psi_c(\mathbf{s}\phi_c - \mathbf{c}\phi_c) + \mathbf{s}\theta_c \mathbf{c}\psi_c(\mathbf{s}\phi_c + \mathbf{c}\phi_c))(x_{pc}-x_c) \\
& + (\mathbf{s}\theta_c \mathbf{s}\psi_c(\mathbf{s}\phi_c + \mathbf{c}\phi_c) - \mathbf{c}\psi_c(\mathbf{s}\phi_c - \mathbf{c}\phi_c))(y_{pc}-y_c) + \\
& \mathbf{c}\theta_c(\mathbf{s}\phi_c + \mathbf{c}\phi_c)z_c] - \delta\theta[\mathbf{s}\phi_c \mathbf{c}\psi_c(\mathbf{s}\theta_c + \mathbf{c}\theta_c)(x_{pc}-x_c) + (\mathbf{s}\phi_c \mathbf{s}\psi_c(\mathbf{s}\theta_c + \mathbf{c}\theta_c))(y_{pc}-y_c) \\
& - \mathbf{s}\phi_c(\mathbf{s}\theta_c - \mathbf{c}\theta_c)z_c + (\mathbf{c}\psi_c(\mathbf{s}\theta_c - \mathbf{c}\theta_c)(x_{pc}-x_c) + \mathbf{s}\psi_c(\mathbf{s}\theta_c - \mathbf{c}\theta_c)(y_{pc}-y_c) + (\mathbf{s}\theta_c + \mathbf{c}\theta_c)z_c)y_{xf}] \\
& + \delta\psi[(\mathbf{c}\phi_c(\mathbf{s}\psi_c - \mathbf{c}\psi_c) - \mathbf{s}\theta_c \mathbf{s}\phi_c(\mathbf{s}\psi_c + \mathbf{c}\psi_c))(y_{pc}-y_c) \\
& + (\mathbf{c}\phi_c(\mathbf{s}\psi_c + \mathbf{c}\psi_c) + \mathbf{s}\theta_c \mathbf{s}\phi_c(\mathbf{s}\psi_c - \mathbf{c}\psi_c))(x_{pc}-x_c) \\
& - (\mathbf{c}\theta_c(\mathbf{s}\psi_c - \mathbf{c}\psi_c)(x_{pc}-x_c) - \mathbf{c}\theta_c(\mathbf{s}\psi_c + \mathbf{c}\psi_c)(y_{pc}-y_c))y_{xf} \\
& + \delta x_p(\mathbf{c}\theta_c \mathbf{c}\psi_c y_{xf} - (\mathbf{s}\theta_c \mathbf{s}\phi_c \mathbf{c}\psi_c - \mathbf{s}\psi_c \mathbf{c}\phi_c)) + \delta y_p(\mathbf{s}\psi_c \mathbf{c}\theta_c y_{xf} - (\mathbf{s}\theta_c \mathbf{s}\phi_c \mathbf{s}\psi_c + \mathbf{c}\phi_c \mathbf{c}\psi_c)) \\
& + \delta y_{xf}(\mathbf{c}\theta_c \mathbf{c}\psi_c(x_{pc}-x_c) + \mathbf{s}\psi_c \mathbf{c}\theta_c(y_{pc}-y_c) - \mathbf{s}\theta_c z_c)
\end{aligned} \tag{E.47}$$

where  $y_{xf}$  is found by substituting the nominal values for the A/C Euler angles into Eq. (E.44).

## Bibliography

- [1] Davison, A.J., I.D. Reid, N.D. Molton, and O. Stasse. “MonoSLAM: Real-Time Single Camera SLAM”. *Pattern Analysis and Machine Intelligence, IEEE Transactions on*, 29(6):1052 –1067, june 2007. ISSN 0162-8828.
- [2] Durrant-Whyte, H. and T. Bailey. “Simultaneous localization and mapping: part I”. *Robotics Automation Magazine, IEEE*, 13(2):99 –110, june 2006. ISSN 1070-9932.
- [3] Giebner, M. *Tightly-Coupled Image-Aided Inertial Navigation System via a Kalman Filter*. Master’s thesis, AFIT, WPAFB, OH, 2003.
- [4] Hoffman, Michael. “Schwartz warns against dependence on GPS”. *Military Times*, January 2010.
- [5] Ke, Y. and R. Sukthankar. “PCA-SIFT: A more distinctive representation for local image descriptors”. *2004 IEEE Computer Society Conference on cumputer Vision and Pattern Recognition (CVPR’04) - Volume 2*, volume 2, 506–513. 2004.
- [6] Maybeck, Peter S. *Stochastic Models, Estimation, and Control Volume 2*. Academic Press, New York, NY, 1983.
- [7] Pachter, M. and G. Mutlu. *Dynamics of Information Systems: Theory and Application*, chapter The Navigation Potential of Ground Feature Tracking, 287–303. Springer, 2010.
- [8] Pachter, M., A. Porter, and M. Polat. “INS Aiding Using Bearing-Only Measurements of an Unknown Ground Object”. *ION Journal Navigation*, 53(1):1–20, 2006.
- [9] Titterton, David and John Weston. *Strapdown Inertial Navigation Technology 2nd Edition*. The Institution of Engineernig and Technology, London, UK, 2004.
- [10] Veth, M., J. Raquet, and M. Pachter. “Stochastic constraints for efficient image correspondence search”. *Aerospace and Electronic Systems, IEEE Transactions on*, 42(3):973–982, 2006.

<b>REPORT DOCUMENTATION PAGE</b>				Form Approved OMB No. 074-0188
<p>The public reporting burden for this collection of information is estimated to average 1 hour per response, including the time for reviewing instructions, searching existing data sources, gathering and maintaining the data needed, and completing and reviewing the collection of information. Send comments regarding this burden estimate or any other aspect of the collection of information, including suggestions for reducing this burden to Department of Defense, Washington Headquarters Services, Directorate for Information Operations and Reports (0704-0188), 1215 Jefferson Davis Highway, Suite 1204, Arlington, VA 22202-4302. Respondents should be aware that notwithstanding any other provision of law, no person shall be subject to an penalty for failing to comply with a collection of information if it does not display a currently valid OMB control number.</p> <p><b>PLEASE DO NOT RETURN YOUR FORM TO THE ABOVE ADDRESS.</b></p>				
1. REPORT DATE (DD-MM-YYYY) 22-Mar-2012	2. REPORT TYPE Master's Thesis	3. DATES COVERED (From – To) September 2010 – March 2012		
4. TITLE AND SUBTITLE  Covariance Analysis of Vision Aided Navigation by Bootstrapping		5a. CONTRACT NUMBER		
		5b. GRANT NUMBER		
		5c. PROGRAM ELEMENT NUMBER		
6. AUTHOR(S)  Relyea, Andrew L, Capt		5d. PROJECT NUMBER		
		5e. TASK NUMBER		
		5f. WORK UNIT NUMBER		
7. PERFORMING ORGANIZATION NAMES(S) AND ADDRESS(S) Air Force Institute of Technology Graduate School of Engineering and Management (AFIT/EN) 2950 Hobson Way Wright-Patterson AFB OH 45433-7765			8. PERFORMING ORGANIZATION REPORT NUMBER AFIT/GE/ENG/12-36	
9. SPONSORING/MONITORING AGENCY NAME(S) AND ADDRESS(ES) Air Force Research Laboratory Munition Guidance Division Division Technical Advisor Dr. Robert Murphey 101 W Eglin Blvd Room 267 Eglin AFB, FL 32542 Robert.Murphey@eglin.af.mil			10. SPONSOR/MONITOR'S ACRONYM(S) AFRL/RWG	
			11. SPONSOR/MONITOR'S REPORT NUMBER(S)	
12. DISTRIBUTION/AVAILABILITY STATEMENT DISTRIBUTION STATEMENT A. APPROVED FOR PUBLIC RELEASE; DISTRIBUTION IS UNLIMITED.				
13. SUPPLEMENTARY NOTES This material is declared a work of the U.S. Government and is not subject to copyright protection in the United States.				
14. ABSTRACT Inertial Navigation System (INS) aiding using bearing measurements taken over time of stationary ground features is investigated. A cross country flight, in two and three dimensional space, is considered, as well as a vertical drop in three dimensional space. The objective is to quantify the temporal development of the uncertainty in the navigation states of an aircraft INS which is aided by taking bearing measurements of ground objects which have been geolocated using ownship position. It is shown that during wings level flight at constant speed and a fixed altitude, an aircraft that tracks ground objects and over time sequentially transitions to tracking new ground objects which were geolocated by the aircraft as they came into view, will have the beneficial effect of considerably reducing the long term uncertainty in the INS-provided navigation state. It is also shown that a munition in “free fall” tracking previously geolocated ground features will also have the beneficial effect of reducing the uncertainty in the INS-provided navigation state.				
15. SUBJECT TERMS Vision Aided Navigation Covariance Analysis Kalman Filter				
16. SECURITY CLASSIFICATION OF: REPORT U		17. LIMITATION OF ABSTRACT UU	18. NUMBER OF PAGES 115	19a. NAME OF RESPONSIBLE PERSON Dr. Meir Pachter
				19b. TELEPHONE NUMBER (Include area code) (937) 255-3636 Ext:7247 meir.pachter@afit.edu

Standard Form 298 (Rev: 8-98)

Prescribed by ANSI Std Z39-18